2008

Paleohydrologic Reconstruction of Three Shallow Basins, Slave River Delta, NWT, Using Stable Isotope Methods

Cherie Mongeon
Wilfrid Laurier University

Your file Votre référence
ISBN: 978-0-494-38718-4
Our file Notre référence
ISBN: 978-0-494-38718-4

Paleohydrologic Reconstruction of Three Shallow Basins, Slave River Delta, NWT, Using Stable Isotope Methods

By

Cherie Mongeon

Honours Bachelor of Arts, Wilfrid Laurier University, 2003

Submitted to the Department of Geography and Environmental Studies
in partial fulfillment of the requirements
for the Masters of Environmental Studies degree
Wilfrid Laurier University
Waterloo, Ontario, Canada
2008

Abstract

The long-term natural hydrological variability of the Slave River Delta (SRD), NWT, is not well documented and needs to be further developed to provide temporal context to understand and evaluate impacts of Slave River (SR) floodwater influence and climate variability and change on contemporary hydro-ecological conditions of the SRD. The SRD has broad ecological and cultural significance, as it provides extensive habitat for wildlife and is important for local First Nations community who have an historical connection with the delta and its resources. Concerns have been raised over recently reported drying trends in the SRD over the past few decades and have largely been attributed to regulation of the Peace River (PR), which supplies the SR with ~65% of its annual flow.

Modern lake water balances (2003 to 2005) of three lakes from different hydrological settings within the SRD were assessed using oxygen ($\delta^{18}O$) and hydrogen ($\delta^{2}H$) stable isotope analyses. Contemporary lake water balance was used to constrain paleohydrological interpretations of cellulose-inferred $\delta^{18}O$ from lake sediment cores. Past hydro-ecological conditions of each lake was also reconstructed using bulk organic carbon and nitrogen elemental and stable isotope analyses. Lead-210 (^{210}Pb) and caesium-137 (^{137}Cs) analyses were conducted to establish sediment core chronologies.

Results from lake water $\delta^{18}O$ and $\delta^{2}H$ analyses of SD20, an evaporation-dominated basin, indicate seasonal precipitation, snowmelt runoff and evaporation predominantly control the water balance of this lake. An ~215-year cellulose-inferred $\delta^{18}O_{lw}$, $\delta^{13}C$ and $\delta^{15}N$ record of SD20 provides paleoclimatological evidence that recently reported dry conditions in the SRD are not outside of the range of natural variability for the delta. SD20 paleohydrological records follow a similar pattern as PAD5, a climate-driven basin in the Peace-Athabasca Delta (PAD), and align with paleoclimate records reconstructed from tree-ring sequences from the Athabasca River headwaters. Results provide long-term documentation of how hydrological conditions have varied in an area of the SRD that is largely beyond the reach of river flooding.

Lake water $\delta^{18}O$ and $\delta^{2}H$ analyses of SD2, a flood-dominated basin, indicate that SR floodwaters control the water balance of SD2. An ~100 year carbon and nitrogen elemental and isotope record for SD2 documents event-scale flooding on the SR and indicates that regulation of the PR has not decreased flood frequency at this site over the past ~40 years. The late 1940s and 1950s likely represent the period of lowest river discharge over the past century. The SD2 C/N record is similar to the C/N record of PAD15, an oxbow lake in the PAD, indicating common upstream drivers control flood frequency in both deltas.

Lake water $\delta^{18}O$ and $\delta^{2}H$ analyses of SD28, an exchange-dominated basin, suggest that SR flooding and evaporation predominantly control the water balance of SD28. Reconstructed cellulose-inferred $\delta^{18}O_{lw}$ suggest an increase in river flooding may have occurred over the past ~40 years. However, reconstructing past hydro-ecological conditions is more difficult at this site due to its long channel connection to the SR, which suppresses the geochemical signals recorded in the lake sediment.

Acknowledgements

First and foremost, I would like to thank my advisor Dr. Brent B. Wolfe for his time, patience, support and constructive criticisms over the last several years, which have helped me to be a better academic writer and critical thinker. I would also like to thank him for his encouragement to pursue other opportunities while I was still in the process of finishing my research and writing of my thesis. Your understanding and guidance are greatly appreciated. Additionally, I would like to say thank you to my co-advisor Dr. Thomas W. Edwards for his time and patience as well. His constructive criticisms have helped me to think beyond what is right in front of me, which has helped to make this thesis a better piece of work. Lastly, I am truly grateful to both of my advisors for the opportunity to take part in a ground breaking and exciting research project.

I am indebt to the following people for providing me with help and support during fieldwork, lab work and all other components of the thesis process: Dr. Brent Wolfe, Dr. Thomas Edwards, Dr. Roland Hall, Dr. Mike English, Ken Clogg-Wright, Johan Wiklund, Natalie St. Amour, Bronwyn Brock, Mike Sokal, Joscelyn Bailey and Gabby Lafferty. I would like to thank the following organizations for providing funding for fieldwork and analytical support: NSERC Northern Research Chair Program, Northern Scientific Training Program, BC Hydro, Premier's Research Excellence Award, and Polar Continental Shelf Project. Lastly, I would like to thank the following supporting and partner organizations for their contributions to this research project: Deninu Kue First Nation and Fort Resolution Deninu School for use of their school during fieldwork.

I owe a sincere and from the bottom of my heart thank you to my daughter Brynn Mongeon and partner Robert Henderson. For the first decade of her childhood, I was a student (enough said!). Through good times and hard times, as well as lost times, she has been accepting of whatever I wanted or needed her to do so that I could pursue my studies. This I will never forget, and will surely try to make up for, for a long time to come. To Robert I am thankful to have such a supportive and patient partner who was always there to listen and to encourage. I know that this process was not easy for the three of us and I value your support, help and advice. This work is dedicated to the both of you.

Lastly, I would like to thank the many friends and fellow graduate students and the staff and faculty in the Geography Department at Wilfrid Laurier University. You have all helped to make this process a happy memory, and your support, advice, help and friendship will never be forgotten. To Michelle Wiszniowski, Kellie Mongeon (my sister) and Nicole Bunning, I thank you for lending your ear whenever I needed it, for taking time out of your busy lives to enjoy life with me (when we could squeeze it in!), for helping Brynn and I out when we needed it and for just being the greatest friends anyone could ask for. Thank you.

Table of Contents

List of Tables

List of Figures

Chapter 1 INTRODUCTION

1.1 THE SLAVE RIVER DELTA, NWT

The Slave River Delta (SRD), located in the Northwest Territories, Canada (**Figure 1**), is an important hydrological node of the Mackenzie Basin drainage system, which drains approximately 1,805,200 km^2 of inland waters into the Arctic Ocean and is one of the world's largest freshwater drainage systems (Natural Resources Canada, 2003). Northern deltaic systems such as the SRD are important both ecologically and hydrologically as these ecosystems are more biologically productive and environmentally sensitive compared to other components of northern riverine systems (Milburn et al., 1999). The SRD is home to a variety of waterfowl and other bird species, migratory fish species, mammal populations such as muskrat, beaver, river otter and mink, as well as a variety of riparian plant communities (Milburn et al., 1999). The Slave River is thought to play an essential role in supplying the SRD with water and nutrient-rich sediment during flood events, considered crucial in maintaining extensive shoreline habitat and the overall sustainability of this northern ecosystem (English et al., 1997; Prowse et al., 2002). However, Sokal (2007) discovered that flooding does not control the nutrient or water balance of precipitation-supported delta lakes that are not typically influenced by Slave River floodwater inputs. Sokal (2007) suggests that precipitation-supported lakes have enough in-lake nutrients and receive enough seasonal precipitation to continually support the nutrient balance within the lake. The SRD has significant cultural importance as well. The rich hunting and fishing

grounds of the delta are a natural resource for the local Deninu Kue First Nation community of Fort Resolution, providing residents a means to support their traditional lifestyle (Wolfe et al., 2007b).

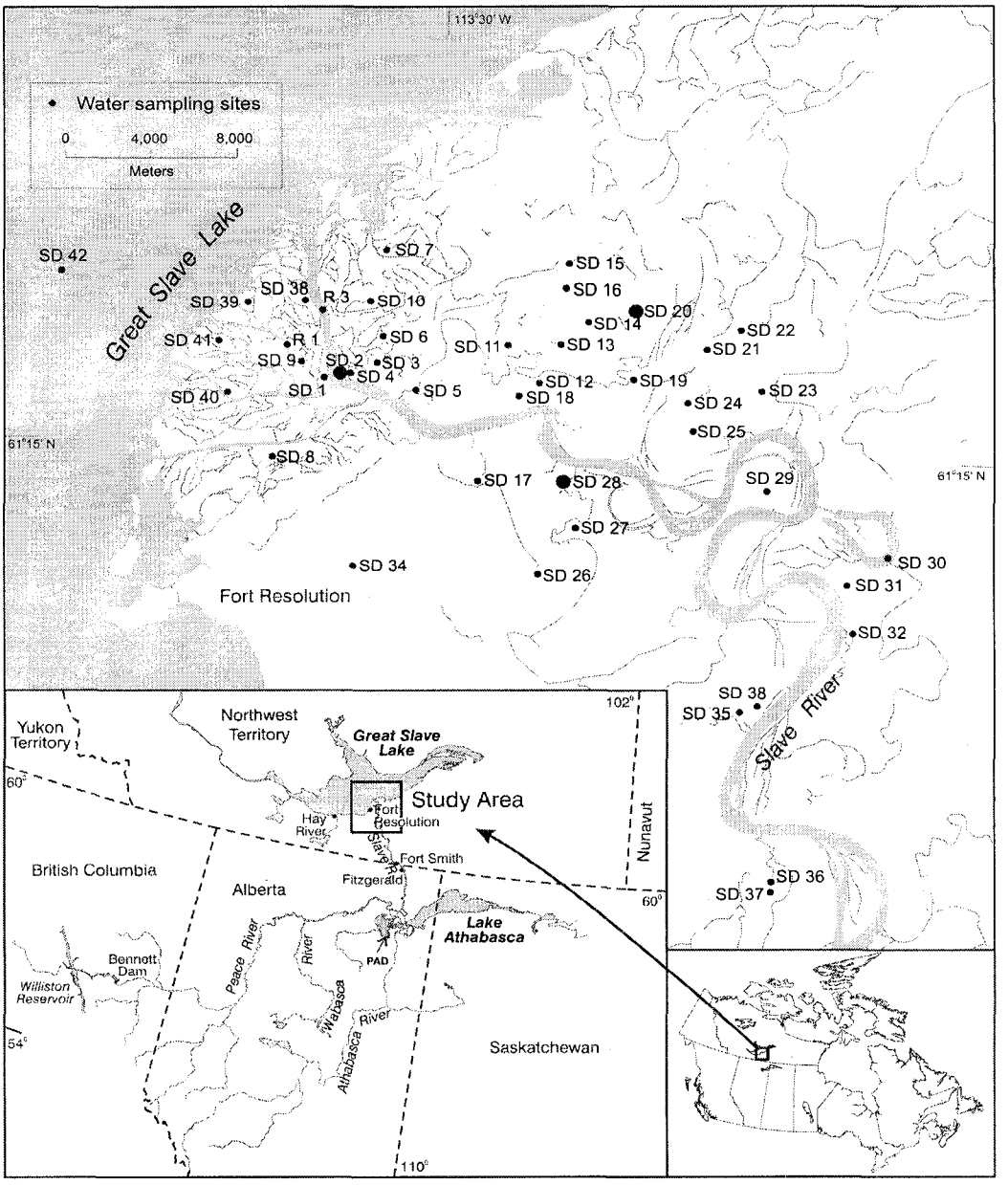

Figure 1. Map of the Slave River Delta, showing lake and river sampling sites, location of SD20, SD2 and SD28 and the Peace-Athabasca Delta (PAD).

The Slave River receives approximately 66% of its annual flow from the Peace River, which was regulated in 1968 by the construction of the WAC Bennett Dam at Hudson's Hope, British Columbia (English et al., 1996). Lake Athabasca, the Athabasca River (via the Rochers River) and other northward-flowing tributaries upstream of the Peace-Rochers confluence provide the remainder (34%) of the Slave River's annual flow. In turn, the Slave River provides approximately 75% of all inflow to Great Slave Lake (Gardner et al., 2006), which is the main source of water for the Mackenzie River.

Notable changes in geomorphological development and plant assemblage communities in the active part of the delta are thought to be caused by rapid changes in Slave River discharge levels, as well as seasonal hydrological processes (such as ice cover formation) on the Slave River (English et al., 1997). Geomorphological and biological changes in the SRD affect wildlife and waterfowl habitat and their food sources. English et al. (1997) documented geomorphological and botanical evolution on the outer margin of the SRD before and after regulation of the Peace River through examination of aerial photos. Observations of plant assemblage changes provide evidence of a shift from wetter, more productive environments, to drier, less productive environments, and a decrease in the growth of cleavage bar islands in the Outer Delta (English et al., 1997). These geomorphological and botanical changes are thought to be the result of substantial reductions in sediment loads initiated by impoundment (English et al., 1997).

River regulation and climate variability have elicited concerns from local community members over the current and future state of the SRD ecosystem (Wolfe et al., 2007b; Wesche, 2007). Previous research by Bill et al. (1996), English (1984) and English et al. (1997) in the SRD, as well as local observations, have focused mainly on geomorphic and

botanical evolution of the delta as evidence of overall drier and less productive conditions, which have been attributed to river regulation. However, long-term documentation of the natural hydrologic and climatic variability of the SRD is lacking. This needs to be further developed to establish temporal context to evaluate the impacts of river regulation and climate variability on the contemporary hydro-ecological conditions of the SRD, and to anticipate future hydrological evolution (Timoney, 2002).

1.1.1 Climatic and Hydrologic Setting

The Slave River Delta (61°15' N, 113°30' W) is located in a Subarctic Climate Zone (Natural Resources Canada, 2003). This climatic zone has short cool summers and long cold winters, and experiences expansive temperature ranges mainly due to continentality (Christopherson and Byrne, 2006). Sporadic discontinuous permafrost underlies approximately 10% to 50% of the SRD region (Natural Resources Canada, 2003). The average mean daily temperature is 10.3°C during the ice-off period (May to October), and -14.9°C during the ice-on period (November to April) (Environment Canada, 2004). Average mean annual precipitation is 362 mm (Environment Canada, 2004).

The delta is 170 km long, and comprises an area of approximately 8,300 km^2, 400 km^2 of which is active. English et al. (1997) classified the SRD into three distinct zones based on geomorphology and vegetation, which are based on the apparent frequency of floodwater inundation of the Slave River. The outer delta zone is the youngest part of the delta. It supports aquatic and emergent vegetation and is thought to flood annually during the spring freshet as its low levee heights are within 0.1 m of Great Slave Lake summer water

levels. The mid-delta zone supports alder-willow vegetation and is thought to flood approximately every 5-7 years as levee heights here are 1.0 m higher than Great Slave Lake summer water levels. The apex zone is the oldest part of the delta. Forest communities dominate the apex and it is thought to flood only every few decades as it has levee heights of approximately 2-2.5 m above Great Slave Lake summer water levels.

To further explore the hydrological processes that control the water balances of lakes in the SRD, Brock et al. (2007) sampled 41 basins within the SRD in 2003 and analysed them for oxygen and hydrogen stable isotope composition. The modern water balance for each study lake was evaluated using an isotopic framework calculated from 2003 hydroclimatic data. Results captured the variation of lake water balances over the 2003 ice-off period (May to October) and lake water balance responses to variations in hydrological processes such as precipitation, snowmelt runoff, river flooding, Great Slave Lake seiche events and evaporation. From this spatial and temporal lake water balance study, Brock et al. (2007) concluded that the geographical position of a lake in the SRD largely determines the hydrological setting of a lake, and the hydrological setting determines the hydrological processes that influence the water balance of a lake in the delta. In addition, the study recognized that biogeographical zones do reflect the hydroecological variability of the 41 study lakes to some degree, but that a hydrologically-based classification of delta lakes is a more appropriate way to describe SRD hydrology, as levee height and flood susceptibility are not the only factors that control SRD lake water balances. Brock et al. (2007) identified three hydrologic classes of lakes based on dominant hydrologic inputs and outputs in 2003: flood-dominated lakes, which are found in the active part of the delta, evaporation-

dominated lakes, which are found in the apex zone, and exchange-dominated lakes located in the outer margin of the active delta and along the Slave River (**Figure 2**).

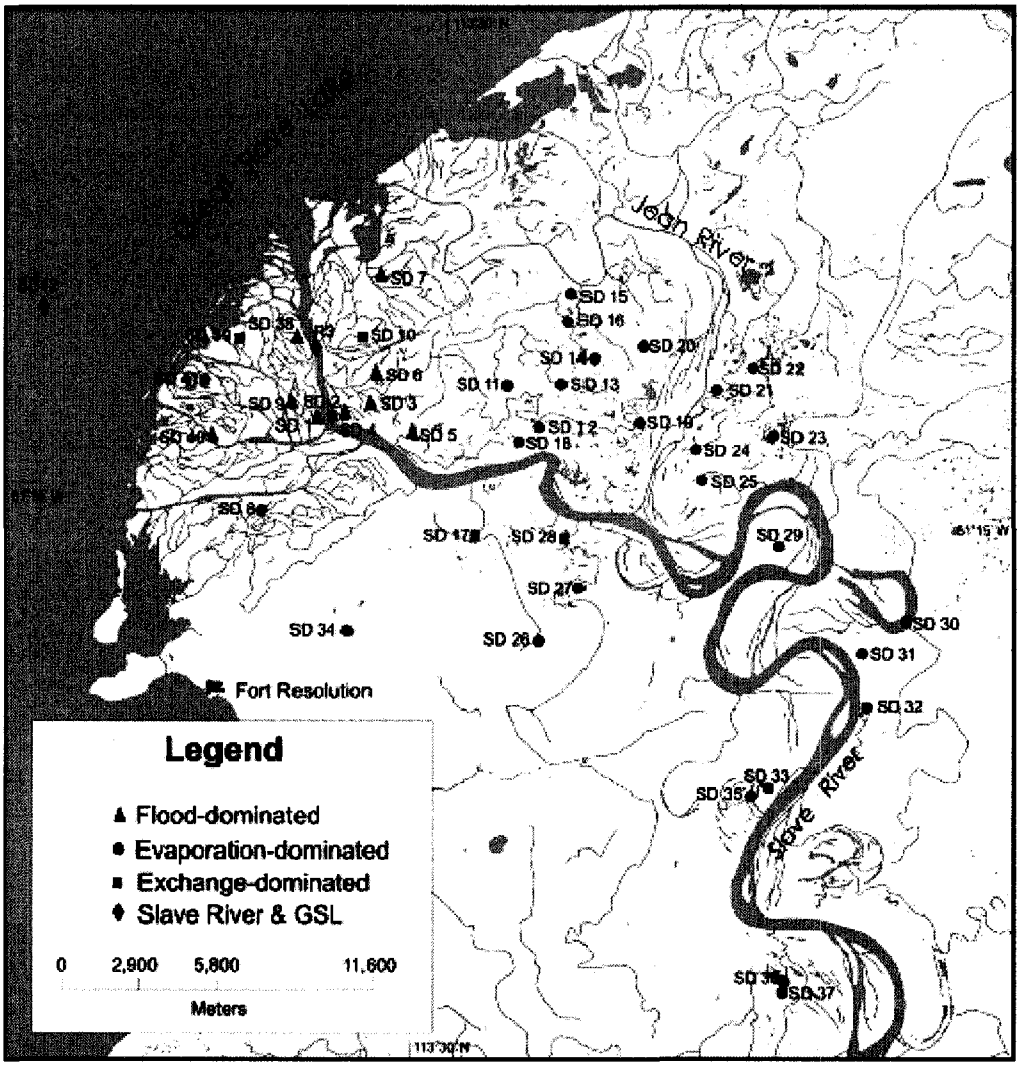

Figure 2. Forty-one lakes in the Slave River Delta, NWT, classified according to hydrological processes that control lake water balances (after Brock et al., 2007, page 398).

Major hydrological processes that play a key role in controlling the water balance of lakes in the SRD include: 1) flooding from the Slave River, which is predominately driven by river ice processes as well as periodic surface seiche events on Great Slave Lake (GSL) (Brock et al., 2007; Gardner et al., 2006; Milburn et al., 1999), 2) precipitation and runoff (Brock et al., 2007), and 3) evaporation (Brock et al., 2007).

River ice processes such as ice cover formation, ice floes and ice jams, play a large role in the hydrologic behaviour of the Slave River, as they influence or determine water levels, flow velocity and flow pathways, flooding regimes, sediment transport and loading, and geomorphology of the delta (Prowse et al., 2002). Ice jams are essential for the replenishment of perched basins at elevations that open-water floods would not normally reach, as ice jams induce reverse flow direction of a river and causing overbank flooding (Beltaos, 2000). Prowse et al. (2002) suggested that ice jam flooding has not been as prevalent during the last few decades in the SRD as ice cover break up has been predominantly thermally induced, as opposed to mechanically induced. Ice covers have been observed "rotting out" in situ due to slower climatic transitions from winter daily temperatures to spring daily temperatures. This causes less and less mechanical break-up of ice covers, which are induced by substantial freeze-up stage and ice cover thickness, large spring-freshet flows, and, usually, a rapid thermal deterioration of ice cover (Prowse et al., 2002). Brock et al. (2007) reported that river flooding occurred on the Slave River after ice break-up in 2003 and that river floodwater contributed largely to the water balance of many of the lakes in the delta, specifically those lakes in the delta that are flood-dominated (see **Figure 1**).

Surface seiche events on GSL predominantly occur during late summer and autumn, and are controlled by northwesterly winds (Gardner et al., 2006). Gardner et al. (2006) discovered GSL surface seiche events impact sedimentation distribution as well as erosional processes, which affect the growth of the outer delta. Basins with hydrological connections to the Slave River and, or, that are proximal to the river, are subject to frequent seiche event flooding each year, suggesting seiche event flooding is important to the water balance and ecological sustainability of these basins (Gardner et al., 2006).

Precipitation contributes to the water balance of evaporation-dominated, exchange-dominated and flood-dominated lakes in the SRD. The degree to which the water balance of a lake is affected by thaw season precipitation or snowmelt varies from lake to lake and is dependent on the surface area and volume of a lake, the catchment characteristics of a lake and the intensity and duration of the precipitation event (Brock et al., 2007). The response of delta lake water isotopic compositions to late thaw season precipitation in 2003 indicated that all lakes, regardless of their hydrologically-based classification showed a depletion in lake water isotopic composition to some degree (Brock et al., 2007). Snowmelt also contributes to the water balance of lakes in the delta during spring melt, as well as to the building of river ice, lake ice and snow packs during the ice-on season. Brock et al. (2007) identified that water balance of several lakes within the SRD, which do not have a hydrological connection to the Slave River and/or are not within geographical extent of river floodwaters, are influenced predominantly by snowmelt in early spring. It was also determined that several of the lakes that were flooded by the Slave River in 2003 were more isotopically-depleted than the Slave River, suggesting that snowmelt influenced these lakes in addition to river floodwater.

Evaporation influences water balance of all lakes in the SRD to varying degrees, as well as the Slave River (Brock et al., 2007). Delta lakes located in the apex zone that do not have channel connections to the Slave River (**Figure 2**) and were not influenced by 2003 spring flooding, were identified by Brock et al. (2007) as having the greatest response to evaporation. A lesser response to evaporation was identified in lake water balance of delta lakes that have channel connections to the Slave River or Great Slave Lake, as well as lakes that received floodwaters during spring melt of 2003.

1.2 OBJECTIVES

Drivers of hydroecological variability and change in the SRD, over varying timescales, may include climate variability and change, regulation of the Peace River upstream, geomorphic evolution, and Great Slave Lake and Slave River hydrology. However, little is known about how much any one of these drivers contributes to hydroecological variability in the SRD. Lack of substantial long-term documentation of geomorphological change, shifts in plant assemblages and Slave River hydrology inhibits the ability to critically compare temporal and spatial changes in the SRD pre- and post-regulation.

The objectives of this thesis, which is a part of a multi-proxy contemporary and paleolimnology study (Wolfe et al., 2007b), are to use stable isotope methods on lake sediment cores taken from three lakes located in different hydrological settings in the SRD to reconstruct hydrological variability of the SRD over the past few hundred years.

Understanding the long-term hydrological variability of the SRD region is essential to assess the relative importance of various drivers of change.

Specific questions that this research addresses include: (1) how have hydrological conditions varied in lakes of the SRD over the past few hundred years?, (2) is there evidence in the past of drier conditions in the SRD similar to the past few decades as reported by residents of the local community of Fort Resolution (Wesche, 2007)?, and (3) how does the hydrological setting of lake basins in a deltaic environment influence the paleohydrological information that is contained in the sediment records?

1.3 SITE DESCRIPTIONS

1.3.1 Study Basins

SD20, SD2 and SD28 (**Figure 1**) were chosen for a multi-proxy paleolimnological analysis to develop an understanding of historical lake water balance of lakes from different hydrological settings within the Slave River Delta. Although all three basins are located in the apex zone, their hydrological settings in the delta are very different from one another. Additionally, it was later determined by Brock et al. (2007) that the hydrological classifications of each of the lakes are also very different from one another. SD2 is adjacent to the Slave River, separated by a low levee and the lake water balance is largely influenced by Slave River floodwaters, thus SD2 is classified as a flood-dominated basin (Brock et al., 2007). The dominant hydrologic input for SD2 includes river floodwater and output includes evaporation. SD28 has a direct connection to the Slave River, making this basin's water balance also strongly influenced by influx of river water, thus SD28 is classified as an

exchange-dominated basin (Brock et al., 2007). The dominant hydrologic input for SD28 includes river water and outputs include surface outflow and evaporation. In contrast, SD20 is more distant from the Slave River and its water balance is strongly influenced by local climate, and so, SD20 is classified as an evaporation-dominated basin (Brock et al., 2007). The dominant hydrologic inputs for SD20 include catchment-sourced snowmelt and precipitation, and output includes evaporation.

The hydrological-based classification scheme of delta lakes is summarized in **Table 1** below. The dominant processes in the water balance of each classification of delta lakes are highlighted in bold (**Table 1**). Groundwater in the lake water balances is considered to be negligible because the SRD is in a zone of discontinuous permafrost and lowland drainage is generally poor (Day, 1972). Additionally, because delta lake sediments comprise predominantly of fine silt and clays the hydraulic conductivity is presumed to be relatively low.

Hydrologically-based Classification Scheme of Delta Lakes			
	Flood-dominated SD2	Evaporation-dominated SD20	Exchange-dominated SD28
Inputs	$\mathbf{R_F}$ + S + P	**S + P**	$\mathbf{R_F}$ + $\mathbf{R_N}$ + S + P
Outputs	O_F + **E**	**E**	$\mathbf{O_F}$ + $\mathbf{O_N}$ + E

Table 1. R is river inputs during elevated (spring flood) flow conditions (R_F) and normal summer flow conditions (R_N), S is catchment-sourced snowmelt input, P is thaw season precipitation, O is surface outflow following elevated (spring flood) flow conditions (O_F) and during normal summer flow conditions (O_N), and E is surface water evaporation (Brock et al., 2007).

1.3.2 SD20

Hydrological Setting of SD20

SD20 is located within close proximity to the Jean River, a distributary of the Slave River (**Figure 2**). It is surrounded by wetlands and mature trees and is approximately 3 m at maximum depth (**Figure 3**). Present day vegetation patterns, such as dead willow fringes, and encroaching jack pine surrounding the basin, indicate water levels have fluctuated in the past. For example, the outer margins of the lake currently contain dead willows, which indicates that at some point in the past the shoreline of the lake did not extend to these areas and willows were able to thrive.

Based on 2003 to 2005 field observations and seasonal photographs, SD20 water levels are visibly higher in the spring due to snowmelt runoff and then decrease over the summer months and into fall due to evaporation. Field observations also indicate that SD20 was not flooded at any time by either the Slave or Jean River during the period of monitoring from 2003 to 2005. In early May 2004, while ice-cover was still intact, visible hydrologic connections to wetlands that surround SD20 were observed. In summer and fall 2003 to 2005, these hydrologic connections were still visible but water levels were greatly reduced due to evaporation and lack of precipitation over the warm summer period.

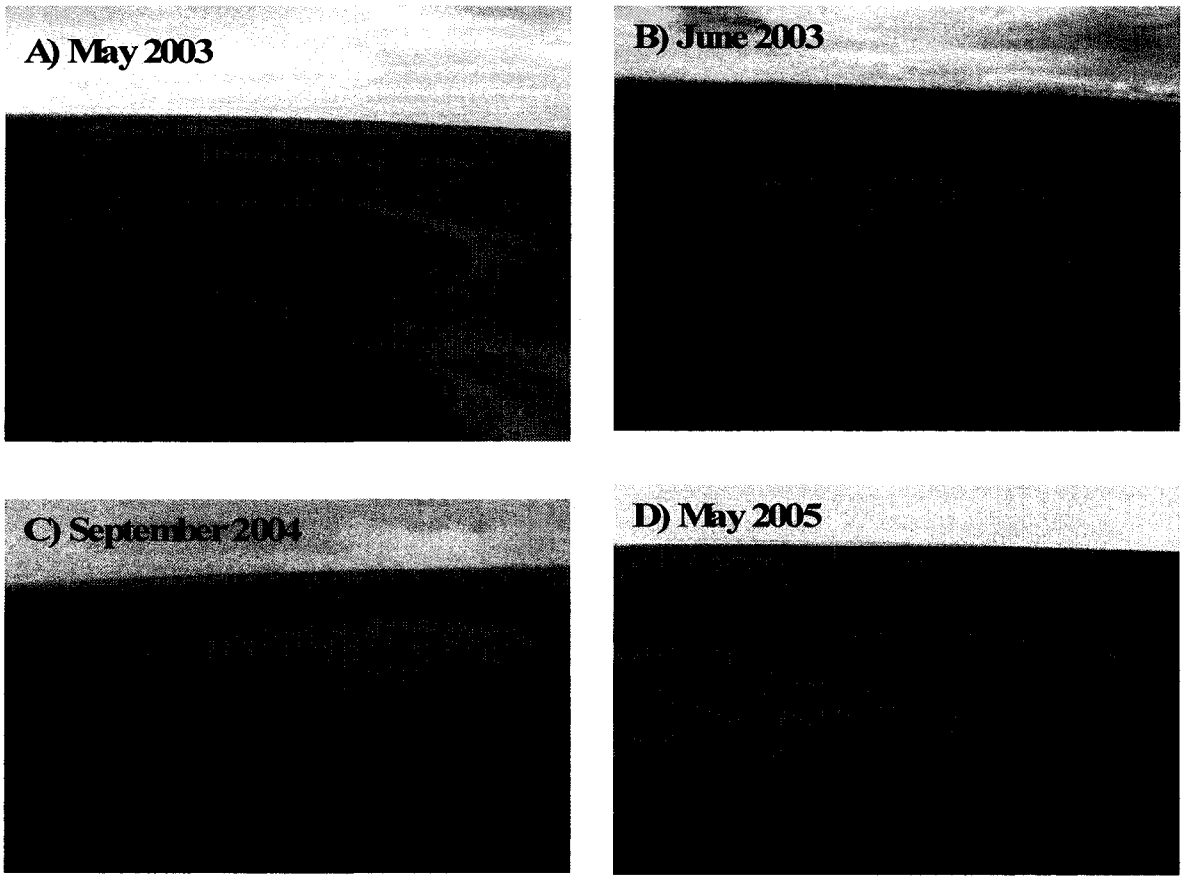

Figure 3. Seasonal photographs of SD20, which illustrate seasonal water level fluctuations.

1.3.3 SD2

Hydrological Setting of SD2

SD2 is located on the border of the apex and mid delta zones of the SRD, and is approximately 50 m from Resdelta Channel, the main distributary of the Slave River (**Figure 2**). SD2 is 1.5 m at maximum depth and has very low levees of about 0.5 to 1.5 m in height. Due to the low levees around the lake and because it is located where the Slave River bifurcates, where ice jams are likely to develop, SD2 is susceptible to floodwaters from the Slave River (**Figure 4**).

Based on field observations and seasonal photographs, it is evident that the Slave River can readily inundate SD2 during high-water events. SD2 was flooded at the onset of spring thaw in 2003 and again in May 2005. A large amount of river sediment (approximately 5-10 cm deep) was found throughout the catchment around the outer margins of the lake following the May 2005 flood event. Water levels visibly decreased at SD2 during each monitoring year (2003 to 2005) indicating that evaporation was the dominant influence on the basin's lake water balance during the summer months.

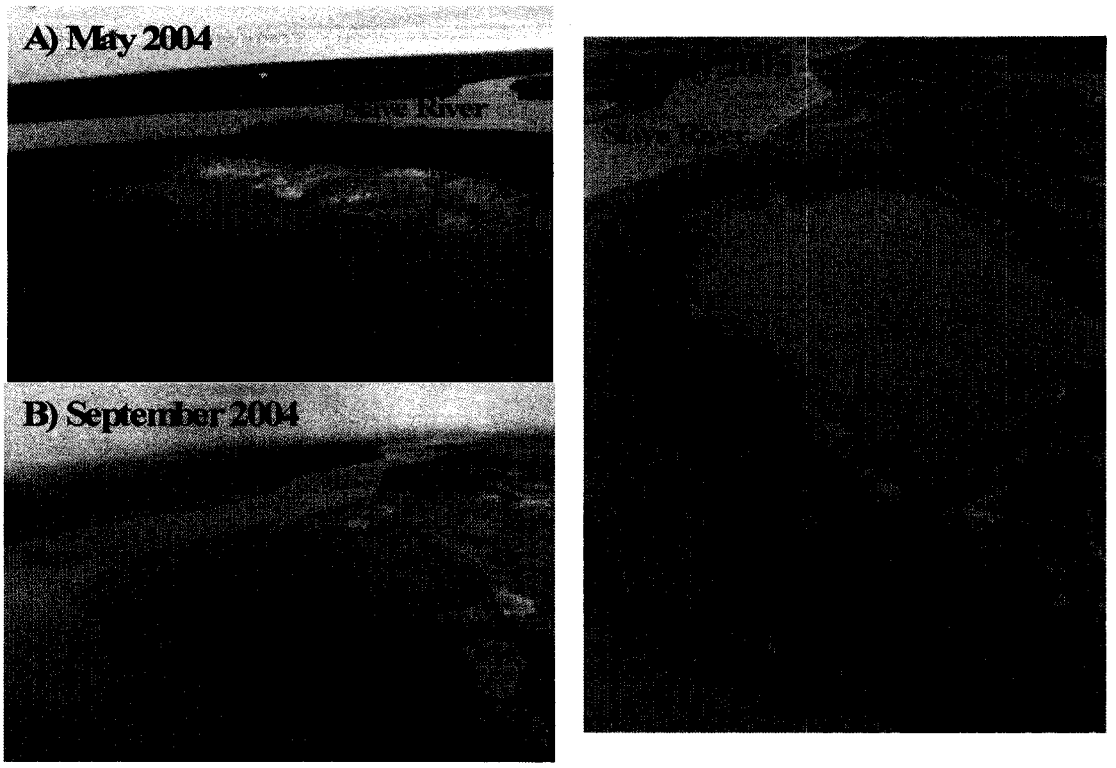

Figure 4. Seasonal photographs of SD2. Photographs illustrate non-flooded conditions (A), conditions after Slave River floodwaters have entered the lake (C), and lower water level conditions (B) at SD2.

1.3.4 SD28

Hydrological Setting of SD28

SD28 is adjacent to the Slave River and is connected to the river by a channel (**Figure 2**). The channel is approximately 1 km long and ranges from 0.5-8 m wide at varying locations during the ice-on and ice-off periods. At maximum depth, SD28 is 2.5 m. The pattern of vegetation surrounding the outer fringes of the lake (**Figure 5**) suggests fluctuations in water levels occurred in the past. For example, vegetation around the lake

consists mainly of sedges and fringing shrub and tree communities. These vegetation types are unable to thrive on the outer fringes of SD28 due to seasonal fluctuations in water levels, which causes periodic inundation along the outer fringes of the lake.

It is visibly evident from field observations and seasonal photographs that during periods of high flow and high water levels on the Slave River, SD28 is influenced by Slave River waters through its channel. Similar to SD2, it was evident that SD28 was strongly influenced by the Slave River during the May 2005 large-scale flood event as sediment from the river was deposited around the outer margins of the lake (**Figure 5 (D)**). During field monitoring in May 2005, photographs were taken to document the presence of high water marks as well as Slave River sediment deposits on trees and vegetation that surround the basin (**Figure 5**). As summer progressed into fall during each monitoring year (2003 to 2005), lake water levels decreased due to decreased river water influence. Lower water levels during this period of each monitoring year were also evident in the channel at the lake/channel mouth.

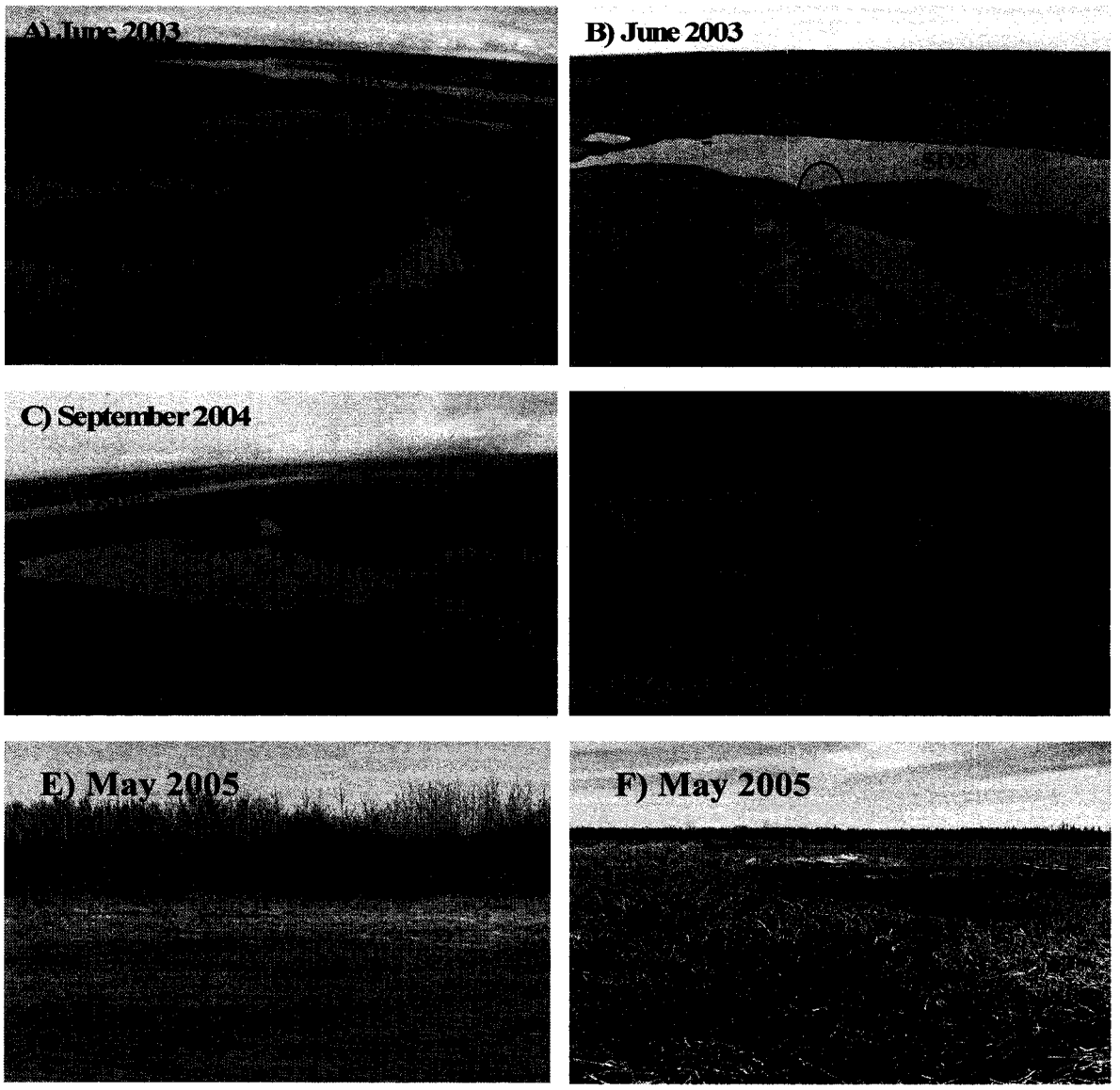

Figure 5. Seasonal photographs of SD28. Photographs illustrate seasonal channel constrictions during warmer summer months and early fall (A, B and C) as well as periods where the Slave River and SD28 freely exchange waters at times of spring flooding (D). May 2005 photographs showing high-water marks on trees adjacent to the lake and Slave River sediment deposits on trees and vegetation that surround the basin ((E) and (F)).

1.4 Field and Laboratory Methods

To meet research objectives, a two-pronged approach was taken during this research project. The first approach was to assess contemporary hydrology of the study sites using water isotope tracers and field observations. The second was to assess the paleohydrology of the study sites using aquatic cellulose oxygen isotope analysis, bulk organic carbon and nitrogen elemental and isotope analysis, loss-on-ignition, macrofossils (Adam, 2007), diatoms (Sokal, 2007) and lead-210 (^{210}Pb) and caesium-137 (^{137}Cs) analyses.

Isotope Hydrology

1.4.1 Water Sampling

Water samples from SD2, SD28, SD20, the Slave River and rain were collected in September of 2002 and on several occasions during the ice-off period from May to October of 2003, 2004 and 2005. Snow samples were collected in May 2004. Samples were collected in 30 ml high-density polyethylene (HDPE) bottles and were sealed tightly to prevent evaporation and were analysed for oxygen and hydrogen isotope composition.

1.4.3 Water $\delta^{18}O$ and $\delta^{2}H$ Analyses

Lake water, Slave River water, rain and snow samples were analysed for oxygen and hydrogen isotope composition to assess modern lake water balance of each of the study lakes. Samples were submitted to the University of Waterloo Environmental Isotope Laboratory (UW-EIL) and analysed by continuous flow isotope ratio mass spectrometry

(CF-IRMS). Water isotope results are expressed as δ–values which represent deviations in per mil (‰) from the Vienna-Standard Mean Ocean Water (VSMOW) standard for oxygen and hydrogen, $\delta_{sample}=[(R_{sample}/R_{standard})-1] \times 10^3$, where R is the $^{18}O/^{16}O$ or $^{2}H/^{1}H$ ratio in the sample and standard. $\delta^{18}O$ and $\delta^{2}H$ results are normalized to –55.5 ‰ and –428 ‰, respectively (Standard Light Antarctic Precipitation; Coplen, 1996). The analytical uncertainty for $\delta^{18}O$ is ±0.2 ‰ and ±2.0 ‰ for $\delta^{2}H$, based on replicated analyses.

Isotope Paleolimnology

1.4.4 Lake Sediment Coring

Multiple sediment cores for SD28 and SD20 were obtained with a Maxi-Glew™ gravity corer from a helicopter on floats; the SD2 sediment core was extracted with a Maxi-Glew™ gravity corer (Glew, 1988) from a canoe. Cores were sectioned vertically into 0.5 cm intervals at the field station.

Five cores were obtained in September 2002 from SD28. The longest core was chosen for analysis (SD28 KB-5; 33 cm). The longest of five cores taken from SD20 in September 2002 was also chosen (SD20 KB-1; 27cm long). A 32 cm long sediment core, SD2 KB-3, extracted from SD2 in August 2003, was analysed for diatoms (Liu, 2004) and carbon and nitrogen elemental and stable isotope composition (Jermyn, 2004). The 49 cm core was extracted from a different location in SD2 to develop a longer paleohydrological record for this basin.

1.4.5 ^{210}Pb and ^{137}Cs Analyses

Sediment samples from the three lakes were analyzed for ^{210}Pb and ^{137}Cs to establish chronologies for each sediment core. Wet weight for each sediment sample from each of the sediment cores was determined. Samples were put into Whirlpack™ bags when sectioned, therefore, the weight of each sample plus the Whirlpack™ bag was weighed, then, the average weight of a Whirlpack™ bag was subtracted from each sediment sample increment to determine its wet weight.

Sediment sample increments were freeze-dried and 20.0 mm aliquots were then packed into plastic Nalgene™ dating tubes, which were then sealed with 1.0 cc of epoxy. Concentrations of total ^{210}Pb, ^{214}Bi (supported ^{210}Pb) and ^{137}Cs contained in each sediment sample were measured using gamma spectrometry at the University of Waterloo. Sediment core chronologies and sedimentation rates of each lake were determined using the constant rate of ^{210}Pb supply (CRS) model (Appleby, 2001). The CRS model accounts for changes in initial unsupported ^{210}Pb concentrations that occur due to changes in sedimentation rates over time (Appleby, 2001).

1.4.6 Loss-On-Ignition

Loss-On-Ignition (LOI) was conducted to provide an approximation of the organic and carbonate contents of sediment samples (Dean, 1974; Heiri et al., 2001). Sub-samples of wet sediment (approximately 0.5 grams) were weighed before and after sequential heating at 90°C, 550°C and 1000°C. The weight loss between reactions was measured and provided an estimate of the water content, organic content and carbonate content of the sediment samples.

1.4.7 Carbon and Nitrogen Elemental and Isotope Analyses

Organic carbon and nitrogen content and stable isotope composition were analysed on sediment samples from SD2 KB-5, SD28 KB-5 and SD20 KB-1 cores to determine whether organic matter in the sediment samples was terrestrial or aquatic, as well as to further investigate past nutrient dynamics for each basin. Carbonate carbon was removed from the lake sediment samples by applying 10% (by volume) hydrochloric acid (HCl) to each sediment sample at 60°C (Wolfe et al., 2001). Samples were then rinsed with deionized water until the pH of each sample was that of the deionized water being used to rinse the samples. Samples were then freeze-dried and sieved through a 500μm dry sieve to remove coarse-grained material. Samples of the fine fraction were then weighed into tin capsules and analyzed by EA-CF-IRMS at the UW-EIL. Carbon stable isotope results are reported in standard δ notation, representing deviations in per mil (‰) from the Peedee Belemnite (PDB) standard. Nitrogen stable isotope results are reported in standard δ notation, representing deviations in per mil (‰) from the AIR standard. The analytical uncertainty for elemental carbon is ± 0.1 %, for elemental nitrogen is ± 0.01 %, for $\delta^{13}C$ is ± 0.1 ‰, and for $\delta^{15}N$ is ± 0.1 ‰.

1.4.8 Cellulose Oxygen Isotope Analyses

Oxygen stable isotope ($\delta^{18}O$) analysis of aquatic plant cellulose extracted from SD20 and SD28 lake sediments was used to reconstruct lakewater $\delta^{18}O$ (Edwards and McAndrews, 1989; Edwards, 1993; Wolfe et al., 2001, 2007a). Cellulose is a bio-molecule that exists in the

cell walls of higher and lower plants, and some algae. Cellulose is preserved in sediments as algal cells within zooplankton fecal pellets, or as amorphous organic matter (Edwards, 1993). Oxygen stable isotope ($\delta^{18}O$) analysis was not conducted on the SD2 KB-5 sediment core as evidence from LOI, elemental carbon and nitrogen stable isotope analysis suggested that the sediment likely contains organic matter derived from outside the lake basin.

Cellulose extraction involves several steps (Wolfe et al., 2001; 2007a). These techniques closely follow those that are used to extract cellulose from wood powder as explained by Green (1963) and Sternberg et al. (1984). Acid-washing to remove carbonate (see section 1.4.6 Carbon and Nitrogen Elemental and Isotope Analyses) was performed first. This was followed by solvent extraction, bleaching, and alkaline hydrolysis to remove non-cellulose organic constituents. Next, removal of iron and manganese oxyhydroxides was completed through hydroxylamine leaching, followed by heavy-liquid density separation using sodium polytungstate to separate the cellulose fraction from the minerogenic residue. Cellulose oxygen isotope composition was then measured by CF-IRMS at the UW-EIL using standard methods (Wolfe et al., 2007a). Oxygen isotope results are expressed as δ–values which represent deviations in per mil (‰) from the Vienna-Standard Mean Ocean Water (VSMOW) standard for oxygen, $\delta_{sample}=[(R_{sample}/R_{standard})-1] \times 10^3$ where R is the $^{18}O/^{16}O$ ratio in the sample and standard, normalized to –55.5 ‰ for Standard Light Antarctic Precipitation (SLAP) (Coplen, 1996). Cellulose-inferred lake water $\delta^{18}O$ values were then calculated by applying a cellulose-water oxygen isotope fractionation factor of 1.028 (see Wolfe et al., 2001). Analytical uncertainty for cellulose-inferred lake water $\delta^{18}O$ values for SD20 is ± 0.6 ‰ and for SD28 is ± 0.4 ‰.

Chapter 2 THEORY

2.1 ISOTOPE HYDROLOGY

2.1.1 $\delta^{18}O$ and $\delta^{2}H$ in the Hydrologic Cycle: Isotopic Framework

Mass differences of water molecules containing various combinations of heavy and light oxygen and hydrogen stable isotopes leads to isotopic fractionation, or partitioning, of water as it passes through the hydrological cycle (Edwards et al., 2004). Precipitation that has not undergone evaporation generally plots close to the Global Meteoric Water Line (GMWL), which is described by $\delta^{2}H = 8\ \delta^{18}O + 10$ (Craig, 1961). The GMWL represents the relationship described by mean annual amount-weighted precipitation worldwide (Edwards et al., 2004). At any specific site on the globe, precipitation will plot along a Local Meteoric Water Line (LMWL). This is a result of the progressive rain-out of mass and heavy isotope species as atmospheric moisture progresses poleward during atmospheric transport. The poles receive precipitation that is strongly depleted in heavy isotopes as a result of this progressive rain-out effect (Edwards et al., 2004).

Surface waters that have undergone evaporation tend to cluster along a Local Evaporation Line (LEL). The LEL can be determined through calculations using local climatic and isotopic data. δp is an estimate of the mean annual isotopic composition of precipitation for a specific region, which commonly anchors the LEL (**Figure 6**). Surface waters that undergo evaporation typically cluster along the LEL (Gibson and Edwards, 2002). The quantification of the degree to which a lake is evaporatively enriched with the stable isotopes of ^{18}O and ^{2}H, allows for water balance modelling of a reservoir.

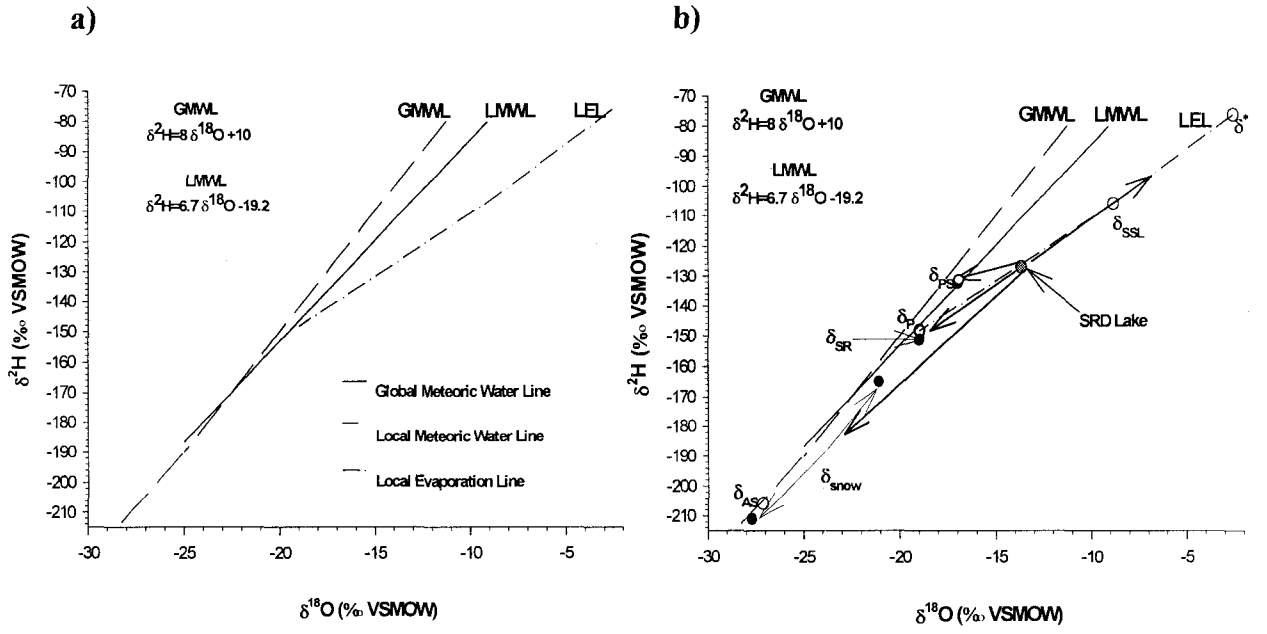

Figure 6. Isotopic framework for defining the LMWL and LEL for the Slave River Delta, based on an isotopic framework calculated from 2003 hydroclimatic data (a), and the potential isotopic trajectory of a theoretical SRD lake superimposed on the 2003 isotopic framework (b). The potential isotopic trajectory of a theoretical SRD lake is superimposed on the 2003 isotopic framework to show the trajectory of a SRD lake in response to 1) evaporation, 2) thaw season precipitation (δ_{PS}; Gibson and Edwards, 2002), 3) Slave River (δ_{SR}) flooding, and 4) snowmelt (δ_{snow}) input (the $\delta^{18}O$ and $\delta^{2}H$ range of snow, -27.7‰ to -21.1‰ and -211‰ to -165‰ is shown). Isotopic framework parameters (shown as open circles) include the isotopic composition of amount weighted mean annual (1962-1965) precipitation (δ_P) obtained from Fort Smith, NWT (Birks et al., 2004), the isotopic composition of evaporation-flux-weighted thaw season precipitation (δ_{PS}) (Gibson and Edwards, 2002) and atmospheric moisture (δ_{AS}), steady-state isotopic composition for a terminal basin (δ_{SSL}) where evaporation exactly equals inflow, and the limiting non-steady-state isotopic composition (δ^*), which indicates the maximum potential transient isotopic enrichment of a lake as it approaches complete desiccation (Brock et al., 2007).

The δ notation is used to express isotopic composition values, which indicate deviations in per mil (‰) from the isotopic composition of the Vienna Standard Mean Ocean Water (VSMOW) standard. The VSMOW value is an approximation of the present-day global ocean reservoir, defined as exactly 0‰ for both ^{18}O and ^{2}H (Gibson et al., 1996b). VSMOW values are used in hydrological studies with the understanding that evaporation from the oceans is the main source of global atmospheric moisture, and provides precipitation inputs for continental water cycles (Edwards et al., 2004).

Parameters used to construct the isotopic framework for this study are calculated using parameters described in detail in Edwards et al. (2004), Gibson and Edwards (2002), Gonfiantini (1986) and Barnes and Allison (1983), and are based on the linear resistance model of Craig and Gordon (1965). Equilibrium liquid-vapour isotopic fractionation ($\alpha^*_{L\text{-}V}$) is calculated based on Horita and Wesolowski (1994), where:

$$\alpha^*_{L\text{-}V} = \exp\left((-7.685 + 6.7123\,(10^3/T) - 1.6664\,(10^6/T^2) + 0.35041\,(10^9/T^3))/1000\right) \quad (1)$$

for $\delta^{18}O$ and

$$\alpha^*_{L\text{-}V} = \exp\left((1158.8\,(T^3/10^9) - 1620.1\,(T^2/10^6) + 794.84\,(T/10^3) - 161.04 + 2.9992\,(10^9/T^3))/1000\right) \quad (2)$$

for $\delta^{2}H$, where T represents the interface temperature in K. Equilibrium separation, for both $\delta^{18}O$ and $\delta^{2}H$, between the liquid and vapour phases ($\varepsilon^*_{L\text{-}V}$) is calculated based on

$$\varepsilon^*_{L\text{-}V} = (\alpha^*_{L\text{-}V} - 1)\,1000 \quad (3)$$

Kinetic separation (ε_K) is

$$\varepsilon_K = 14.2\ (1\text{-}h) \tag{4}$$

for $\delta^{18}O$ and

$$\varepsilon_K = 12.5\ (1\text{-}h) \tag{5}$$

for $\delta^{2}H$ (Gonfiantini, 1986).

The slope (S) and intercept (d) of the local evaporation line are calculated using the approach described by Barnes and Allison (1983), as

$$S = (\alpha^{*2}/\ \alpha^{*18})\ [(\varepsilon_K^{\ 2} + \varepsilon^{*2}/\ \alpha^*)\ (1+\delta_p^{\ 2}) - (h\ (\delta_p^{\ 2} - \delta_{AS}^{\ 2}))\ /\ (\varepsilon_K^{\ 18} + \varepsilon^{*18}/\ \alpha^*)\ (1 + \delta_p^{\ 18}) - (h\ (\delta_p^{\ 18} - \delta_{AS}^{\ 18}))] \tag{6}$$

where δ_p is the isotopic composition of input water, and

$$d = \delta_p^{\ 2} - S\ \delta_p^{\ 18} \tag{7}$$

where δ_{AS} is the isotopic composition of atmospheric moisture, calculated with

$$\delta_{AS} = (\delta_{PS} - \varepsilon^*_{L\text{-}V})\ /\ \alpha^*_{L\text{-}V} \tag{8}$$

(Gonfiantini, 1986).

The depleted end of the LEL is constrained by δ_p, while the limiting isotopic composition (δ^*) falls at the enriched end. δ^* is calculated using

$$\delta^* = (h\,\delta_{AS} + \varepsilon_K + \varepsilon^*_{L\text{-}V} / \alpha^*_{L\text{-}V}) / (h - \varepsilon_K - \varepsilon^*_{L\text{-}V} / \alpha^*_{L\text{-}V}) \quad (9)$$

(Gonfiantini, 1986). Steady state isotopic conditions (δ_{SSL}) are achieved under special circumstances in which the isotopic composition of evaporated moisture (δ_E) is equal to δ_P. The isotopic composition of δ_E can be calculated using

$$\delta_E = [[(\delta_L - \varepsilon^*) / \alpha^*] - h\,\delta_{AS} - \varepsilon_K]] / (1 - h + 10^{-3}\varepsilon_K) \quad (10)$$

(Gonfiantini, 1986).

2.2 PALEOLIMNOLOGY

2.2.1 Sediment Chronology

To establish sediment core chronology, lead-210 (^{210}Pb) and caesium-137 (^{137}Cs) radiometric dating was employed on SD 20 KB-1, SD28 KB-5 and SD 2 KB-5 sediment cores. ^{210}Pb is commonly used to establish depth-time scales for the past 150 years, based on its half-life of 22.29 years (Smol, 2002). ^{210}Pb is derived from the uranium-238 (^{238}U) radioactive decay series. ^{238}U has a half-life of 4.5 x 10^9 yr (Flett, 2003). Concentrations of ^{238}U in the earth's crust present today are considered to be constant, and even though concentrations of ^{238}U vary spatially, it is present at some concentration in all soils and sediments on Earth (Flett, 2003). ^{238}U radioactively decays over a long period of time ($t_{½}$ = 4.5 x 10^9 years) into uranium-234, which then decays into thorium-230, and then into

radium-226 (^{226}Ra). Radon-222 gas is derived from the radioactive decay of ^{226}Ra at the air-soil interface, which then escapes into the atmosphere, undergoes a series of several radioactive decays, and eventually decays to ^{210}Pb. ^{210}Pb then falls into water bodies (and on land), and eventually makes its way into the sediment column, becoming permanently bound to sediment particles (Holmes et al., 2002). A constant input of ^{210}Pb from the atmosphere is assumed when using most ^{210}Pb dating techniques. ^{210}Pb that was deposited into lake sediments 22.29 years ago will therefore be half the concentration as it was when it was first deposited. This enables the age of lake sediments at various depths to be calculated as well as the rate of sedimentation (Flett, 2003).

The ^{210}Pb dating technique used in this study is the Constant Rate of Supply (CRS) model developed by Krisnaswami et al. (1971). Methods followed for the CRS model are described in Appleby (2001) and Krisnaswami et al. (1971). Total ^{210}Pb activity in a sediment core compares two components: 1) supported ^{210}Pb (measured as ^{214}Bi), derived from the in situ decay of the parent radionuclide ^{226}Ra, and 2) unsupported ^{210}Pb derived from atmospheric flux (Appleby, 2001). The CRS method is based on a number of assumptions; 1) there is a constant rate of unsupported ^{210}Pb derived from atmospheric deposition, 2) ^{210}Pb is quickly absorbed to suspended particles in the water column, 3) post-depositional processes do not redistribute the ^{210}Pb within the sediments, and 4) ^{210}Pb decays exponentially over time, which follows the law of radioactive decay (Krisnaswami et al., 1971). The CRS model has been challenged by some paleolimnologists because unsupported ^{210}Pb inputs to a water system could possibly include additional amounts derived from soil erosion, which in turn can be lost by outflow, causing redistribution by hydrological processes and sediment focusing (Smol, 2002). From these conflicting views,

the Constant Initial Concentration, or CIC of ^{210}Pb dating method was established (Appleby et al., 1978). As noted by Smol (2002) however, the CRS model has proven to be a better dating method for most studies, but the CIC model provides a more reliable dating record when applied to studies where the sediment at the core site has been compacted and the primary sedimentation rates are constant (Appleby, 2001). For this study, the CRS method of ^{210}Pb was employed because the sedimentation rates of the study basins are assumed to be variable. Previous studies, for example Hall et al. (2004), have shown that in deltaic environments, sedimentation rates of aquatic basins are variable due to influx of river sediments during times of flood events.

^{137}Cs can provide a stratigraphic marker when plotted versus core depth, and is often used to validate ^{210}Pb age-depth chronologies (Jarvis et al., 2006). ^{137}Cs is an anthropogenic radioisotope, generated from nuclear bomb testing in the Northern Hemisphere in the late 1950s and early 1960s, and has a half life of 30.17 years. ^{137}Cs absorbs readily into liquid in the atmosphere and is then returned to the Earth's surface via radioactive fallout, whereby it attaches to sediment particles (Flett, 2003). The distribution of ^{137}Cs in the sediment core depth profile, or more specifically at what depth a ^{137}Cs peak is observed in the sediment core profile, marks the year A.D. 1963, based on known ^{137}Cs fallout rates (Appleby, 2001). ^{137}Cs may be preserved in basins with high sedimentation rates, and can be mobile in organic-rich sediments, or sediments that do not contain many clays and have large particle sizes (Longmore, 1982; Foster et al., 2006). In addition, available oxygen levels and pH can also influence ^{137}Cs absorption and mobility as can saltwater or groundwater incursion (Longmore, 1982; Foster et al., 2006).

2.2.2 Carbon and Nitrogen Elemental and Isotope Composition of Lake Sediment Organic Matter

Organic matter found in lake sediment is primarily from plants and organisms that are either in or around a lake (Meyers et al., 2001). Bulk organic carbon and nitrogen elemental and stable isotope composition was analyzed in the SD20, SD2 and SD28 sediment cores to further investigate past variability in nutrient cycling. Additionally, these analyses (i.e. C/N ratios) provided a means to determine if the organic matter found in the lake sediments was of terrestrial or aquatic origin. This is of great importance, as aquatic organic matter is essential for the reconstruction of lake water $\delta^{18}O$ histories from sediment cellulose $\delta^{18}O$ (Wolfe et al., 2001).

To help identify past intervals of river influence and/or changes in in-lake nutrient cycling the origin, or source, of organic matter, as well as organic content % (LOI at 550°C) and moisture content % (derived from LOI results) of lake sediments will be analysed. The coupling of these analyses with reconstructed lake sediment cellulose-inferred oxygen isotope composition will provide further insight into river influence intervals, changes in nutrient cycling, as well as with the interpretation of long-term natural hydroecological variability of the SRD. For example, Jermyn (2004) determined the carbon and nitrogen elemental and isotope composition of sediment core SD2 KB-3, extracted from SD2 in August 2003. Jermyn (2004) found that increases in organic matter content, carbonate and moisture content indicated periods of increased lake productivity and little to no Slave River flood water influence, and the opposite being true of decreases in organic matter content, carbonate and moisture content.

2.2.3 Oxygen Isotope Composition of Lake Sediment Cellulose

Aquatic cellulose $\delta^{18}O$ can be used to reconstruct past lake water $\delta^{18}O$ based on lab and field studies (DeNiro et al., 1981; Sternberg et al., 1984; Edwards et al., 1985; Edwards et al., 1989; Wolfe et al., 2001; Wolfe et al., 2007a) that indicate a near constant cellulose-water oxygen-isotope fractionation factor of ~1.028. Edwards and McAndrews (1989) first developed the method of extracting cellulose from sediment cores and concluded that fine-grained cellulose components in the offshore sediments of Weslemkoon Lake, Ontario, were dominantly aquatic. They discovered that the ability to trace past lake water $\delta^{18}O$ was possible through analyzing lake sediment cellulose $\delta^{18}O$ and by applying a cellulose-water fractionation factor similar to that of the one that exists between terrestrial cellulose and leaf water (DeNiro and Epstein, 1981; Sternberg et al., 1984; Edwards et al., 1985; Hall et al., 2004; Wolfe et al., 2005). A study by Wolfe et al. (2005) on Spruce Island Lake, a perched basin in the Peace-Athabasca Delta, highlights the usefulness of reconstructing past lake water $\delta^{18}O$ through lake sediment cellulose $\delta^{18}O$ analysis. Wolfe et al. (2005) were able to reconstruct the historical lake water balance of Spruce Island Lake, which enabled them to assess past impacts of climate and river flooding on the hydro-ecology of the basin. In addition, recent progress in sample preparation techniques and mass spectrometry have expedited oxygen isotope analysis of aquatic cellulose from lake sediment cores, increasing the ability to use this approach on high-resolution, multi-site, and multi-proxy studies (Wolfe et al., 2007a). These findings conclude that by analyzing aquatic cellulose within sediment intervals, shifts along the local evaporation line and/or meteoric water line can be documented, and paleohydrologic and paleoclimatic information can be derived (Edwards et al., 2004).

2.3 WATER BALANCE RECONSTRUCTION

2.3.1 Cellulose-inferred Lake Water Balance Reconstruction

Historical water balance reconstruction of a lake can be quantified using the cellulose-inferred lake water $\delta^{18}O$ record of a lake, as long as water balance is the predominant signal recorded in the lake sediments, and evaporative isotopic enrichment has occurred under conditions of hydrologic steady-state (Wolfe et al., 2005). Water balance is expressed as an evaporation-to-inflow (E/I) ratio through the use of isotope-mass balance equations and the linear resistance model of Craig and Gordon (1965). E/I is defined as:

$$E/I = (\delta_L - \delta_I) / (\delta_E - \delta_I) \quad (11)$$

where δ_E is calculated from Equation (10) in section 211. *$\delta^{18}O$ and $\delta^{2}H$ in the Hydrologic Cycle.*

Chapter 3 RESULTS AND INTERPRETATION

3.1 MODERN ISOTOPE HYDROLOGY: ISOTOPIC FRAMEWORK

The GMWL, as defined by Craig (1961) to be $\delta^2H = \delta^{18}O + 10$, describes the relationship between $\delta^{18}O$ and δ^2H for global amount–weighted annual precipitation. The LMWL for the SRD, which is approximated by $\delta^2H = 6.7\ \delta^{18}O - 19.2$ (Birks et al., 2004) is based on analysis of weighted monthly precipitation collected at Fort Smith, AB, from 1962-65. The GMWL and LMWL are used to develop the isotopic framework for the SRD (discussed in detail in section *2.1.1 $\delta^{18}O$ and δ^2H in the Hydrologic Cycle: Isotopic Framework).*

The LEL (discussed in detail in section *2.1.1 $\delta^{18}O$ and δ^2H in the Hydrologic Cycle: Isotopic Framework*) for the SRD for monitoring years 2003, 2004 and 2005 was calculated using $\delta^{18}O$ and δ^2H values of local precipitation from the years 1962-1965, and $\delta^{18}O$ and δ^2H values of ambient atmospheric moisture, relative humidity and air temperature during the open-water season of each specific monitoring year. Steady-state isotopic composition for a terminal basin (δ_{SSL}) and the limiting non-steady-state isotopic composition (δ^*) are two important reference points along the LEL (Barnes and Allison, 1983; Gibson and Edwards, 2002; Edwards et al., 2004). Climate normals were not used to calculate δ_{SSL} and δ^*, which are essential in evaluating the lake water balance of SD20, SD2 and SD28, as it was determined by Brock et al. (2007) that climate normal conditions may either under-, or, over-estimate potential evaporative enrichment, leading to inappropriate δ_{SSL} and δ^* values. Amount-weighted mean annual precipitation (δ_p) calculated from 1962-1965 was taken from

Fort Smith, NWT (Birks et al., 2004). This introduces a degree of analytical uncertainty to the slope of the LEL for 2003, 2004 and 2005, as δ_P anchors the LEL and may not represent the actual isotopic composition of annual precipitation for these monitoring years. Temperature (T) values for each monitoring year are based on evaporation-flux-weighted air temperatures from Hay River, NWT climate data (Environment Canada, 2004; 2005; 2007). Relative humidity (*h*) values for each monitoring year are based on flux weighted *h* values obtained from Hay River, NWT climate data (Environment Canada, 2004; 2005; 2007). Evaporation-flux-weighted thaw season precipitation (δ_{PS}) is taken from Gibson and Edwards (2002), which is based on GNIP data (Birks et al., 2004). Ambient atmospheric moisture (δ_{AS}) is assumed to be in approximate isotopic equilibrium with evaporation-flux weighted summer precipitation (δ_{PS}) (Gibson and Edwards, 2002). **Table 2** below provides the parameters used to develop the isotopic framework for evaluating lake water balance of SD20, SD2 and SD28 for 2003, 2004 and 2005 using equations (1) to (9) (see *Chapter 2* Theory).

Table 2. Parameters used to develop the isotopic framework for evaluating lake water balance of SD20, SD2 and SD28 for 2003, 2004 and 2005 using equations (1) to (9) (see *Chapter 2* Theory).

Parameter	Year: 2003		Year: 2004		Year: 2005	
h (%)	62.8		63.2		63.0	
T (°)	Celsius	Kelvin	Celsius	Kelvin	Celsius	Kelvin
	13.4	286.55	12.63	285.78	11.0	285.05
	$\delta^{18}O$	$\delta^{2}H$	$\delta^{18}O$	$\delta^{2}H$	$\delta^{18}O$	$\delta^{2}H$
δ^* (‰)	-2.38	-74.10	-2.58	-74.52	-2.42	-73.48
δ_{SSL} (‰)	-8.72	-104.63	-8.77	-104.60	-8.71	-104.16
δ_P (‰)	-19.0	-148.3	-19.0	-148.3	-19.0	-148.3
δ_{PS} (‰)	-17.0	-132.3	-17.0	-132.3	-17.0	-132.3
δ_{AS} (‰)	-27.11	-205.73	-27.18	-206.46	-27.25	-207.16
LEL	Slope	Intercept	Slope	Intercept	Slope	Intercept
	4.19	-68.60	4.23	-68.01	4.24	-67.73

The trajectory of the LEL for each monitoring year is very similar (**Figure 7**). Relative humidity for each of the three monitoring years is similar at ~ 63%. The isotopic composition of ambient atmospheric moisture is slightly more enriched in 2003 and 2004

than in 2005 due to slightly higher temperatures in 2003 and 2004. δ* for 2004 is slightly more isotopically depleted than in 2003 and 2005 due to a slightly higher *h* (**Table 2**).

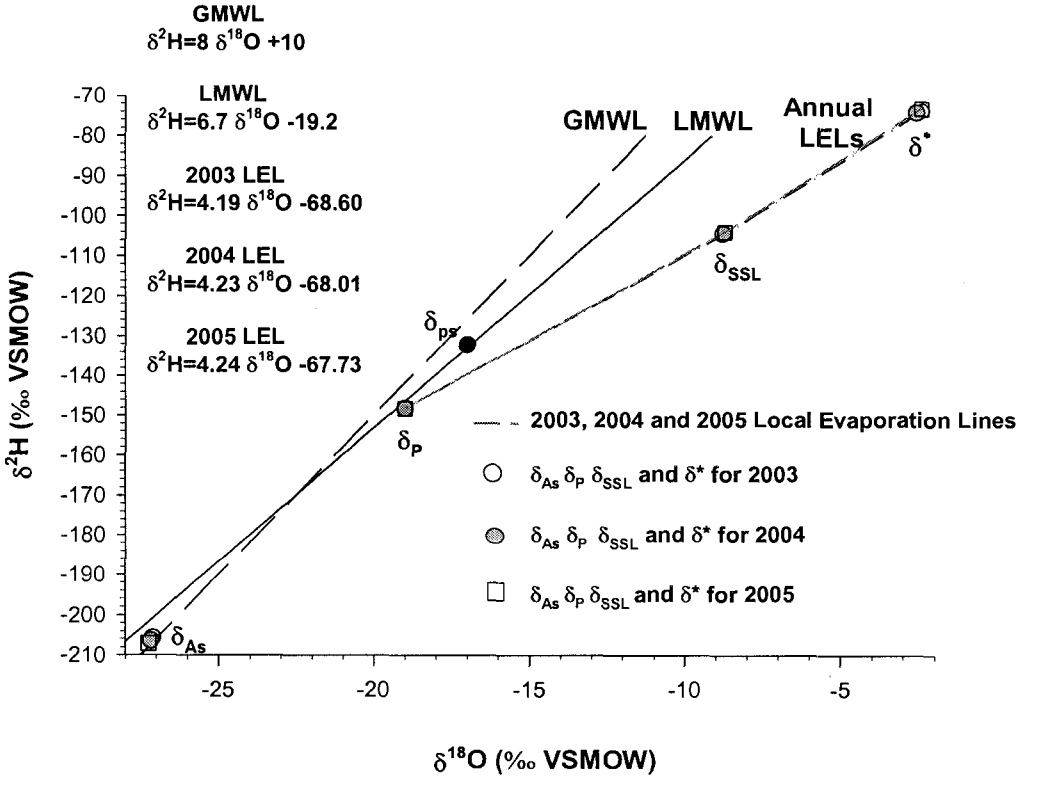

Figure 7. Isotopic framework for 2003, 2004 and 2005 showing Local Evaporation Lines for each monitoring year.

3.2 SD20 EVAPORATION-DOMINATED BASIN

Results from the isotope analysis of lake water samples collected from SD20 during the open-water season of 2003 plot along the LEL and values are more enriched than the Slave River for the entire 2003 sampling period (**Figure 8 (a)**). For example, the May sample for SD20 ($\delta^{18}O$ = -13.7‰ and $\delta^{2}H$ = -127‰) plots just slightly below the LEL and further along the LEL in comparison to the Slave River ($\delta^{18}O$ = -19‰ and $\delta^{2}H$ = -151‰) (**Figure 8 (a)**). From May 4th to May 5th a total of 4 cm of snowfall was measured and from May 14th to May 19th a total of 15.8 mm of rainfall was measured (Environment Canada, 2005). This suggests that the May sample reflects the influence of precipitation, and possibly snowmelt runoff, and not the influence of Slave River flood waters. Although an ice jam led to some flooding of the Slave River Delta, SD20 did not receive river floodwater (Brock et al., 2007). In contrast, isotopic composition of lakes in the delta whose water balance is defined as flood-dominated (such as SD2) and exchanged-dominated (such as SD28) were similar to the Slave River at the onset of ice-break up in May 2003 (Brock et al., 2007) (see **Figures 9 (a) and 10 (a)**). SD20 approaches δ_{SSL} in 2003, however, it does not reach δ_{SSL} composition. A total of 95.3 mm of rainfall was recorded from June until August 15th (Environment Canada, 2005), which is the date the SD20 August sample was extracted. Isotopic analysis of SD20 for June ($\delta^{18}O$ = -12.77‰ and $\delta^{2}H$ = -121.99‰), July ($\delta^{18}O$ = -11.7‰, and $\delta^{2}H$ = -118‰) and August 2003 ($\delta^{18}O$ = -10.9‰, and $\delta^{2}H$ = -113‰) show that samples are highly constrained along the LEL.

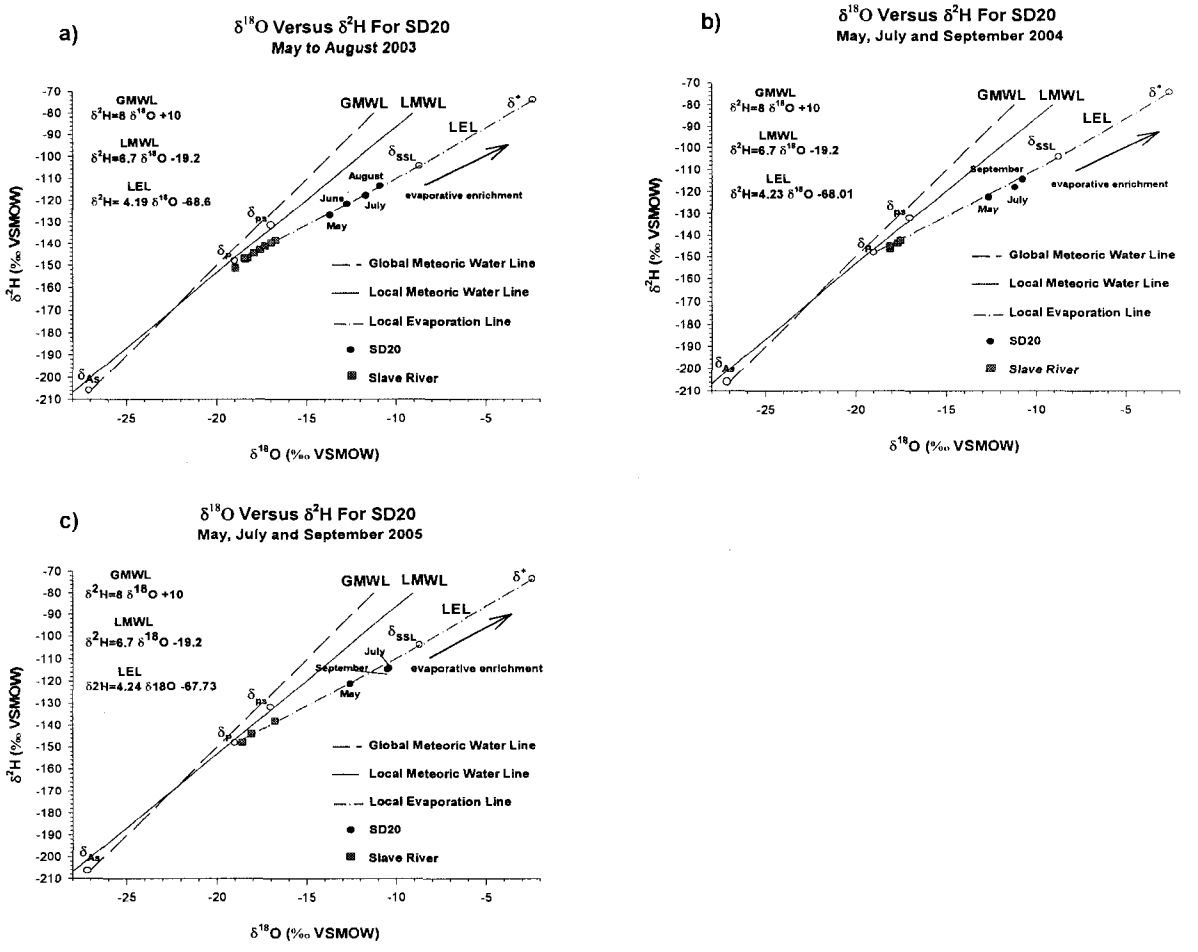

Figure 8. Isotope results from water samples collected from SD20 and the Slave River shown in $\delta^{18}O$-$\delta^{2}H$ space for May-August 2003 (a), May, July and September 2004 (b), and May, July and September 2005 (c).

Isotopic compositions of water samples taken in 2004 from SD20 plot below the LEL and do not reach δ_{SSL} values. Compositions may fall below the LEL simply because the LEL is anchored by δ_P values that are based on 1962-1965 amount-weighted mean annual precipitation, which is a conservative estimate of the isotopic composition of source water input (δ_I). It is possible that if amount-weighted mean annual precipitation for 2004 was used to calculate δ_P, and that the isotopic composition of δ_P for 2004 was lower than the value for 1962-1965, SD20 compositions may have plotted on the LEL and the slope of the LEL would decrease. Yi et al. (2008) suggest that even though lakes in the same region experience similar atmospheric conditions, it is more reasonable to use a lake-specific LEL to assess the water balance of a lake, as each lake may have different source water inputs (δ_I). Although this causes the slope of the LEL to be different for each lake, it conforms to the theory that with increasing evaporation, the lake water compositions of all lakes in a region, regardless of the slope of their unique LEL, would eventually converge at the same δ^* (Yi et al., 2008).

Overall, isotope analysis of all SD20 2004 water samples are more enriched in comparison to the Slave River throughout the entire 2004 monitoring season (**Figure 8 (b)**). $\delta^{18}O$ and $\delta^{2}H$ values for SD20 in May were -12.7‰ and -123‰, whereas $\delta^{18}O$ and $\delta^{2}H$ values for the Slave River were -17.7‰ and -144‰, indicating that SD20 was much more isotopically enriched in comparison to the river at the on-set of ice break-up and that the lake was not influenced by river flood waters. Lake water isotopic compositions for July 2004 ($\delta^{18}O$ = -11.2‰, and $\delta^{2}H$ = -118‰) and September ($\delta^{18}O$ = -10.8‰, and $\delta^{2}H$ = -115‰) indicate that SD20 was slightly more enriched in September than in July, which

suggests that evaporation was the dominant control on lake water balance from mid summer and into the fall (**Figure 8 (b)**).

Lake water isotope analysis of water samples taken in 2005 plot below the LEL and between δ_P and δ_{SSL} (**Figure 8 (c)**). Similar to 2004 sampling year, this suggests that using a conservative estimate of δ_P (1962-1965 amount-weighted mean annual precipitation) may not be appropriate for the 2005 sampling year. If the isotopic composition of δ_P was more depleted for 2005, the composition of SD20 would theoretically fall directly on the LEL. SD20 2005 values are more enriched in comparison to the Slave River throughout the 2005 monitoring season. For example, the isotopic composition of the May sample was $\delta^{18}O$ = -12.6‰, and δ^2H = -122‰, whereas the isotopic composition of the Slave River was $\delta^{18}O$ = -18.6‰, and δ^2H = -148‰, indicating that SD20 was much more evaporatively enriched in comparison to the river and that river flood waters did not enter the basin at the onset of ice break-up (**Figure 8 (c)**). The July ($\delta^{18}O$ = -10.4‰, and δ^2H = -115‰) and September ($\delta^{18}O$ = -10.5‰, and δ^2H = -115‰) values are essentially the same.

Overall, the distribution of lake water isotope values for SD20 are very similar for all three monitoring years. Analyses indicate that SD20 is fed by waters that closely approximate estimated mean annual isotopic composition of precipitation. Although evaporation is an important process that greatly influences the lake water balance of this basin, SD20 did not reach closed-basin steady-state conditions (δ_{SSL}) in 2003 to 2005. This can be attributed to the amount of seasonal precipitation and snowmelt the lake received during these three years.

3.3 SD2 FLOOD-DOMINATED BASIN

Results from the isotope analysis of lake water samples collected from SD2 during the open-water season of 2003 from May to July plot below and parallel to the LEL (**Figure 9**). Lake water isotope analysis for SD2 taken at the onset of ice break-up in May 2003 show that SD2 essentially had the same isotopic water composition as the Slave River, because floodwaters from the Slave River entered SD2 (**Figure 9 (a)**). Additionally, Brock et al. (2007) report that total suspended solids (TSS) results for the May 2003 water sample indicated that SD2 received Slave River floodwaters. The isotopic composition of SD2 in May ($\delta^{18}O$ = -19.2‰, and $\delta^{2}H$ = -155‰) was however slightly more depleted than the isotopic composition of the Slave River ($\delta^{18}O$ = -19‰, and $\delta^{2}H$ = -151‰) likely due to the addition of even more isotopically-depleted snowmelt (**Figure 9 (a) and Figure 6 (b)**). Lake water samples plot below the LEL during the months of May, June and July and values indicate that the basin became more evaporatively enriched from May to July. The August samples plot on the LEL, indicating that the lake was influenced by an appreciable summer precipitation event. A total of 17 mm of rainfall was measured from August 1st to the date of the August sample collection on August 15, 2003 (Environment Canada, 2005). Results indicate that SD2 became much more isotopically depleted in September and October. Values plot above the LEL and closer to the LMWL and in the vicinity of summer precipitation (δ_{PS}) values, indicating the lake was influenced by thaw season precipitation (**Figure 9 (a)**). The September 4th sample ($\delta^{18}O$ = -16.3‰, and $\delta^{2}H$ = -136‰) and October 14th sample ($\delta^{18}O$ = - 16.5‰, and $\delta^{2}H$ = -133‰), which are essentially the same, are believed to be more depleted than August values due to the influence of a lake-effect

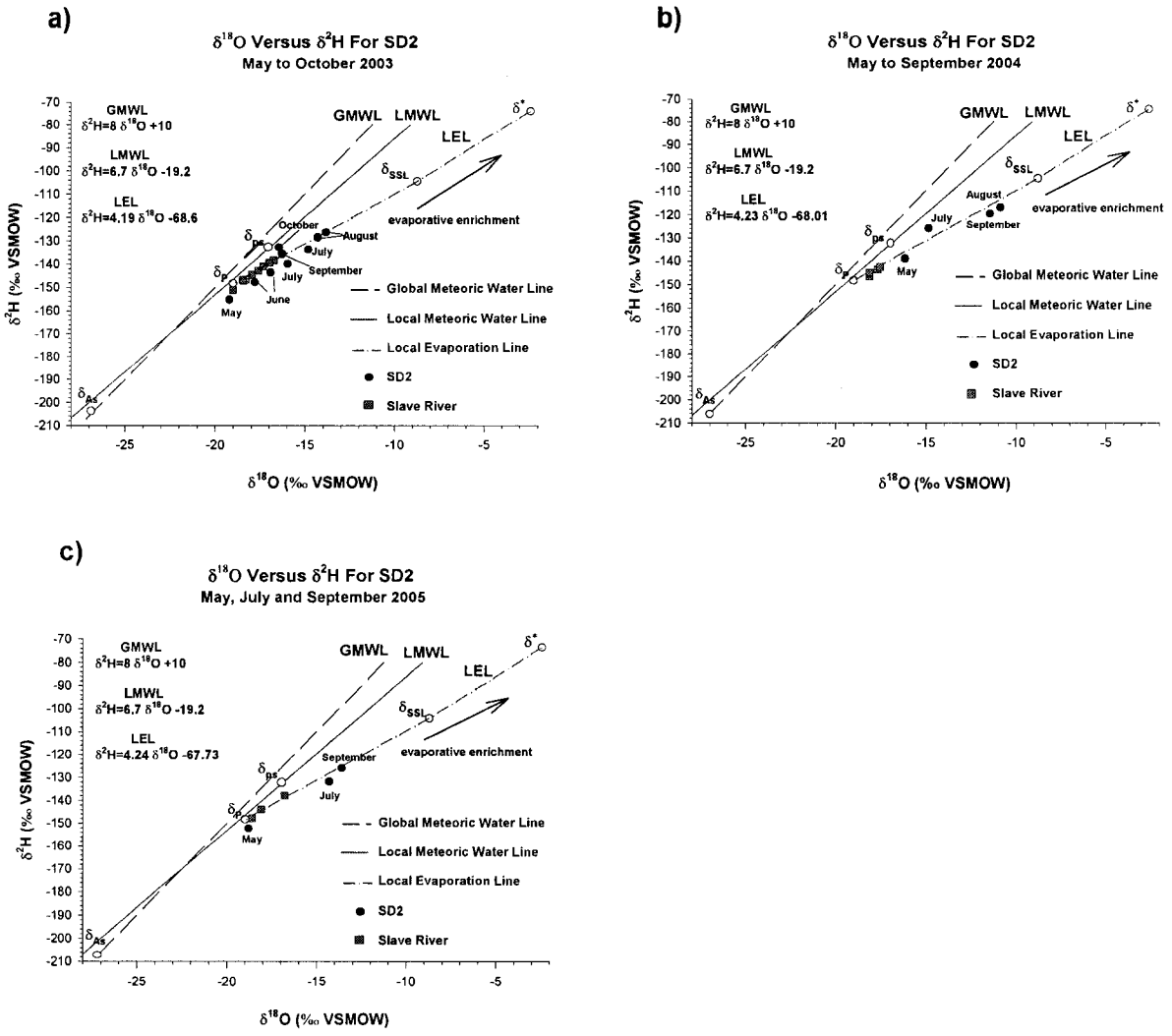

Figure 9. 2003 Isotope results from water samples collected from SD2 and the Slave River shown in $\delta^{18}O$-$\delta^{2}H$ space for May-October 2003 (a), May, July, August and September 2004 (b), and May, July, and September 2005 (c).

snowstorm generated by Great Slave Lake, which was reported by residents of Fort Resolution on September 1, 2003 (Brock et al., 2007). However, between September 1st and September 4th, 10.6 mm of rainfall was recorded, and from September 4th to October 14th a total of 40.2 mm of rain was recorded (Environment Canada, 2005), which suggests that the basin was influenced by a combination of thaw season precipitation and snowmelt during these months.

Lake water isotope results for the 2004 monitoring season plot slightly below and parallel to the LEL during the months of May, August and September, and above the LEL in July (**Figure 9 (b)**). Values for SD2 are more enriched than values for the Slave River during the 2004 monitoring season, which is attributed to the absence of flooding on the Slave River at the on-set of ice break-up. For example, in May the isotopic composition of SD2 was $\delta^{18}O$ = -16.2‰, and $\delta^{2}H$ = -139‰, whereas the isotopic composition of the Slave River was $\delta^{18}O$ = -17.7‰, and $\delta^{2}H$ = -144‰ (**Figure 9 (b)**). The May sample does however plot below the LEL indicating that snowmelt runoff or depleted precipitation did influence the basin (**Figure 6 (b)**). A total of 2 cm of snowfall was measured as well as 4 mm of rainfall in May (Environment Canada, 2005), which may also have influenced the isotopic composition of the lake. In contrast, the July ($\delta^{18}O$ = -14.8‰, and $\delta^{2}H$ = -126‰) sample plots above the LEL, indicating that local thaw season precipitation (shown as: δ_{PS} ($\delta^{18}O$ = -17‰, and $\delta^{2}H$ = -132‰) in **Figure 9 (b)**) influenced the basin. There is no independent precipitation data (i.e. from Environment Canada) available for July 2004 to support this idea; however, the trajectory of the July value is towards the thaw season precipitation value (δ_{PS}), which suggests that the July value reflects the influence of enriched thaw season

precipitation. The isotopic composition of SD2 in August ($\delta^{18}O$ = -10.8‰, and $\delta^{2}H$ = -117‰) was slightly more evaporatively enriched than in September ($\delta^{18}O$ = -11.5‰, and $\delta^{2}H$ = -120‰), which may likely be attributed to the influence of depleted precipitation input to the lake in September.

Results from isotope analysis of lake water samples collected from SD2 during the open-water season of 2005 for the months of May and July plot below and parallel to the LEL (**Figure 9 (c)**). At the beginning of ice-break-up in May 2005, a large amount of river sediment (approximately 5-10 cm deep) was observed throughout the catchment surrounding SD2 due to a large-scale flood event caused by an ice-jam on the Slave River. Similar to the May 2003 lake water sample, the May 2005 sample ($\delta^{18}O$ = -18.8‰, and $\delta^{2}H$ = -152‰) plots close to the isotopic composition of the Slave River ($\delta^{18}O$ = -18.6‰, and $\delta^{2}H$ = -148‰) indicating that river floodwaters entered the lake. However, the May 2005 value is slightly more depleted than the Slave River due to the additional influence of snowmelt runoff (**Figure 6 (b)**). The July 22nd sample ($\delta^{18}O$ = -14.3‰, and $\delta^{2}H$ = -132‰) plots just below the LEL and in the trajectory of δ_{SSL}. However, if a lake-specific LEL was used to assess this monitoring year, it is possible that this value would fall on the LEL indicating a trend towards evaporative enrichment. The September 22nd sample ($\delta^{18}O$ = -13.6‰, and $\delta^{2}H$ = -126‰) is more enriched than the May and July samples and plots the closest to the LEL. If the slope of the LEL were to decrease, the September composition may have plotted above the LEL, which would reflect the influence of thaw season precipitation. This may be reasonable to suggest, as 47.2 mm of precipitation was recorded during the month of August, and an additional 22 mm was recorded from September 1st to

September 22nd (Environment Canada, 2005), which would cause the September value to be offset from where the July value plots.

It is recognized that the calculated LEL for 2003, 2004 and 2005 is based on conservative estimates of δ_p, and so the location of SD2 values in relation to the calculated LELs used to assess the modern hydrology of the lake introduces a degree of uncertainty to interpretations. However, it is evident that the isotopic composition of SD2 was essentially the same as the Slave River after the May 2003 and 2005 flood events, as discussed above. Additionally, the composition of SD2 in May of 2003 and 2005 were very similar to one another (May 2003; $\delta^{18}O$ = -19.2‰, and $\delta^{2}H$ = -155‰ and May 2005; $\delta^{18}O$ = -18.5‰, and $\delta^{2}H$ = -152‰). In contrast, in the absence of flooding on the river and river water input into the basin, as in 2004, the isotopic composition of SD2 is controlled predominantly by precipitation. For example, the May 2004 value for SD2 ($\delta^{18}O$ = -16.2‰, $\delta^{2}H$ = -139‰) was not essentially the same as the Slave River ($\delta^{18}O$ = -17.7‰, and $\delta^{2}H$ = -144‰), nor was it similar to the Slave River and SD2 May 2003 and 2005 values. These findings strongly indicate that river floodwaters and seasonal precipitation are the important processes controlling the input of water to SD2.

3.4 SD28 Exchange-dominated Basin

Results from the isotope analysis of lake water samples collected from SD28 during the open-water season of 2003 are strongly constrained along the LEL (**Figure 10 (a)**). As noted in section *3.2* and *3.3*, the calculated LEL for 2003, 2004 and 2005 is based on

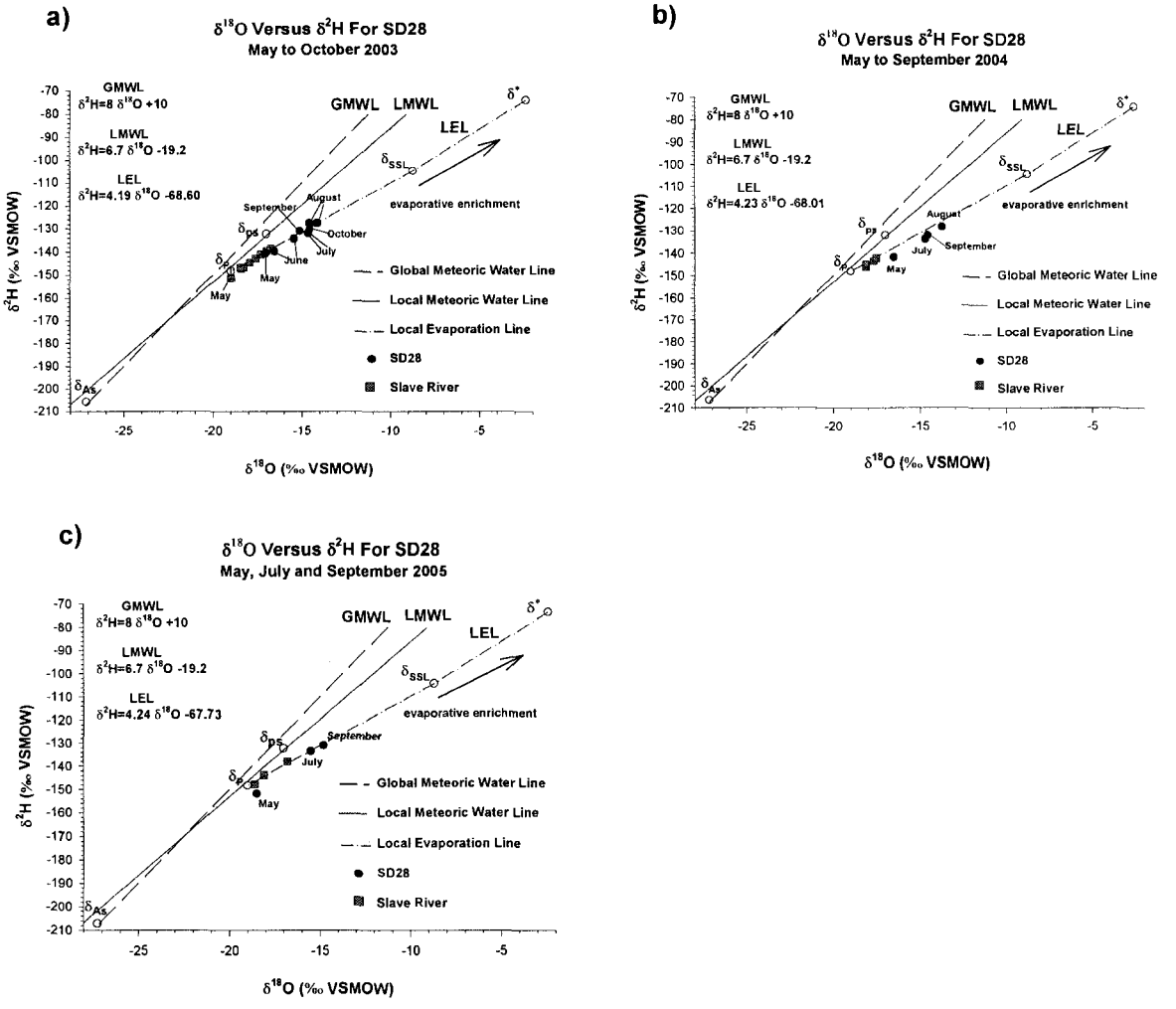

Figure 10. Isotope results from water samples collected from SD28 and the Slave River shown in $\delta^{18}O$-$\delta^{2}H$ space for May-October 2003 (a), May, July, August and September 2004(b), and May, July and September 2005 (c).

conservative estimates of δ_p, and so the location of SD28 values in relation to the calculated LELs used to assess the modern hydrology of the lake introduces a degree of uncertainty to the interpretations. Values from SD28 indicate that the lake is more enriched than the Slave River during the entire 2003 monitoring year. For example, in May the lake water isotopic composition of SD28 was $\delta^{18}O$ = -17‰, and $\delta^{2}H$ = -141‰, whereas the isotopic composition of the Slave River was $\delta^{18}O$ = -19‰, and $\delta^{2}H$ = -151‰. SD28 was less influenced by Slave River floodwaters in May than SD2 and other exchange-dominated basins in the delta, which is probably a result of the spatial distribution of flooding as well as the length and depth of the channel that connects SD28 to the Slave River (Brock et al., 2007) (**Figure 10 (a)**). Two samples were taken from SD28 in each of June, July and August. The June 10th sample ($\delta^{18}O$ = -17‰, and $\delta^{2}H$ = -140‰) is slightly more depleted than the June 23rd sample ($\delta^{18}O$ = -15.4‰, and $\delta^{2}H$ = -135‰), suggesting that the basin became progressively more evaporatively enriched. Additionally, samples taken in July (July 6th, $\delta^{18}O$ = -14.7‰, and $\delta^{2}H$ = -132‰ and July 25th, $\delta^{18}O$ = -14.6‰, and $\delta^{2}H$ = -130‰) and in August (August 2nd, $\delta^{18}O$ = -14.6‰, and $\delta^{2}H$ = -128‰ and August 15th, $\delta^{18}O$ = -14.1‰, and $\delta^{2}H$ = -128‰) indicate that the trend towards evaporative enrichment continued into the summer. The September 4th sample ($\delta^{18}O$ = -15.1‰, and $\delta^{2}H$ = -131‰), however, interrupts this trend, as it plots above the LEL and towards the δ_{PS} value, and is more depleted than samples taken on August 2nd and August 15th. Similar to SD2, this is thought to be attributed solely to a lake-effect snowstorm that occurred on September 1st. However, a total of 58.4 mm of rainfall was measured in August 2003, 38.2 mm of which fell on August 24, 2003 just 11 days prior to the September 4th sample being taken, and in the

month of September a total of 10.6 mm of rainfall was recorded by the 4th (Environment Canada, 2005). This indicates that the September sample was influenced by thaw season precipitation, and/or possibly exchanged water with the SR, as the trajectory of the September sample is towards the SR value (**Figure 10 (a)**). In October, the isotopic composition of the lake ($\delta^{18}O$ = -14.2‰ and $\delta^{2}H$ = -128‰) becomes slightly more enriched than it was in September and plots to the right of the September sample, returning to the previous trajectory of summer compositions (**Figure 10 (a)**).

Isotopic composition values for SD28 for the 2004 monitoring season plot just below and parallel to the LEL (**Figure 10 (b)**). The Slave River did not flood during 2004, which is reflected in the results for SD28, as the lake was more evaporatively enriched at the onset of ice break-up in May ($\delta^{18}O$ = -16.5‰, and $\delta^{2}H$ = -142‰) in comparison to the Slave River ($\delta^{18}O$ = -17.7‰, and $\delta^{2}H$ = -144‰) (**Figure 10 (b)**). The May sample does however plot below the LEL, which may be due to the influence of snowmelt runoff (**Figure 6 (b)**). By July ($\delta^{18}O$ = -14.7‰, and $\delta^{2}H$ = -134‰), SD28 is even more enriched in comparison to the Slave River ($\delta^{18}O$ = -18.1‰, and $\delta^{2}H$ = -146‰). This could either indicate that there was little to no river water input to the lake during this month, or it could be due to the fact that SD28 was offset by evaporative enrichment in comparison to the SR from the beginning of the 2004 sampling season. In August ($\delta^{18}O$ = -13.7‰, and $\delta^{2}H$ = -128‰), the lake is more evaporatively enriched in comparison to July. The August composition plots closer to the LEL than the May and July samples, suggesting that evaporation is controlling the basin's water balance during this month. The September composition ($\delta^{18}O$ = -14.6‰, and $\delta^{2}H$ = -132‰) is more isotopically depleted than the

August composition. However, it is more isotopically enriched than the Slave River September composition ($\delta^{18}O$ = -18.1‰, and $\delta^{2}H$ = -145‰). This shift from an isotopically enriched value in August to a more isotopically depleted value in September may be due to input from the Slave River via the channel connection between SD28 and the river, as the trajectory of the September composition relative to the August composition supports this notion (**Figure 10 (b)**).

Results for 2005 indicate that SD28 was influenced by Slave River flood water and snowmelt influence at the onset of ice break-up, as the value for this time period plots below the LEL and is more depleted than the isotopic composition of the river (**Figure 10 (c)**). Values for the rest of the 2005 monitoring year plot on the LEL indicating evaporation was influencing the lake water balance during these months. Similar to SD2, SD28 was inundated by the Slave River during the large-scale flood event at the onset of ice-break-up in May of 2005. The lake water isotopic composition of SD28 was $\delta^{18}O$ = -18.5‰, and $\delta^{2}H$ = -152‰ in May, whereas the isotopic composition of the Slave River was $\delta^{18}O$ = -18.6‰, and $\delta^{2}H$ = -148‰, which is indicative of river floodwater and isotopically depleted snowmelt runoff influence (**Figures 6 (b) and 10 (c)**). Lake water samples for July 2005 ($\delta^{18}O$ = -15.5‰, and $\delta^{2}H$ = -134‰) and September 2005 ($\delta^{18}O$ = -14.8‰, and $\delta^{2}H$ = -131‰) plot along the LEL and are more enriched, indicating that evaporation influenced the water balance of the basin during these two months (**Figure 10 (c)**).

Additionally, it was observed during fieldwork and from viewing seasonal and annual photographs of SD28 over the course of the ice-off period from spring to fall from 2003 to 2005, that water levels in SD28 were at their maximum in the spring and at their minimum in

the summer. It is apparent that the channel connecting SD28 to the Slave River becomes flooded during spring melt periods and lake and river water freely exchange where the channel meets the basin (at the channel/basin mouth). As summer progresses, the channel becomes more narrow and constricted, and water levels decrease substantially. This narrowing is especially evident at the channel/basin mouth, as it is here where the channel becomes constricted by a thick growth of *Equisetum* and the channel becomes somewhat disconnected from the basin, making boat access to the basin via the channel very difficult (**Figure 5**). Turbidity differences between the basin and the channel were observed in July and August 2003, and July and September 2004 during times of very low water levels in the channel/basin mouth. It was apparent that river water was entering the channel at the channel/river mouth, but river water was not entering the basin due to the thick *Equisetum* growth and very low water levels in the channel at the channel/basin mouth. In the fall, the *Equisetum* dies back, re-opening the connection.

Lake water isotopic compositions of SD28 for 2003, a flood year, and 2004, a non-flood year, during the months of May (2003; $\delta^{18}O$ = -17‰, and $\delta^{2}H$ = -141‰, and 2004; $\delta^{18}O$ = -16.5‰, and $\delta^{2}H$ = -142‰), July (2003; $\delta^{18}O$ = ~ -14.7‰, and $\delta^{2}H$ = ~ -132‰ and 2004; $\delta^{18}O$ = -14.7‰, and $\delta^{2}H$ = -134‰), August (2003; $\delta^{18}O$ = ~ -14.1‰, and $\delta^{2}H$ = ~ -128‰, and 2004; $\delta^{18}O$ = -13.7‰, and $\delta^{2}H$ = -128‰) and September (2003; $\delta^{18}O$ = -15.1‰, and $\delta^{2}H$ = -131‰, and 2004; $\delta^{18}O$ = -14.6‰, and $\delta^{2}H$ = -132‰) are very similar. In contrast to SD2, the isotopic compositions of SD28 and the Slave River in May 2003 are not similar. However, isotopic compositions of SD28 ($\delta^{18}O$ = -18.5‰, and $\delta^{2}H$ = -152‰), SD2 ($\delta^{18}O$ = -18.5‰, and $\delta^{2}H$ = -152‰) and the Slave River ($\delta^{18}O$ = -18.6‰, and $\delta^{2}H$ =

-148‰) after the May 2005 flood event were essentially the same. The May 2005 flood event was of larger scale in comparison to the May 2003 flood event. Findings suggest that river water input most strongly influences SD28 under conditions such as larger scale flood events. Additionally, findings indicate that river water influence on lake water composition of SD28 is controlled by the length and depth of the basin's channel connection to the river.

3.5 PALEOLIMNOLOGY

3.5.1 SD20 KB-1 Sediment Core Chronology

Total ^{210}Pb activity for SD20 KB-1 generally declines exponentially (**Figure 11 (a)**). Supported ^{210}Pb (^{214}Bi) levels (0.021 Bq/g) are estimated to be reached at approximately 18.25 cm midpoint depth (0.021 Bq/g) resulting in a basal Constant Rate of Supply (CRS) ^{210}Pb date of ~ 1884 at this sediment horizon (**Figures 11 (a) and 12 (a)**). The mean sampling resolution for SD20 KB-5 from 0-18.50 cm is 3.3 years, which is a longer time interval, for example, than the mean sampling resolution for the SD2 KB-5 and SD28 KB-5 sediment cores (see sections 3.5.3 and 3.5.5), indicating that the sedimentation rate at this basin is relatively slow.

CRS dates for samples from 0 to 16.50 cm depth were calculated using the values of samples that were measured in the gamma spectrometer with outliers removed (2.75 cm, 9.75 cm, 12.75 cm, 13.75 cm, 14.75 cm, and 15.75 cm midpoint depths) and values interpolated for samples that were not analysed in the gamma spectrometer (**Figure 11 (a)**). Dates from 16.75 cm to the bottom of the sediment core were extrapolated using an average

sedimentation rate (0.057 g/cm^2/year), which was calculated from sediment increments 15.25 cm (0.069 g/cm^2/yr), 15.75 cm (0.062 g/cm^2/yr), and 16.25 cm (0.039 g/cm^2/yr) midpoint depths. This resulted in a basal date of 1788 for the bottom of the sediment core (27.25 cm depth) (**Figure 12 (b)**). Dates were extrapolated from 16.25 cm depth to the bottom of the core and not from 18.50 cm where supported levels of ^{210}Pb were estimated to be reached, as calculated CRS dates for samples from 16.75 cm to 18.25 cm spanned relatively large time intervals (~ 10-20 years) that ware likely overestimated and thus they were determined to be less reliable.

There is no evidence of a well defined ^{137}Cs peak in the SD20 KB-1 sediment core. Small peaks occur in the ^{137}Cs profile at 1.25 cm, 2.25 cm, 4.25 cm, 5.25 cm and 7.75 cm midpoint depths, after which the ^{137}Cs profile declines from 0.01 to 0.001 Bq/g to the bottom of the core (**Figure 11 (b)**). A complacent ^{137}Cs profile in the top portion of the sediment core (0-6 cm for SD20 KB-1) such as this is likely indicative of ^{137}Cs mobility. ^{137}Cs mobility occurs more frequently in organic rich sediments (Longmore, 1982; Foster et al., 2006), consistent with the LOI (at 550°C) results of the uppermost sediment extracted from SD20 KB-1 (see **Figure 11 (b) and 13 (c)**).

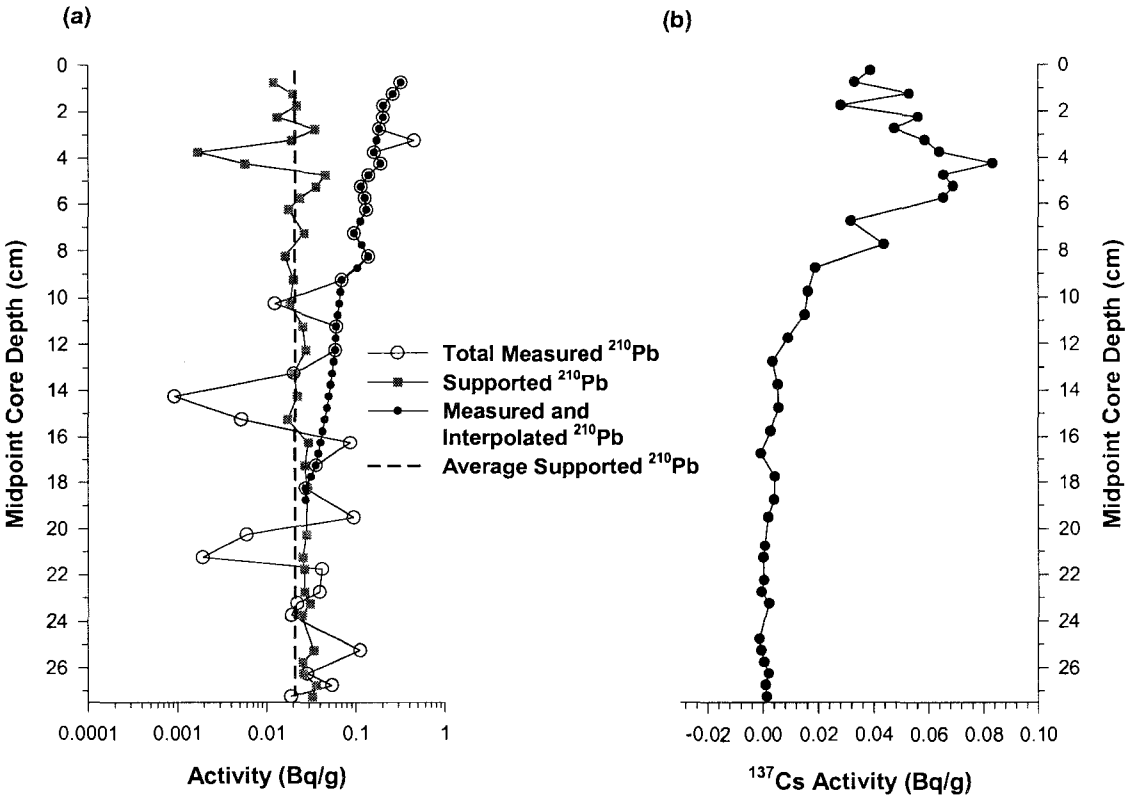

Figure 11. (a) Total and supported ^{210}Pb, and (b) ^{137}Cs activity profiles for SD20 KB-1. 'Total Measured ^{210}Pb' profile represents activity values measured in samples analysed in the gamma spectrometer. 'Measured and Interpolated ^{210}Pb ' profile is based on 'Total Measured ^{210}Pb' with outliers removed (removed outliers are: 2.75 cm, 9.75 cm, 12.75 cm, 13.75 cm, 14.75 cm and 15.75 cm mid point depths) and values interpolated for samples that were not analysed in the gamma spectrometer. Background supported ^{210}Pb is 0.021 Bq/g based on average ^{214}Bi values. Supported ^{210}Pb is estimated to be reached at 18.25 cm depth (0.021 Bq/g).

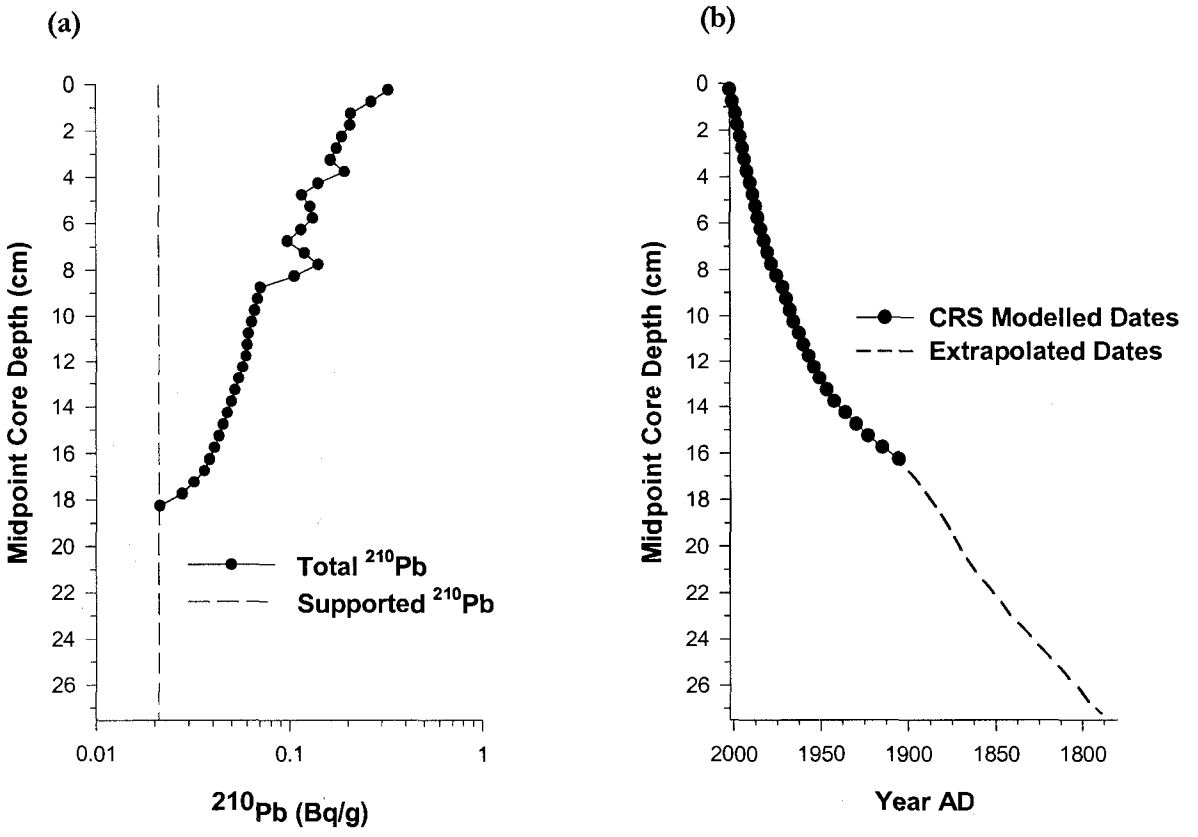

Figure 12. (a) Total ^{210}Pb activity (includes measured and interpolated ^{210}Pb) and average background levels of supported ^{210}Pb (^{214}Bi) versus depth for SD20 KB-1 and (b) SD 20 KB-1 sediment core chronology based on the Constant Rate of Supply model, extrapolated down core using an average sedimentation rate of 0.057 g/cm^2/yr.

3.5.2 SD20 KB-1 Cellulose Inferred Lake Water Oxygen Isotope Stratigraphy

Sediment core results show that cellulose-inferred lake water $\delta^{18}O$ ($\delta^{18}O_{lw}$) values have varied from -18 to -8 ‰ indicating a broad range of hydrological variability characterized SD20 over the past ~215 years (**Figure 13 (a)**). Inferred $\delta^{18}O_{lw}$ values in the top portion of the sediment core range from -14.4 to -9.1 ‰, which are in excellent agreement with measured lake water $\delta^{18}O$ values from 2003-2005 (-13.8 to -10.4 ‰). Reconstructed $\delta^{18}O_{lw}$ values indicate periods when evaporation, as well as when inflow, was the dominant control on the water balance of SD20 (**Figure 13 (a)**). Floods from the Slave River may have also periodically influenced the basin; however, they would have had to be of very high magnitude in order to have influenced the water balance of SD20. For example, it is possible that a large flood event occurred on the SRD in 1974, as has been documented in the Peace Athabasca Delta (PAD) (Pietroniro et al., 1999). If this flood reached SD20 it could account for the very low cellulose-inferred $\delta^{18}O_{lw}$ value at ~1984 (-17.5 ‰), which is similar to modern Slave River $\delta^{18}O$ values (2003-2005 range is from ~-19 to –16.8 ‰). Fluctuations in geochemical proxies at ~1984 support this notion (**Figure 13 (a) to (h)**). However, if the ~1984 value does represent river water dilution of the lake from the 1974 flood, then this would mean that the chronology of the SD20 KB-5 sediment core is off by ~10 years at this stratigraphic horizon. With the exception of the ~1984 value, it is also reasonable to suggest that more depleted values in the $\delta^{18}O_{lw}$ record are due to the influence of large-scale snowmelt runoff, or summer precipitation events. Modern lake water $\delta^{18}O$ measurements from 2003 to 2005 help to support this interpretation, as modern measurements show that the water balance of SD20 is driven primarily by evaporative loss

and local precipitation dilution and that during times of high-magnitude floods such as those in 2003 and 2005, the basin is not influenced by Slave River flood waters. Analysis of the $\delta^{18}O_{lw}$ record for SD20 suggest that changes and/or fluctuations in lake water balance are predominantly controlled by local hydroclimatic factors such as snowmelt inputs, thaw season precipitation, and surface water evaporation, perhaps with the exception of a large flood in 1974.

Four zones were defined in the geochemical stratigraphic profiles for SD20. Zones are based primarily on stratigraphic changes in the cellulose-inferred $\delta^{18}O_{lw}$ record. Zone one spans from ~1788 to ~1801, zone two spans from ~1802 to ~1905, zone three spans from ~ 1906 to ~1971 and zone four spans from ~1972 to ~2002.

In zone one, during the late 1700s, $\delta^{18}O_{lw}$ values range from -11.2 to -10.2 ‰ documenting a period when the basin was dominated by evaporation, while trends to overall lower $\delta^{18}O_{lw}$ values in zone two during the 1800s (ranging from -14.1 to -9.2 ‰) suggest a shift to wetter conditions. $\delta^{18}O_{lw}$ values during the 1900s in zones three (ranging from -16.1 to -10.3‰) and four (ranging from -17.5 to -9.1 ‰) and are much more variable in comparison to the late 1700s and 1800s. Distinct periods of wetter conditions in zone three include ~1914 (-14.2 ‰), from ~1936 to ~1942 (range from -16.1 to -14.4 ‰), ~1962 to ~1967 (range from -14.9 to -14.2 ‰), and in zone four from ~1982 to 1989 (range from -17.5 to -15.6 ‰). In contrast, there are several brief excursions where the basin shows strong evaporative enrichment trends during the 1900s, such as in zone three at ~1946 (-10.3 ‰), ~1954 (-11.8 ‰), ~1969 (-12 ‰), and in zone four in 2002 (-9.1 ‰) (**Figure 13 (a)**).

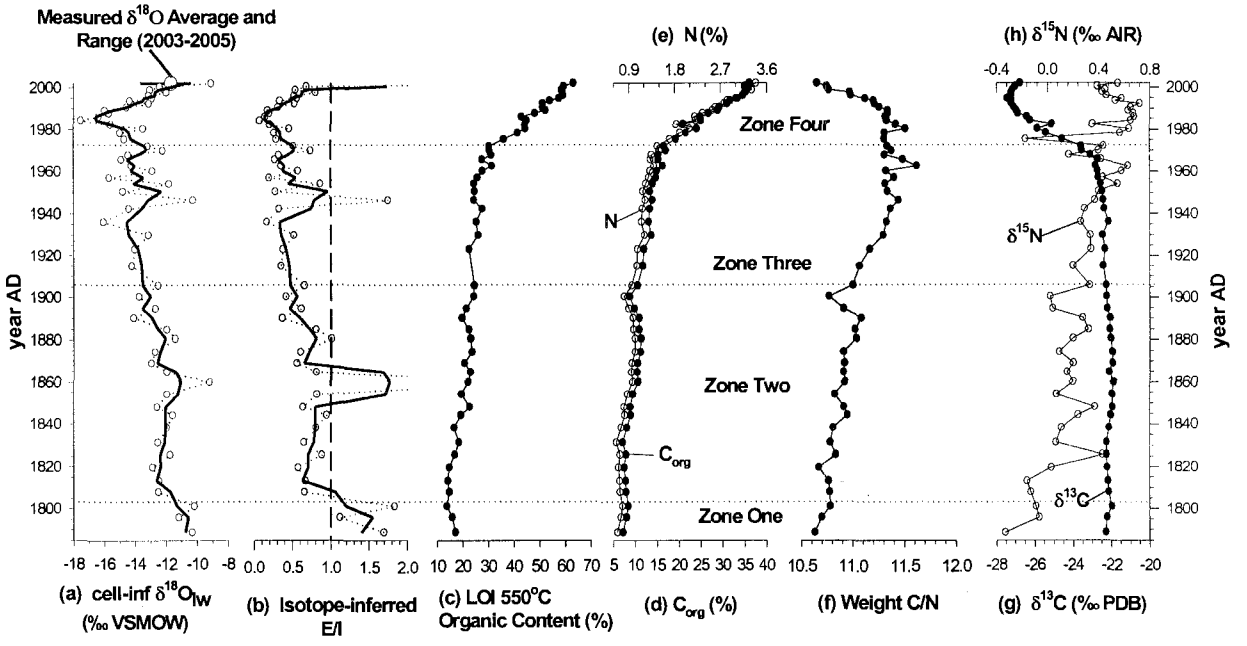

Figure 13. SD20 KB-1 Geochemical Stratigraphy. (a) An ~215 year lake water $\delta^{18}O$ history for SD20 inferred from oxygen isotope analysis of aquatic plant cellulose extracted from the SD20 KB-1 sediment core. Raw data (open circles) and smoothed (three-point running mean represented by solid black line) profiles are shown. The range and average lake water $\delta^{18}O$ composition measured from lake water samples taken during sampling seasons in 2003-2005 are also shown. (b) Isotope-inferred evaporation-to-inflow (E/I) ratios were estimated using the cellulose-inferred lake water $\delta^{18}O$ record and an isotope-mass balance model (raw data are represented by open circles, and the three-point running mean is represented by solid line) using a *h* value of 69.2% (Hay River 30-year climate normal) assuming steady-state evaporative enrichment fed by source waters of constant isotopic composition. Other geochemical stratigraphic profiles include: organic content estimated from loss-on-ignition (c), organic carbon content (d), nitrogen content (e), weight C/N ratios (f), bulk organic $\delta^{13}C$ (g) and $\delta^{15}N$ (h). Zones are primarily based on stratigraphic changes in the cellulose-inferred $\delta^{18}O_{lw}$ record.

3.5.3 SD20 KB-1 Lake Water Balance Reconstruction

Quantifying the cellulose-inferred lake water $\delta^{18}O$ record of SD20 KB-1 is possible assuming that water balance is the predominant signal captured in the lake sediments, evaporative enrichment in the basin has occurred under conditions of hydrologic steady-state and that δ_I is constant. In order to quantify evaporation/inflow (E/I) values for SD20, modern evaporation-flux-weighted *h* (69.2%), $\delta_I = \delta_P$ (-19 ‰) and δ_A (-29.28 ‰) based on Hay River 30-year Climate Normals (Environment Canada, 2004), CNIP amount weighted seasonal precipitation composition, and *T* (13.4°C) based on air water interface temperature, were used in equation (11) (see Chapter 2, section 2.3 Water Balance Reconstruction).

Evaporation-to-inflow ratios (E/I) for SD20 show that E/I < 1 (positive steady-state water balance) for the most part dominated zones two, three and four, from years ~1807 to ~1990. The lowest value occurs at ~1984 (E/I = 0.07) when the basin was dominated by a very strong positive water balance (**Figure 13 (b)**). As discussed above, if the chronology for SD20 is underestimated, then year ~1984 may be year 1974. This would imply that the E/I value (0.07) for this time period reflects river flood water input to the lake (**Figure 13 (b)**). Periods of strong negative water balance (E/I>1) are evident in zone one from ~1788 to ~1801 (E/I ranges from 1.1 to 1.8), in zone two from ~1854 to ~1864 (E/I ranges from 0.8 to 3.7), and in zone three at ~1946 (E/I = 1.7) indicating evaporation dominated the water balance during these time periods (**Figure 13 (b)**). In zone four, a negative water balance is evident, however, because these samples are from the uppermost portion of the sediment core (0-1.75 cm), they may in fact reflect summer evaporation over a short period of time.

3.5.4 SD20 KB-1 Carbon and Nitrogen Elemental and Stable Isotope Stratigraphy

C/N ratios indicate low values throughout all zones, ranging from 10.63 to 11.62 from ~1788 to 2002 and are characteristic of organic matter that is of aquatic origin (Meyers et al., 2001). In zone one during the late 1700s, bulk organic carbon (C_{org}) and nitrogen (N), C/N ratios, organic carbon isotope ($\delta^{13}C$) and nitrogen isotope ($\delta^{15}N$) values are relatively stable and coincide with high inferred E/I. Organic content ranges from 13.8 to 17.2 %, C/N ranges from 10.6 to 10.8, C_{org} ranges from 7.2 to 8.4 %, N ranges from 0.68 to 0.78 %, $\delta^{13}C$ ranges from -22.3 to -22.0 ‰, and $\delta^{15}N$ ranges from -0.3 to -0.1‰. Values for these geochemical analyses are relatively lower in this zone in comparison to the other three zones, indicating that there is very little change in organic content during this time period.

Zone two (from ~1807 to ~1905), shows an increase in organic content (%) (ranging from 14.2 to 24.6 %), a slight increase in C/N (ranging from 10.7 to 11.1), C_{org} (%) (ranging from 7.1 to 11.3 %), N (%) (ranging from 0.7 to 1.0 %), and $\delta^{15}N$ (ranging from -0.2 to 0.4‰), and no change in $\delta^{13}C$ (ranging from -22.3 to -22.0 ‰) in comparison to zone one (**Figure 13 (c), (d), (e), (f), (g), and (h)**). All geochemical analyses for this time period suggest that productivity levels in the lake increased slightly in comparison to the late 1700s, which corresponds with a shift towards declining E/I ratios.

In zone three, which spans from ~1914 to ~1971, there is an increase in organic content (%) (ranging from 22.6 to 31.5 %), a slight increase in C/N (ranging from 11.1 to 11.6) and $\delta^{15}N$ (ranging from 0.2 to 0.6 ‰), a large increase in C_{org} (%) (ranging from 11.7 to 17.0 %) and N (%) (ranging from 1.1 to 1.5 %), and a slight decline in $\delta^{13}C$ (ranging from -23.6 to -22.2 ‰) in comparison to zone two (**Figure 13 (c), (d), (e), (f), (g), and (h)**). During

this time period the water balance of SD20 shows an increase in hydrological vaiability. However, E/I ratios indicate that the general trend of the water balance in zone three is towards a declining E/I in comparison to zone two. This may suggest that an increase in lake productivity is associated with overall wetter conditions.

$\delta^{13}C$ sharply declines in zone four, which spans from ~1975 to 2002, with values ranging from -27.5 to -24.6 ‰ (**Figure 13 (g)**). Conversely, organic content (%) sharply increases, and doubles in zone four in comparison to zone three, ranging from 36.2 to 63.2 % (**Figure 13 (c)**). There is also an increase in C_{org} (%) (ranging from 19.3 to 36.1 %) and N (%) (ranging from 1.7 to 3.4 %) and $\delta^{15}N$ (ranging from -0.2 to 0.7 ‰), and a slight decrease in C/N ratios in zone four (ranging from 10.7 to 11.5) (**Figure 13 (d), (e), (f), and (h)**), which may be indicative of a substantive increase in lake productivity. E/I ratios for this time period again document a declining E/I up until ~1994.

3.5.5 SD2 KB-5 Sediment Core Chronology

Results from ^{210}Pb of the SD2 KB-5 sediment core show that ^{210}Pb activity does not decline exponentially with depth and that the profile displays a large amount of variability (**Figure 14**). ^{137}Cs analysis indicates that a peak (0.0207 Bq/g) occurs at 25.25 cm midpoint core depth (**Figure 14**). A ^{137}Cs peak occurs at approximately the same depth (26.75 cm midpoint core depth) in another core taken from SD2 in August of 2003 (SD2 KB-3; Jermyn, 2004), validating the ^{137}Cs peak found in SD2 KB-5 at 25.25 cm and confirming that ^{137}Cs mobility has likely not occurred (Jermyn, 2004). Additionally, Jermyn (2004) and Liu (2004) reported that SD2 had a high sedimentation rate and that clays and silt were found

throughout the SD2 KB-3 sediment core, which is consistent with the SD2 KB-5 core. ^{137}Cs is more likely to be preserved in basins with high sedimentation rates such as SD2, whereas it can be mobile in organic-rich sediments, or sediments that do not contain many clays and have large particle sizes (Longmore, 1982; Foster et al., 2006).

The depth at which the measured ^{137}Cs peak occurs in the SD2 KB-5 core is assumed to represent the year 1963 based on known ^{137}Cs fallout rates (Appleby, 2001). A linear constant sedimentation rate of 0.616 g/cm^2/year was used to calculate dates for all sediment intervals with the exception of 0-0.5 cm and 25.25 cm by:

$$CSR = 25.25 \text{ cm} / (2004 - 1963) \quad (12)$$

where 25.25 cm is the depth at which the ^{137}Cs peak occurs, 2004 is the year the sediment core was extracted and 1963 is the year that the ^{137}Cs peak is assumed to represent.

The mean sampling resolution for the SD2 KB-5 core is 0.8 years from 0-49 cm, resulting in an estimated date of ~1925 at the base of the core. The short mean sampling resolution of 0.8 years is a function of high sedimentation rates.

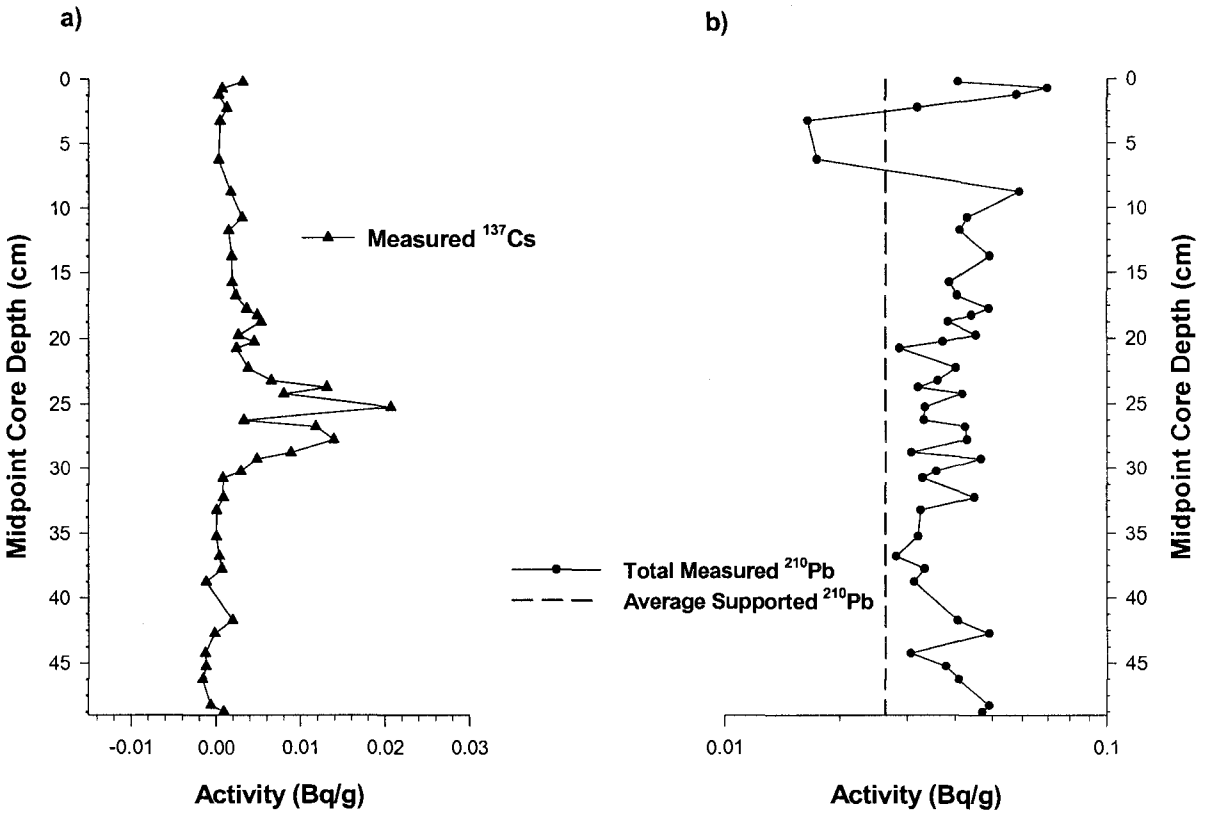

Figure 14. (a) ^{137}Cs, and (b) total and supported ^{210}Pb activity profiles for SD2 KB-5. A ^{137}Cs peak (0.0207 Bq/g) occurs at 25.25 cm depth interpreted to represent 1963. The 'Total Measured Pb-210 series' represents activity values measured in all samples analysed in the gamma spectrometer. Average supported ^{210}Pb (^{214}Bi) (0.026 Bq/g) is also shown.

3.5.6 SD2 KB-5 Geochemical Stratigraphy

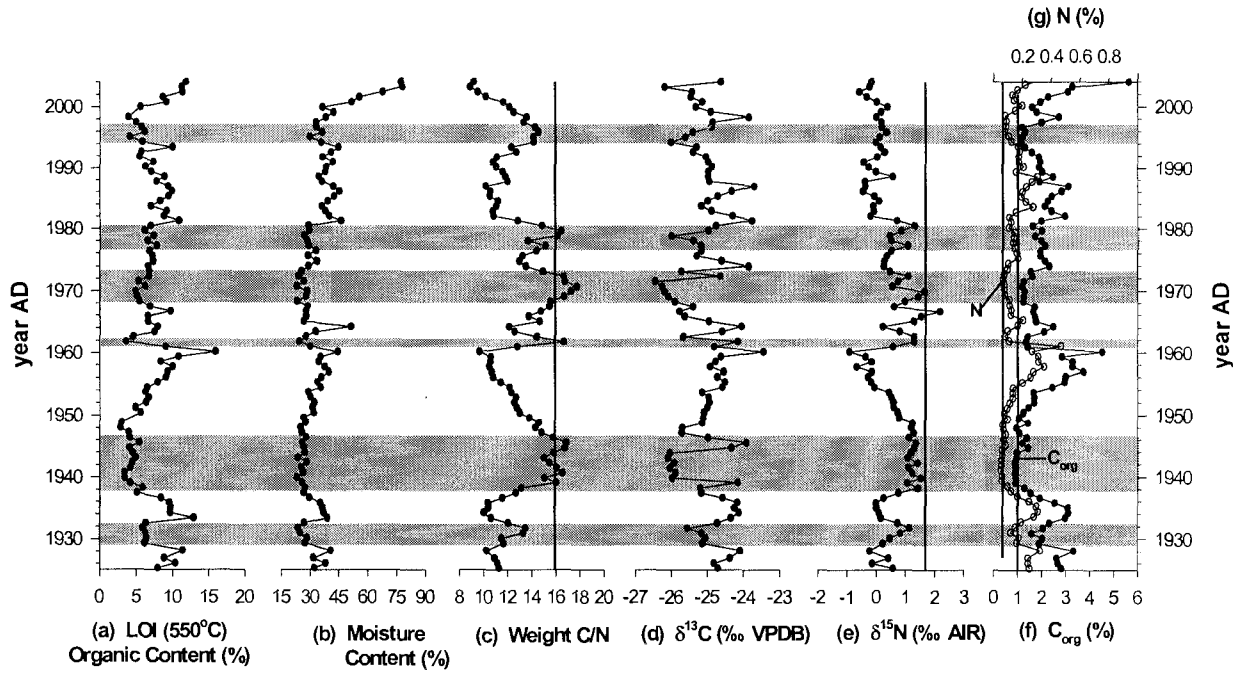

Figure 15. Geochemical stratigraphic records for SD2 KB-5. (a) Organic content estimated from loss-on-ignition at 550°C, (b) moisture content (LOI at 90°C), (c) weight C/N ratios, (d) bulk organic $\delta^{13}C$, (e) $\delta^{15}N$, (f) organic carbon content and (g) nitrogen content. The grey highlighted areas indicate periods of lower organic content, moisture content and $\delta^{13}C$ and higher weight C/N and $\delta^{15}N$ values, which are interpreted to reflect periods of increased Slave River floodwater influence. Vertical solid lines represent analytical results for a flood deposit sampled from the catchment of SD2 following the 2005 ice jam flood.

Organic and moisture content (%), bulk organic C_{org} (%) and nitrogen (%) content, C/N ratios, and organic carbon and nitrogen isotope (‰) stratigraphies for SD2 are variable over the last century (**Figure 15 (a) to (g)**). A sediment sample was taken onshore at SD2 days after the May 2005 large-scale flood event on the Slave River. Very good agreement exists where all geochemical stratigraphies for the SD2 KB-5 core are thought to be influenced by Slave River flood waters (grey bands highlighted in **Figure 15 (a) to (g)**) and measured C/N, $\delta^{13}C$, $\delta^{15}N$, C_{org} and N values of the May 2005 sediment sample taken onshore at SD2 after the May 2005 large-scale flood event (vertical lines in **Figure 15 (c), (d) and (e)**). This lends support to hypothesized periods of Slave River flood influence at the basin. C/N ratios for the SD2 KB-5 record range from 8.90 to 17.75, which is a much larger range in comparison to the range in C/N ratios for SD20 (10.63 to 11.62). Values of 10 or lower are characteristic of organic matter that is of aquatic origin (Meyers et al., 2001). C/N ratios of 11 to 20 are still considered to be characteristic of organic matter that is predominately aquatic in origin; however, it is acknowledged that lakes with C/N ratios greater than 10 are typically influenced by inputs of vascular land plants (Meyers et al., 2001). It is also possible that C/N ratios higher than ~10 may reflect N deficiency within a lake (Hecky et al., 1993). If nitrogen becomes limiting within a lake, C/N ratios can increase due to the sensitivity of algae and zooplankton to nitrogen limitation (Brahney et al., 2006). Dead algal material and zooplankton fecal matter contribute to sediment organic matter in a lake. If nitrogen is limiting in a lake, algae discrimination against uptake of ^{15}N decreases, eventually resulting in an increase in $\delta^{15}N$ uptake by grazing zooplankton (Brahney et al., 2006). $\delta^{15}N$ enriched zooplankton fecal matter is then deposited in lake sediments thus elevating C/N ratios of sediment organic material (Brahney et al., 2006). It is unlikely that N

limitation is the reason for higher C/N ratio values in the KB-5 sediment record, as higher C/N values are similar to measured C/N and $\delta^{15}N$ values of the May 2005 flood deposit sediment sample.

Six periods of Slave River flood influence have been identified in geochemical records of the SD2 KB-5 core. During each of the identified flood periods there is a decrease in organic content, moisture content, $C_{org,}$ N, and $\delta^{13}C$, and an increase in C/N ratios and $\delta^{15}N$, which are changes consistent with input of flood waters from the Slave River containing high loads of suspended inorganic sediment such as fine silt and sand (grey bands highlighted in **Figure 15 (a) to (g)**). In contrast, during suspected periods of less river influence, increases in organic content, moisture content, $C_{org,}$ N, and $\delta^{13}C$ and decreases in C/N ratios, and $\delta^{15}N$ occur (white bands highlighted in **Figure 15 (a) to (g)**).

The first river influence period occurs from ~1929 to ~1932. Organic content (ranging from 6.18 to 6.46 %), moisture content (ranging from 23.8 to 28.6 %), C_{org} (ranging from 1.6 to 2.3 %), N (ranging from 0.1 to 0.2 %) and $\delta^{13}C$ (ranging from -25.1 to -24.7 ‰) are low, whereas C/N ratios (ranging from 11.5 to 13.5) and $\delta^{15}N$ (ranging from 0.2 to 0.8 ‰) are high. However, values for these geochemical indicators do not measure as high as C/N (15.9) and $\delta^{15}N$ (1.7 ‰) values, or as low as C_{org} (1.01 %) and N (0.06 %) measured in the flood deposit sample taken following the 2005 ice jam flood on the Slave River (**Figure 15 (a) to (g)**).

The second river influence period, which spans from ~1937 to ~1947, is the longest identified period of Slave River flood influence recorded in the SD2 record. Periods of river influence are captured in ~1937 to ~1940, and ~1942 to ~1947. Again, during this period

of river influence organic content (ranging from 3.5 to 5.9 %), moisture content (ranging from 23.2 to 28.5 %), C_{org} (ranging from 0.9 to 1.5 %), N (~ 0.1 %) and $\delta^{13}C$ (ranging from -26.1 to -23.9 ‰) are low, and C/N ratios (range from 12.7 to 16.9) and $\delta^{15}N$ (ranging from 0.8 to 1.5 ‰) are high. During this period, however, C/N values measure slightly higher, and $\delta^{15}N$ values measure more closely to, the C/N (15.9) and $\delta^{15}N$ (1.7 ‰) values of the 2005 flood deposit sample. In addition, C_{org} and N values for this period closely approximate the C_{org} (1.01 %) and N (0.06 %) values of the flood deposit sample (**Figure 15 (a) to (g)**).

The third river influence period from ~1961 to ~1962 is brief and may reflect only one single flood event. However, like the first and second flood influence periods, organic content (ranging from 3.68 to 4.64 %), moisture content (ranging from 24.6 to 27.9 %), C_{org} (ranging from 1.4 to 1.4 %), N (~ 0.1 %) and $\delta^{13}C$ (ranging from -24.1 to -25.7 ‰) are low, and C/N ratios (ranging from 14.4 to 16.7 %), and $\delta^{15}N$ (~ 1.3 %) are high. During this period C/N ratios measure slightly higher, and $\delta^{15}N$ values measure close to, the 2005 flood deposit sample C/N (15.9) and $\delta^{15}N$ (1.7 ‰) values and C_{org} and N values closely approximate the C_{org} (1.01 %) and N (0.06 %) values of the 2005 flood deposit sample (**Figure 15 (a) to (g)**). This is similar to the second river influence period.

The fourth river influence period, which spans from ~1966 to ~1973, possibly reflects the strongest river influence period in the SD2 KB-5 sediment record. Low organic content (ranging from 5 to 9.8 %), moisture content (ranging from 23.3 to 28.5 %), C_{org} (ranging from 1.2 to 1.6 %), N (~ 0.1 %) and $\delta^{13}C$ (ranging from –24.6 to –26.4 ‰) are measured during this time period. C/N ratios (ranging from 14.9 to 17.8) are high, and are

higher than the C/N (15.9) value of the 2005 flood deposit sample. $\delta^{15}N$ (ranging from 0.5 to 2.2 ‰) is also high, and reaches the same $\delta^{15}N$ (1.7 ‰) value as the 2005 flood deposit sample (**Figure 15 (a) to (g)**). Decreases in C_{org} and N values occur during this period, and similar to the first three river influence periods, values closely approximate the C_{org} (1.01 %) and N (0.06 %) values of the 2005 flood deposit sample. The response of geochemical indicators for this period suggests that flooding was of larger scale than the 2005 flood event and may possibly reflect the influence of a large-scale flood event that may have occurred in 1974, as has been documented in the Peace-Athabasca Delta (Pietroniro et al., 1999) (see **Figure 16**). This would imply that the chronology for SD2 is slightly too old (by ~3 to 4 years), which is possible, as a constant sedimentation rate for the core was assumed (see section *3.5.5 SD2 KB-5 Sediment Core Chronology*).

Throughout the fifth flood influence period, from ~1976 to ~1981, the sediment record contains predominantly low organic content (ranging from 6.2 to 7.9 %), moisture content (ranging from 31.4 to 56 %), C_{org} (ranging from 1.6 to 2.2 %), N (ranging from 0.1 to 0.2 %), and $\delta^{13}C$ (ranging from -26 to -23.8 ‰), and high C/N ratios (ranging from 13 to 16.4 %) and $\delta^{15}N$ (ranging from 0.5 to 1.3 %). During this period, C/N ratios are slightly higher, $\delta^{15}N$ values are slightly lower, and C_{org} and N values are slightly higher than the C/N (15.9), $\delta^{15}N$ (1.7 ‰), C_{org} (1.01 %) and N (0.06 %) values of the 2005 flood deposit sample (**Figure 15 (a) to (g)**).

The sixth period of increased Slave River floodwater influence spans from ~1995 to ~2000 and has also captured river influence periods. The measured ranges for geochemical indicators for this period are similar to measured ranges of geochemical indicators for the

first period of floodwater influence. Organic content (ranging from 4 to 6.2 %), moisture content (ranging from 31.8 to 48.7 %), C_{org} (ranging from 1.1 to 2.7 %), N (ranging from 0.1 to 0.2 %) and $\delta^{13}C$ (ranging from -26 to -23.8 ‰) are low, while C/N ratios (ranging from 11.6 to 14.5 %) and $\delta^{15}N$ (ranging from 0.5 to 1.3 %) are high. C/N and $\delta^{15}N$ values for this period do not measure as high as the C/N (15.9) and $\delta^{15}N$ (1.7 ‰) values measured in the 2005 flood deposit sample, which is also the case during the first period of river influence (**Figure 15 (a) to (g)**). During this period, C_{org} and N values measure slightly higher than the C_{org} (1.01 %) and N (0.06 %) values of the 2005 flood deposit sample. Additionally, C_{org} and N values measure closer to the C_{org} and N values of the flood deposit sample during this period than they do during the first period of river influence (**Figure 15 (a) to (g)**).

The white highlighted areas identified in **Figure 15** are periods of less river influence that are characterized by higher organic content (average of 8.5%), moisture content (average of 38.6 %), C_{org} (average of 2.4 %), N (average of 0.22 %) and $\delta^{13}C$ (average of -24.8 ‰) and lower C/N (average of 11.6) and $\delta^{15}N$ (average of 0.13 ‰) values. These periods span from ~1918 to ~1928, ~1933 to ~1936, ~1948 to 1960, ~1963 to ~1965, ~1974 to ~1975, ~1983 to 1994 and ~2001 to 2004. Macrofossil analyses by Adam (2007) and diatom analyses by Sokal (2007) identify ~1948 to ~1960 as being a distinct period of decreased SR floodwater influence in the SD2 sediment record (although it should be noted that Adam (2007) and Sokal (2007) use a slightly different chronology that is partly based on the ^{210}Pb data).

A correlation is evident between high spring discharge levels, predominantly while ice cover was intact, on the Slave River and higher C/N ratios and $\delta^{15}N$ (%), and lower C_{org}

(%) and N (%) in the SD2 record (**Figure 16**) from 1960 to 1998. Findings from geochemical analyses are consistent with biological proxy data from the SD2 KB-5 core (Adam 2007; Sokal 2007). Plots show that from 1960 to ~1982, C/N values (ranging from 9.7 to 17.8 %) and $\delta^{15}N$ values (ranging from -0.91 to 2.19 %) are at their highest, a time period when several large peak discharge events on the Slave River were recorded. In contrast, C_{org} values (ranging from 1.2 to 3.0 %) and N values (ranging from 0.07 to 0.28 %) are relatively low in comparison to periods of less river influence (**Figure 16**). As discussed above, the response of geochemical indicators in the SD2 record from ~1966 to ~1973 suggest that flooding was of larger scale than the May 2005 flood event and may in fact reflect a large-scale flood event in 1974, as it is possible that the chronology for SD2 is slightly too old. A similar trend of high C/N values (ranging from 12.7 to 16.9 %) and $\delta^{15}N$ values (ranging from 0.77 to 1.54 %) and lower C_{org} (ranging from 0.9 to 1.6 %) and N values (ranging from 0.06 to 0.12 %) in the SD2 record occurs from ~1937 to ~1947 where the second increased flood influence period was identified (see **Figure 15 (c), (e), (f) and (g)**). C/N (ranging from 10.2 to 12.9 %) and $\delta^{15}N$ (ranging from -0.06 to 0.06 %) values are lower from ~1983 to ~1994 during a period where lower peak discharge events were measured on the Slave River. From ~1995 to ~1998 C/N ratios (ranging from 13.3 to 14.6 %) and $\delta^{15}N$ (ranging from 0.12 to 0.35 %) start to increase, whereas C_{org} values (ranging from 1.2 to 2.7 %) and N values (ranging from 0.08 to 0.20 %) start to decrease. The responses of these specific geochemical proxies from ~1995 to ~1998 correspond to a period where a number of high spring peak discharge events were measured on the Slave River, such as the peak discharge events in 1996, 1997, 1998 and 1999 (Water Survey of Canada, 2006) (**Figure 16**).

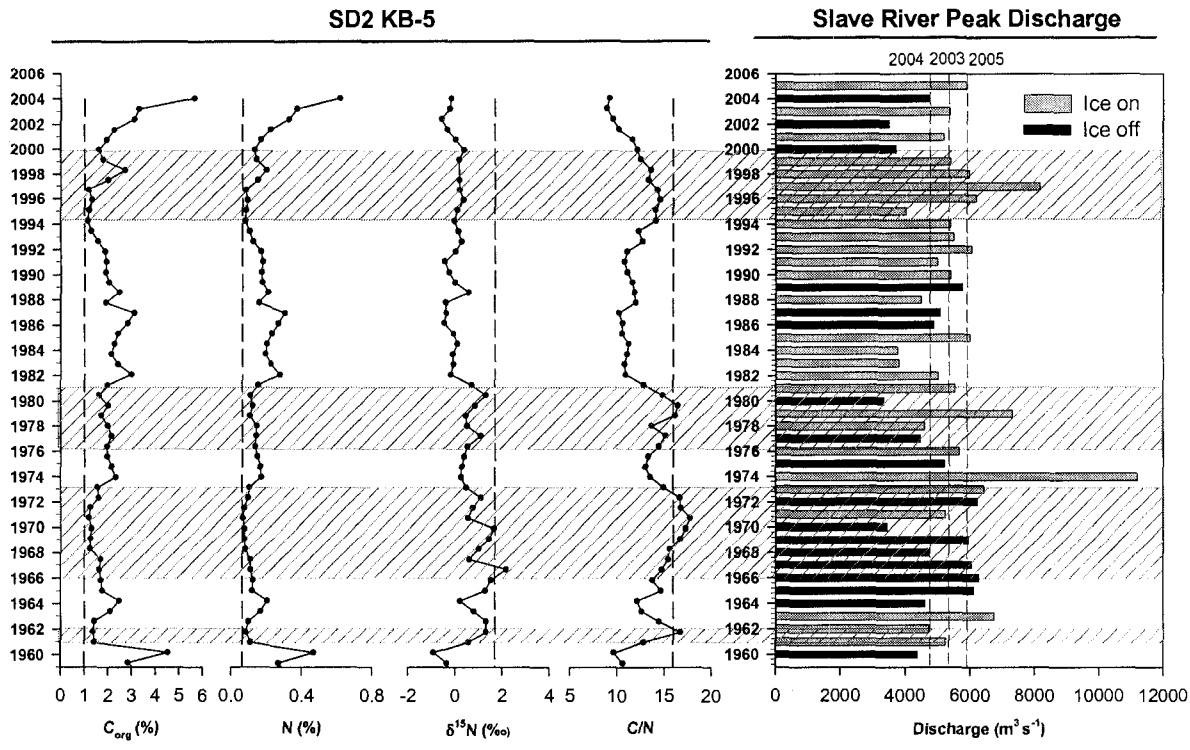

Figure 16. SD2 KB-5 Carbon and nitrogen elemental and stable isotope stratigraphic records and peak Slave River discharge measured between 1960 and 2005 at Fitzgerald, AB (Water Survey of Canada, 2006), during spring melt periods. SD2 KB-5 geochemical records showing values for the May 2005 flood deposit sediment sample (represented by dashed lines). Years with peak discharge occurring, predominantly with ice still intact, on the Slave River correlate with higher C/N ratios and $\delta^{15}N$ (‰), and lower C_{org} (%) and N (%) in the SD2 record and are highlighted by hash marks. Maximum discharge ($m^3 s^{-1}$) measured in Slave River at Fitzgerald, AB (Water Survey of Canada, 2006) during the period 14 days prior to and 3 days post the disappearance of solid and floating ice. Grey bands indicate years in which peak discharge occurred while river ice cover was intact, while black bands represent years in which peak discharge occurred following the disappearance of river ice cover. Peak discharge conditions measured in the SRD in 2003-2005 are indicated by vertical dashed lines on the Slave River discharge graph.

3.5.7 SD28 KB-5 Sediment Core Chronology

It was determined through analysis of the ^{210}Pb profile for the SD28 KB-5 sediment core that measured ^{210}Pb did not decline exponentially and that the profile displayed a large amount of variability (**Figure 17**). Background levels of supported ^{210}Pb (^{214}Bi) (0.027 Bq/g) were estimated to be reached at 29.75 cm (0.027 Bq/g) resulting in a basal date of ~1917 at this depth using the CRS model (**Figure 18 (b)**). Measured ^{210}Pb values that fell between sediment intervals 0-29.25 cm and measured below the average supported ^{210}Pb level (0.027 Bq/g) were excluded from the model because these values measured less than supported ^{210}Pb levels and generated dates younger than the age of the sediment increment above. Excluded sediment intervals are 6.50 to 7.0 cm (^{210}Pb = 0.0178 Bq/g), 15.0 to 15.50 cm (^{210}Pb = 0.012 Bq/g), 18.0 to 18.50 cm (^{210}Pb = 0.0218 Bq/g), 19.0 to 19.50 cm (^{210}Pb = 0.0180 Bq/g), 20.50 to 21.0 cm (^{210}Pb = 0.0134 Bq/g) and 28.50 and 29.0 cm (^{210}Pb = 0.0123 Bq/g) (**Figures 17 and 18 (a)**). Dates from 29.75-33.0 cm (the bottom of the core) were extrapolated using a sedimentation rate of 0.231 (g/cm^2/year), which is the average sedimentation rate for sediment intervals 24.75 to 28.75 cm (**Figure 18 (b)**). Sediment intervals from 24.75 to 28.75 cm were chosen to calculate the average sedimentation rate for the bottom samples of the SD28 KB-5 core, as the sedimentation rate of these intervals were determined to be the most reasonable estimation of the sedimentation rate of the bottom of the unsupported ^{210}Pb profile. The mean sampling resolution is 1.5 years from 0-29.25 cm, and 2.3 years from 29.75-33.0 cm.

CRS modeled dates for sediment intervals 6.50 to 7.0 cm, 15.0 to 15.50 cm, 18.0 to 18.50 cm, 19.0 to 19.50 cm and 20.50 to 21.0 cm correspond to years that have similar

measured peak discharge levels to that of years 2003 and 2005, years in which the Slave River flooded into SD28. For example, 6.50 to 7.0 cm is approximately year 1996, a year in which spring peak discharge on the Slave River while ice cover was intact, measures higher than May 2005 peak discharge (**Figure 19**). Interval 15.0 to 15.50 cm is approximately year 1985, another year in which peak discharge higher than May 2005 was measured on the Slave River while ice cover was intact (**Figure 19**). In 1974, the highest peak discharge while ice cover was intact was measured on the Slave River and this year corresponds to sediment interval 18.0 to 18.5 cm. At 19.0 to 19.50 cm, which is approximately year 1969, peak discharge on the Slave River during ice-off conditions was measured to be approximately the same as the peak discharge in May 2005 (**Figure 19**). At 20.50 to 21.0 cm, which is approximately year 1961, peak discharge on the Slave River while ice cover was intact measured close to that of May 2003 peak discharge (**Figure 19**). Low ^{210}Pb concentrations measured in the specific sediment intervals as mentioned above are likely due to Slave River floodwater dilution of ^{210}Pb concentrations in lake sediments.

There is no evidence of an interpretable ^{137}Cs peak in the sediment core. The ^{137}Cs profile is somewhat variable in the uppermost 7 cm of the core and is relatively constant below that depth **(Figure 17).**

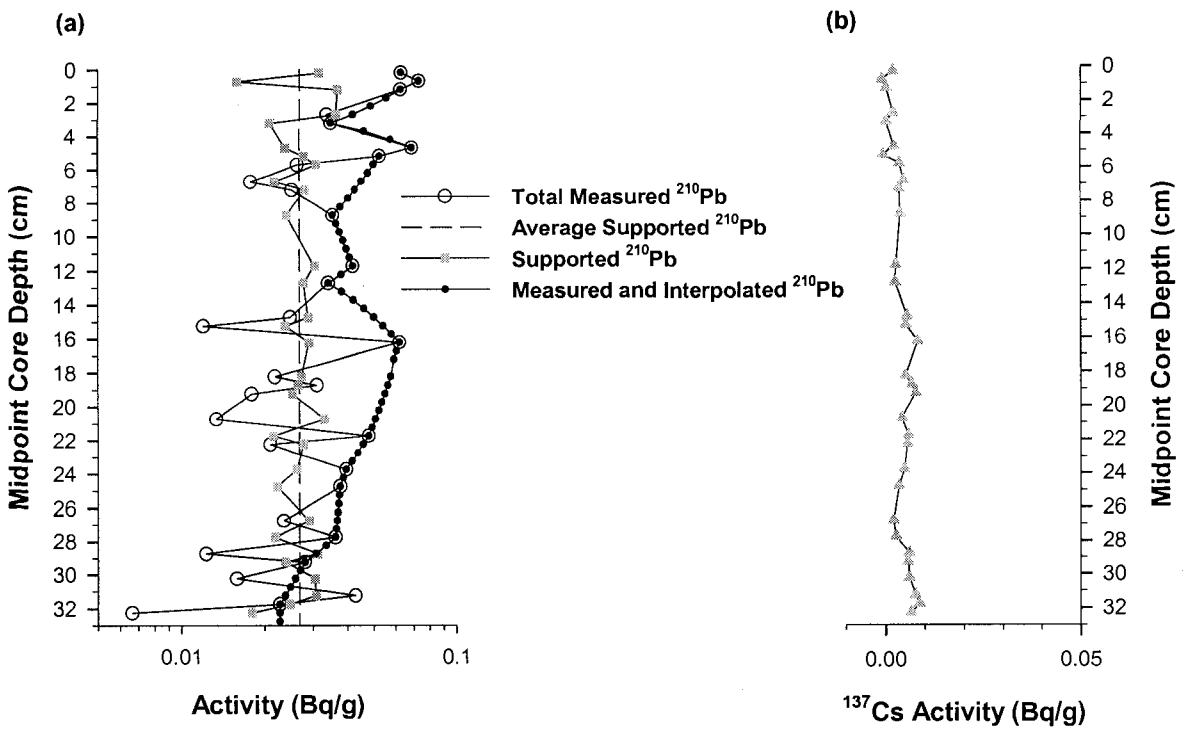

Figure 17. (a) Total and supported ^{210}Pb, and (b) ^{137}Cs activity profiles for SD28 KB-5. The 'Total Measured ^{210}Pb series' represents activity values measured in all samples analysed in the gamma spectrometer. The 'Measured and Interpolated ^{210}Pb' series is based on the 'Total Measured ^{210}Pb' series, with outliers removed (removed outliers are: 2.75, 5.75, 6.75, 7.25, 14.75, 15.25, 18.25, 18.75, 19.25, 20.75, 22.25, 26.75, 28.75, 30.25, 31.25 and 32.25 cm) and values interpolated for samples that were not analysed.

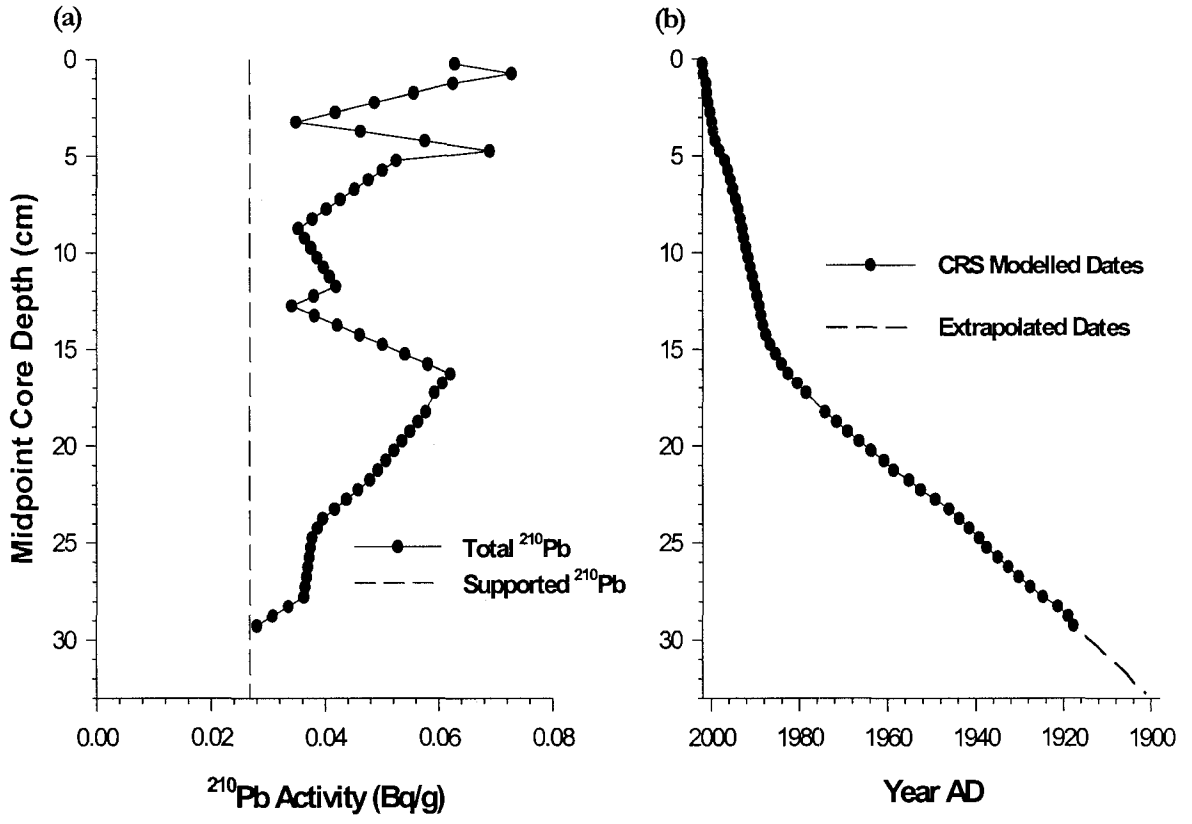

Figure 18. (a) Total ^{210}Pb activity (includes measured and interpolated ^{210}Pb) and average background levels of supported ^{210}Pb (^{214}Bi) versus depth for SD28 KB-5 and (b) SD 28 KB-5 sediment core chronology based on the Constant Rate of Supply model. An average sedimentation rate for interval 24.75 to 28.75 cm depth was used to estimate the sediment chronology below 29.25 cm depth.

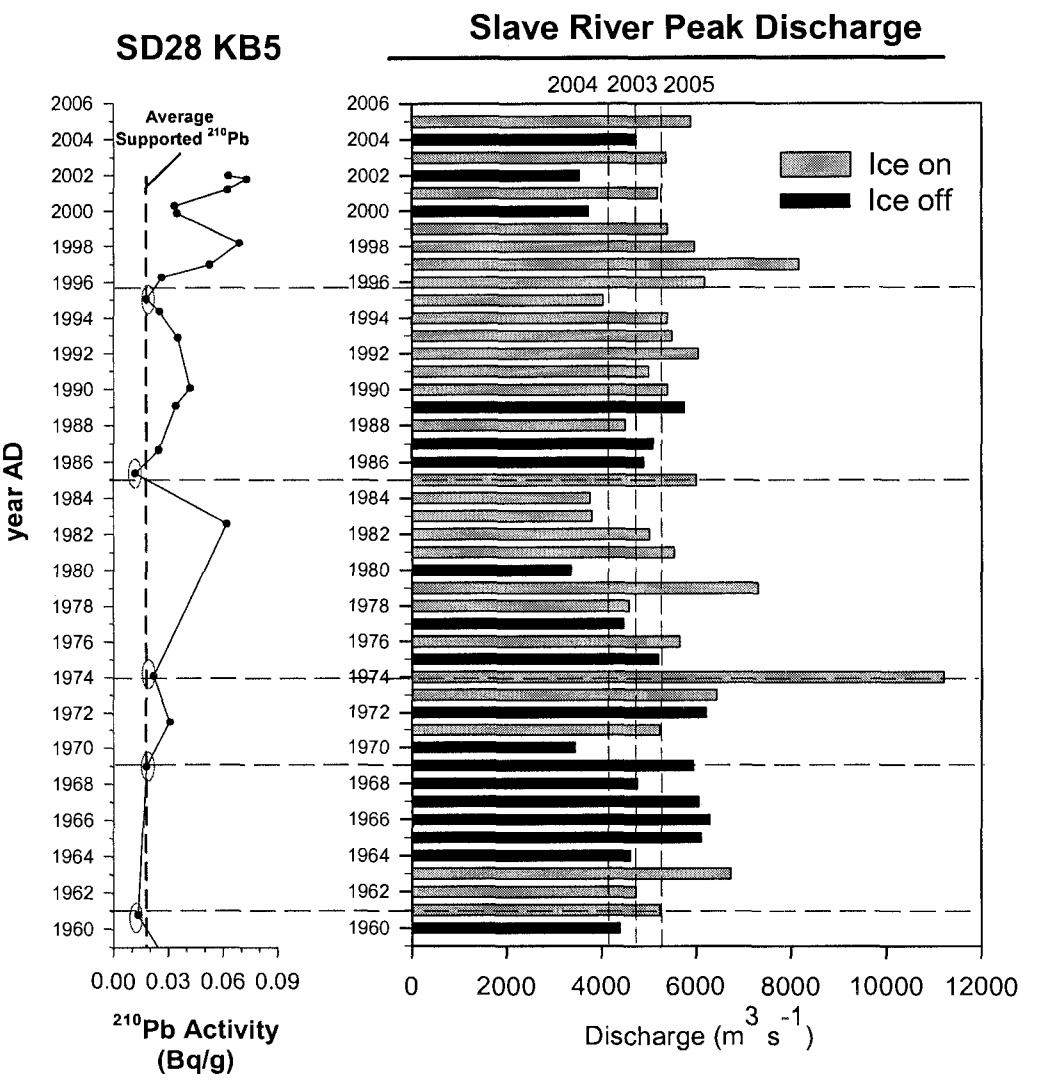

Figure 19. SD28 KB-5 ^{210}Pb stratigraphy from 1960 to 2002 and peak Slave River discharge measured between 1960 and 2005 at Fitzgerald, AB (Water Survey of Canada, 2006), during spring melt periods. Total ^{210}Pb values that are similar to the average supported ^{210}Pb level (0.027 Bq/g) (sediment intervals 6.50 to 7.0 cm, 15.0 to 15.50 cm, 19.0 to 19.50 cm and 20.50 to 21.0 cm) are circled. Dashed lines indicate peak discharge years that correspond to 'diluted' ^{210}Pb values.

3.5.8 SD28 KB-5 Cellulose Inferred Lake Water Oxygen Isotope Stratigraphy

Sediment cellulose-inferred $\delta^{18}O_{lw}$ values vary from -22.5 to -13 ‰ over the last century. Most values are within the range of contemporary lake water $\delta^{18}O$ values, which range from -18.5 to -14 ‰. From ~1901 to ~1973, $\delta^{18}O_{lw}$ values are stable ranging from -15.9 to -13 ‰ (**Figure 20 (a)**). However, at ~1912 (-12.9 ‰) and ~1930 (-12.7 ‰), $\delta^{18}O_{lw}$ values are the highest in the record, but still do not reach contemporary closed-basin isotopic steady-state (δ_{SSI}), a value of -8.9 ‰ (**Figure 20 (a)**). A trend towards lower $\delta^{18}O_{lw}$ values occurs from ~1974 to 2002 with values ranging from -22.5 to -15 ‰ (**Figure 20 (a)**). Overall, the cellulose-inferred $\delta^{18}O_{lw}$ record for SD28 indicates that hydrological conditions in the basin over the last century have remained relatively stable until the last ~30 years when a slight shift towards lower values occurs.

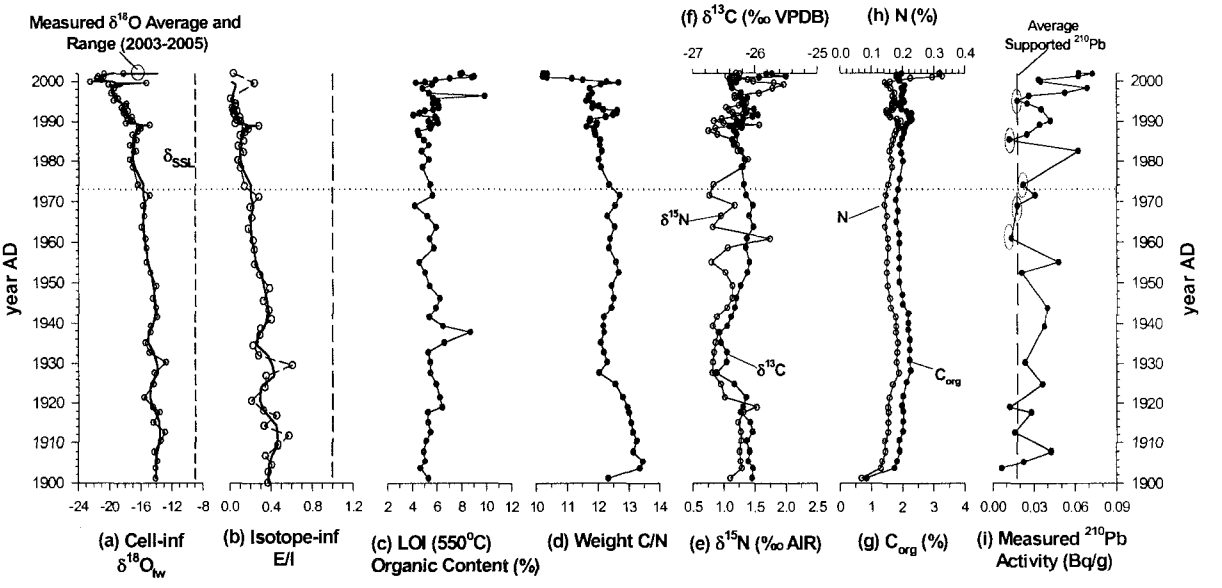

Figure 20. SD28 KB-5 Geochemical Stratigraphy. An ~100 year lake water $\delta^{18}O$ history for SD28 inferred from oxygen isotope analysis of aquatic plant cellulose extracted from SD28 KB- 5 sediment core (a). Raw (open circles) and smoothed (three-point running mean represented by solid line) profiles are shown. The range and average lake water $\delta^{18}O$ composition measured from lake water samples taken during sampling seasons in 2003-2005 is shown. E/I ratios (b) were estimated using the cellulose-inferred lake water $\delta^{18}O$ record and an isotope-mass balance model (raw data are represented by open circles and the three-point running mean is represented by solid line) using a *h* value of 69.2% (Hay River 30-year climate normal), and assumes steady-state evaporative enrichment fed by source waters of constant isotopic composition. Other geochemical stratigraphic records include: organic content estimated from loss-on-ignition at 550°C (c), weight C/N ratios (d), total $\delta^{15}N$ (e), bulk organic $\delta^{13}C$ (f), organic carbon content (g), nitrogen content (h), and ^{210}Pb activity (i). Circles shown on ^{210}Pb activity stratigraphy indicate years where ^{210}Pb concentration is similar to average supported ^{210}Pb concentration of 0.027 (Bq/g), which is likely due to dilution from the Slave River during high magnitude floods (see Figure 26).

3.5.9 Lake Water Balance Reconstruction

The cellulose-inferred $\delta^{18}O_{lw}$ record indicates SD28 has had a consistently positive (E/I <1) water balance during the 20th century, with the past 30 years displaying a trend to lower E/I ratios possibly reflecting an increase in the input of Slave River floodwaters (**Figure 20 (a)**). For example, values are relatively stable from ~1901 to ~1973 ranging from 0.2 to 0.6, and lower values ranging from 0.01 to 0.2 occur from ~1974 to 2002. Three years of modern water balance analyses show that the water balance of SD28 is dominated by ^{18}O depletion due to river water influence and ^{18}O enrichment due to evaporation. Parameters used to quantify the $\delta^{18}O_{lw}$ record of SD28 are the same parameters used to quantify the $\delta^{18}O_{lw}$ record of SD20 (see *2.3 Water Balance Reconstruction*, section *2.3.1*). Note that the δ_I value used for the E/I modelling is average precipitation (-19), which slightly lower than SR composition (-18 to -17) thus E/I values may be slightly overestimated.

3.5.10 Carbon and Nitrogen Elemental and Stable Isotope Stratigraphy

Overall, results for the entire SD28 KB-5 sediment core indicate that organic content (ranging from 4.10 to 9.87), C_{org} (ranging from 0.85 to 3.35 %), N (ranging from 0.07 to 0.33 %), $\delta^{13}C$ (ranging from -26.6 to -25.5 ‰), and $\delta^{15}N$ (ranging from 0.75 to 1.97 ‰) show a narrow range of variability (**Figure 20 (a) to (h)**). The range of C/N values for SD28 is from 10.22 to 13.45, values that are characteristic of organic matter that is predominantly of aquatic origin (Meyers et al., 2001). The range in C/N values for SD28 is much smaller in

comparison to the range in C/N values for SD2 (8.90 to 17.75), and is closer to the smaller range in C/N values measured in SD20 (10.63 to 11.62).

From ~1901 to ~1973, organic content (ranging from 4.2 to 9.0 %), C/N (ranging from 12 to 13.4), $\delta^{13}C$ (ranging from -26.6 to -26 ‰), $\delta^{15}N$ (ranging from 0.8 to 1.5 ‰), C_{org} (ranging from 0.9 to 2.3 %), and N (ranging from 0.1 to 0.2 %) are quite stable (**Figure 20 (a) to (h)**). There is a very small increase in variability in organic content (ranging from 4.1 to 10 %), C/N (ranging from 10.2 to 12.7), $\delta^{13}C$ (ranging from -26.4 to –25.5 ‰), $\delta^{15}N$ (ranging from 0.8 to 2 ‰) and N (ranging from 0.1 to 0.3 %) from ~1974 to 2002. Conversely, there is an increase in variability in C_{org} (ranging from 1.8 to 3.3 %) during this time period (**Figure 20 (a) to (h)**).

Analyses indicate that $\delta^{18}O_{lw}$, E/I ratios and measured ^{210}Pb stratigraphic records may be better indicators of periods of Slave River floodwater influence and flood frequency in the SD28 sediment record in comparison to all other geochemical proxies. All geochemical proxies do however document a slight increase in variability from ~1974 to 2002 (**Figure 20 (a) to (i)**). However, because carbon and nitrogen elemental and stable isotope records, $\delta^{18}O_{lw}$ and consequently E/I ratios record such a narrow range of hydrological variability of the basin, which is due to the hydrological setting of SD28 and its long channel connection to the river, it is difficult to reconstruct the past hydrological variability of the basin. The highly variable ^{210}Pb data also generate greater uncertainties in the sediment chronology in comparison to the SD20 and SD2 records.

Chapter 4 DISCUSSION

4.1 CLIMATE-DRIVEN PALEOHYDROLOGY

SD20

Contemporary isotope-based studies of the lake water balance of SD 20 indicate that precipitation and catchment-derived snowmelt are the predominant inputs into the basin and evaporation is the dominant process controlling water loss from the basin. During the years 2003, 2004 and 2005, river floodwaters did not influence the water balance of SD20. SD20 undergoes pronounced heavy-isotope enrichment due to evaporation, and is constrained along the LEL for each of the sampling years, which is consistent with other evaporation-dominated SRD basins located in the apex of the delta (Brock et al., 2007). Findings indicate that the water balance of SD20 is driven predominantly by local climatic influences and that occasionally, very large-scale flood events, such as one that may have occurred in 1974 (as did in the Peace-Athabasca Delta; see Pietroniro et al., 1999), may reach the basin.

Multi-proxy evidence from the SD20 KB-5 sediment core indicates hydro-ecological conditions have varied substantially over the last ~215 years. An increase in organic content (%) from the bottom to the top of the core (**Figure 13**) may suggests a shift from lower productivity levels in the basin during the later part of the "Little Ice Age" (from ~1788 to ~1900) when air temperatures in the Northern Hemisphere are documented to have been cooler, to an increase in productivity post-Little Ice Age (from ~1901 to 2002), when air temperatures are documented to have increased (Mann et al., 1999). Reconstructed E/I ratios suggest that the lake was influenced by multi-decadal dry and wet periods that follow the same general pattern as "Spruce Island Lake" (Wolfe et al., 2005), a climate-driven perched basin in the Peace-Athabasca Delta (**Figure 22**). SD20 and Spruce Island Lake are

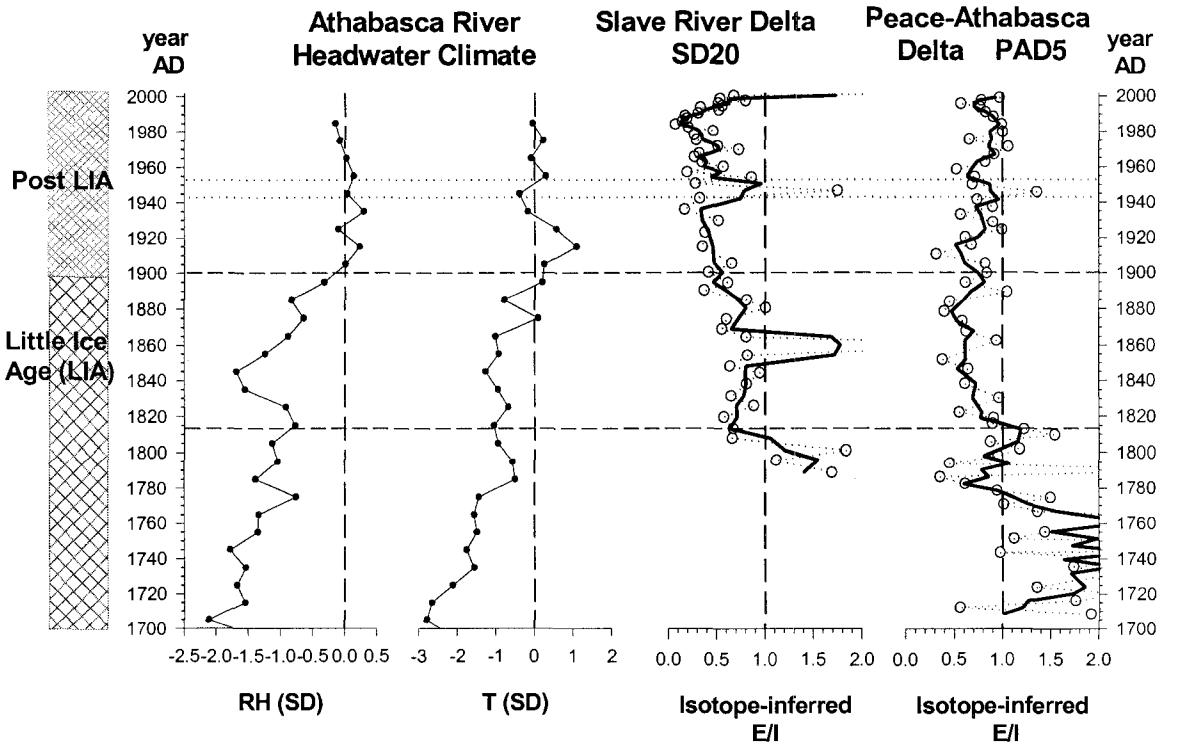

Figure 22. An ~215 year record of isotope inferred evaporation-to-inflow (E/I) ratios for SD20 and "Spruce Island Lake" (Wolfe et al., 2005). Isotope inferred evaporation-to-inflow (E/I) ratios are estimated using the cellulose-inferred lake water $\delta^{18}O$ record and an isotope-mass balance model assuming steady-state evaporative enrichment fed by source waters of constant isotopic composition (Craig and Gordon, 1965) (raw data represented by open circles, and a three point running mean represented by solid lines). Athabasca River headwater climate data is quantified from carbon and oxygen isotope analyses of a composite tree-ring record from the headwaters of the Athabasca River (Hall et al., 2004).

plotted alongside Athabasca River headwater climate records based on isotope analysis of a dendrochronological sequence (Wolfe et al., 2005; Hall et al., 2004), which provides an independent climatic record to assess trends of positive and negative water balance of the two lakes.

Analysis of historical E/I records for SD20 and Spruce Island Lake show that during the 1700s, both basins have E/I ratios indicative of non-steady-state net evaporation (**Figure 22**). Athabasca River headwater climate reconstruction indicates that cool and dry conditions were persistent during this time period associated with the "Little Ice Age" (**Figure 22**). The Athabasca climate record shows an increase in temperature and relative humidity for most of the 1800s, which corresponds with predominantly positive water balance for both basins whereby inputs were the dominant influence on lake water balance during this time period. Throughout the 20th century, temperatures and relative humidity are more stable in comparison to the Little Ice Age and Spruce Island Lake shows a trend towards closed-basin steady-state conditions (E/I values approach 1). During the 20th century, SD20 shows a trend towards a slightly more positive water balance in comparison to Spruce Island Lake, but only up until ~1944 to ~1954 when both basins are influenced by a brief shift towards a negative water balance. This trend is consistent with a period (from ~1948 to ~1960) in the SD2 KB-5 sediment record, which has been documented through geochemical analyses and biological proxy data from the same sediment core (Adam, 2007 and Sokal, 2007) as being a period of decreased SR floodwater influence at the basin. After ~1954, the trend towards a more positive water balance continues at SD20 with the most positive value occurring at ~1984, which may be associated with a major flood event in 1974. This water balance trend only continues until the mid-1980s after which a marked

period of declining water balance occurs at SD20, suggesting a return to steady-state isotopic lake water balance conditions (**Figure 22**).

Evidently, broadly similar climate regimes have influenced the water balance of upland basins in both the SRD and PAD over the last ~215 years, as paleohydrological trends from these two basins closely align with paleoclimate records reconstructed from tree-ring sequences upstream near the headwaters of the Athabasca River (**Figure 22**). A higher degree of variability in historical lake water balance is evident at SD20 during the 20th century in comparison to Spruce Island Lake. This is most likely due to differences in catchment characteristics, specific localized climatic events (e.g. lake-effect snow storms generated by Great Slave Lake) and susceptibility to large-scale flood events (e.g. 1974).

Analyses of paleohydrological trends of SD20 provide long-term documentation of how hydrological conditions have varied in the SRD largely independent of river flooding. Hydrological conditions have shifted from drier conditions in the late 1700s to wetter conditions over the last two centuries. Paleohydrological records provide evidence that drier and less productive conditions identified from aerial photography over the past ~40 years (English et al., 1997) are not outside of the range of natural variability for closed-drainage basins in the SRD. Drier conditions reported by local community members in the SRD since regulation of the Peace River in 1968 (Wesche, 2007) may be similar to multi-decadal dry intervals that have naturally occurred in the recent past.

4.2 SLAVE RIVER FLOOD FREQUENCY

SD2

Contemporary isotope-based studies of SD2 indicate that the basin is predominantly controlled by Slave River floodwater inputs. In 2003 and 2005, during periods of known high flow and high water levels on the Slave River, the Slave River flooded SD2 and the isotopic composition of river floodwaters was reflected in the 2003 and 2005 lake water isotopic composition of the basin. Conversely, in the absence of flooding, as in 2004, the composition of SD2 did not reflect the composition of the Slave River. For sampling years 2003, 2004 and 2005, as the thaw season progressed into fall and peak discharge levels on the Slave River fell, the water balance of SD2 was similar to that of an evaporation-dominated basin and SD2 became much more evaporatively enriched in comparison to the Slave River.

Paleohydrological records derived from multi-proxy evidence for SD2 indicate that the basin is frequently influenced by Slave River flooding. Carbon and nitrogen elemental and stable isotope records for SD2 have provided an excellent archive of Slave River flood frequency over the last century (**Figure 16**). Increases in C/N ratios strongly correspond to higher discharge levels on the Slave River and decreases in C/N ratios strongly correspond to lower discharge levels on the Slave River over the last ~44 years in which discharge records exist. The C/N record also shows that from ~1948 to ~1960 was a period in which the basin received very little floodwater input from Slave River which corresponds with a brief, but strong $\delta^{18}O$ enrichment at SD20. These findings are consistent with biological proxy data from the same sediment core (Adam, 2007; Sokal, 2007).

Flood frequency patterns of the Slave River captured in the C/N record of SD2 are similar to flood frequency patterns of the Peace River as documented by the C/N record of "Pete's Creek", or PAD15, a 4 m deep oxbow lake in the PAD (Wolfe et al., 2006) (**Figure 23**). PAD15 is a hydrologically closed basin, however, it does have an inflow channel connection to the Revillon Coupé (a major distributary of the Peace River when back-flooding occurs during ice-jams on the Peace River), that is typically only connected during high water events on the Peace River. The PAD15 C/N record provides a historical record of flood events in the Peace sector of the PAD. Increases in PAD15 C/N ratios are in good agreement with increases in SD2 C/N ratios and identified SD2 river influence periods (**Figure 23**).

Correlations have been made between upstream flow generation and spring flood magnitudes in the PAD (Prowse and Conly, 1998; Romolo et al., 2006) and SRD (Brock et al., in review). Key tributaries of the Peace River, located in the Wapiti-Smoky drainage basin, provide the source waters that control spring flow magnitudes in the PAD (Prowse and Conly, 1998). Years when high discharge levels and high spring snow pack snow-water equivalents were recorded in the Smoky River basin have been correlated with high river discharge and major historic ice break up events on the Peace River (Romolo, 2006). Brock et al. (in review) report that 2003 and 2005 were years in which high discharge was recorded on the Smoky, Peace and Slave Rivers, which corresponds to years in which flooding occurred on the SRD. High water events on the Peace River are correlated with high water events on the Slave River and are ultimately controlled by drivers such as snow accumulation, melt and river discharge in upstream tributaries of the Peace River.

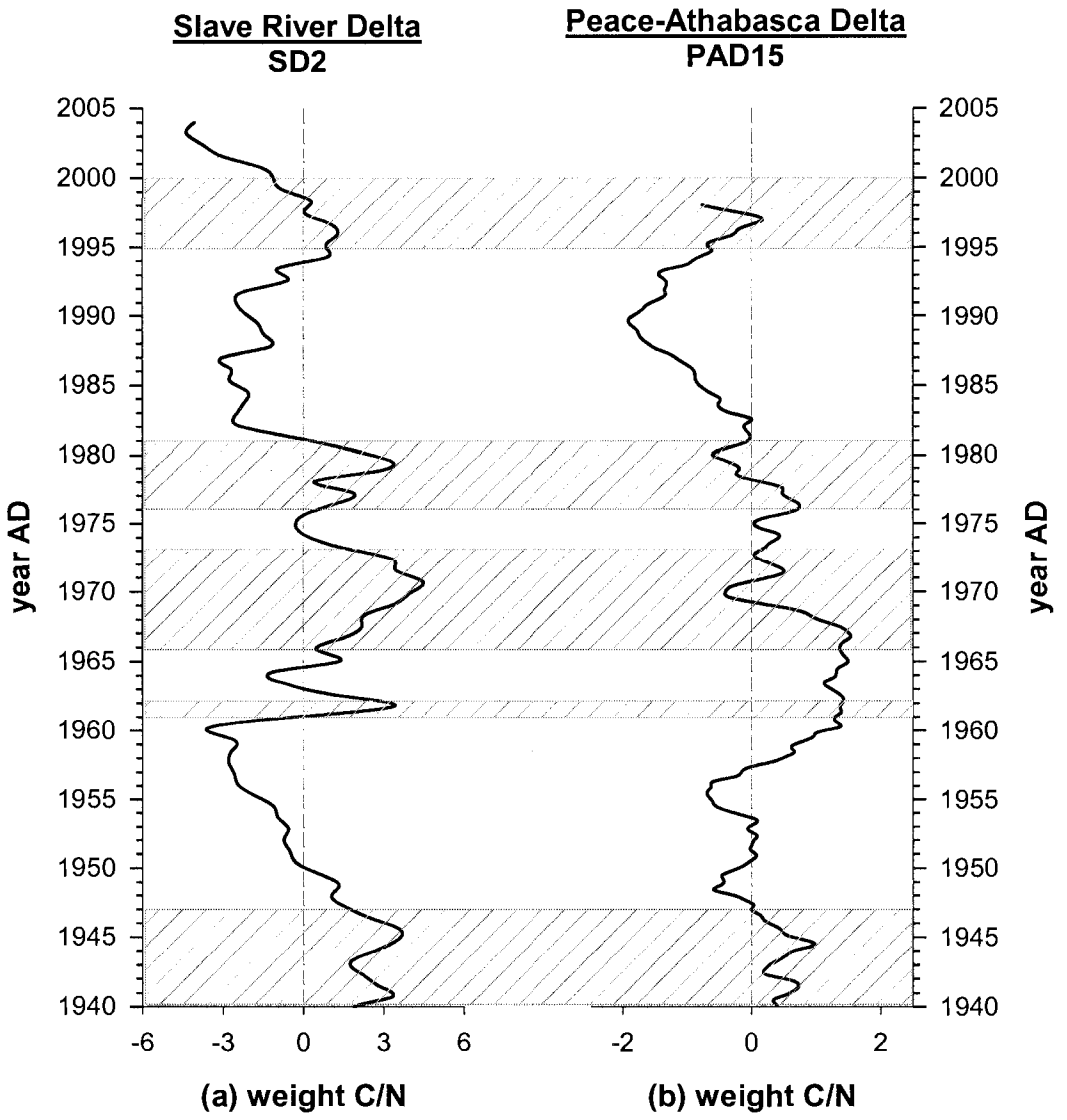

Figure 23. Comparison of SD2 and PAD15 C/N ratio stratigraphies to 1940. The C/N ratios are plotted relative to mean values. Note the C/N ratio plotted for PAD15 is shown as an eleven point running mean to achieve similar temporal resolution as the SD2 C/N record. SD2 river influence periods (~1937 to ~1947, ~1961 to ~1962, ~1966 to ~1973, ~1976 to ~1981, ~1995 to ~2000; see section *3.5.6*) are highlighted with hash marks.

SD28

Contemporary isotope-based studies for SD28 indicate that the lake water balance is influenced by Slave River water via the channel connection to the river, catchment-derived snowmelt and evaporation. Results from 2005 for SD28 show that the lake was flooded because of high discharge on the Slave River and river water was the predominant influence on the lake water balance. Conversely, during periods of lower flow on the Slave River, such as in 2003 and 2004, evaporation more strongly influences SD28 lake water balance. SD28 is typically more evaporatively enriched than the river all year round (**Figure 10 (a to c)**).

In comparison to the strikingly variable SD2 record of flood frequency, the geochemical stratigraphy for SD28 is largely complacent except for a decline in the cellulose-inferred $\delta^{18}O_{lw}$ (and modelled E/I ratio) records beginning at ~1974. This trend may reflect an increase in river flooding into the basin. Low ^{210}Pb values may also be due to dilution from individual flood events. Uncertainties in developing a robust chronology for this site, owing to a highly variable ^{210}Pb profile, hampers any additional interpretation of the paleohydrological record. This is further compromised by the long (~1 km) channel connection between this basin and the river, which likely dilutes geochemical signatures that may be associated with individual flood events entering the basin. Thus, SD2, which has a sill that separates the basin from the adjacent Slave River but which is easily overtopped during flood events, provides a much more sensitive geochemical record of flood frequency.

Chapter 5 CONCLUSIONS AND RECOMENDATIONS

5.1 CONCLUSIONS

Results from contemporary hydrological and paleohydrological analysis of three lakes found in three very different hydrological settings within the Slave River Delta provide insight into long-term and short-term hydro-ecological variability in the SRD. Modern lake water $\delta^{18}O$ and $\delta^{2}H$ analysis of SD20 indicates that this closed-drainage lake is dependent on precipitation and snowmelt runoff in order to maintain standing water within the basin, and that in the absence of these inputs, evaporation strongly controls lake water balance. Paleolimnological and paleohydrological records for SD20 have provided an understanding of long-term natural hydro-ecological variability and change, as these records have shown that shifts from wetter to drier periods and vice versa, have existed in the past and are not outside the natural range of variability. Records also indicate that drier conditions existed in the past (late 1700s) in comparison to present-day conditions. Additionally, the paleohydrological record for SD20 indicates that conditions over the last two centuries have predominantly been wetter and more productive in comparison to the late 1700s. Overall, the paleohydrologic record from SD20 is consistent with a paleohydrologic record from a similar upland basin in the Peace-Athabasca Delta (Wolfe et al., 2005) and an independent record of climate variability from the headwaters of the Athabasca River (Hall et al., 2004).

In contrast, modern lake water $\delta^{18}O$ and $\delta^{2}H$ analysis of SD2 lake water balance indicates that this flood-dominated lake is largely controlled by frequent flooding from the Slave River. Snowmelt runoff is also an important input to this lake, however, it is evident that if floodwater frequency were to decrease the lake would be controlled predominantly by

evaporation and its lake water balance could mirror that of some of the closed drainage lakes in the delta. The paleolimnological record for SD2 has provided an understanding of short-term hydro-ecological change and variability driven by fluctuations in Slave River discharge. The carbon and nitrogen elemental and stable isotope stratigraphic record indicate that there is no strong evidence to support the notion that regulation of the Peace River in 1968 has changed flood frequency at this location. Additionally, the record shows that the late 1940s and 1950s was a period of low flood frequency. The macrofossil record for SD2 KB-5 (Adam, 2007) characterizes the late 1940s and 1950s as the driest interval in the record.

Modern lake water $\delta^{18}O$ and $\delta^{2}H$ analysis of SD28 indicates that this exchange-dominated lake is largely influenced by periodic large-scale flooding from the Slave River as well as catchment-derived inputs. Isotopic analysis of lake water samples taken from SD2 and SD28 in May of 2003 and 2005 after floodwaters entered both lakes illustrates that the water balance of SD28 is less influenced by lower magnitude flood events than higher magnitude flood events in comparison to SD2 (**Figures 9 (a to b) and 10 (a to b)**). Although river flooding to this basin may have increased over the past 40 years, the geochemical stratigraphic record is not particularly sensitive because of its hydrological setting in the delta.

Findings provide insight and understanding into the complexity and sensitivity of different basin types within the SRD deltaic system. Slave River flood frequency and discharge dynamics is less likely to be captured in lake sediments of basins that are directly connected to the river by long channels. When climatic shifts from wetter to drier periods occur in the SRD, they are more likely to be more pronounced in the sediment records of

evaporation-dominated basins and not in flood-dominated basins, or in exchange-dominated basins.

5.2 RECOMMENDATIONS

A longer sediment core has been extracted from SD20 to further develop a longer paleohydrological and paleoclimatological record of hydro-ecological change and variability in the SRD. Additionally, a longer sediment core has been extracted from SD2 in order to further develop a longer historical archive of Slave River flood frequency. Investigation of these longer records will be important to examine variability in delta hydroecology and flood frequency over a broader range of climatic conditions.

This research serves as an example of how to couple modern- and paleo-isotope methods to evaluate hydroecological variability and change in large freshwater ecosystems. Such temporal context is critical to develop for effective water resource management and methods employed here are readily transferable to other large, freshwater ecosystems subject to multiple stressors.

References

Adam, M. E., 2007. Development and application of plant macrofossils for paleolimnology reconstructions in the Slave River Delta, NWT. Unpublished MSc Thesis, Department of Biology, University of Waterloo.

Allison, G. B., and Leaney, F. W., 1982. Estimation of isotopic exchange parameters using constant feed pans. Journal of Hydrology 55: 151-161.

Appleby, P. G. 2001. Chronostratigraphic Techniques in Recent Sediments. In: Last, W. M., and Smol, J. P. (Eds), Tracking Environmental Change Using Lake Sediments: Basin Analysis, Coring, and Chronological Techniques, vol. 1. Kluwer Academic Publishers, Dordrecht, pp 171-230.

Appleby, P. G., and Oldfield, F., 1978. The calculation of lead-210 dates assuming a constant rate of supply of unsupported ^{210}Pb to the sediment. Catena 5: 1-8.

Barnes, C. J., and Allison, G. B., 1983. The distribution of deuterium and ^{18}O in dry soils 1. Theory. Journal of Hydrology 60: 141-156.

Beltaos, S. 2000. Advances in river ice hydrology. Hydrological Processes 14: 1613-1625.

Bill, L., Crozier, J., and Surrendi, D., 1996. A report of wisdom synthesized from the Traditional Knowledge component studies. Northern River Basins Study Synthesis Report NO. 12, Northern River Basins Study, Edmonton, Canada.

Birks, S. J., Edwards, T. W. D., Gibson, J. J., Drimmie, R. J., and Michel, F. A., 2004. Canadian Network for Isotopes in Precipitation. Accessed 6 January, 2006. http://www.science.uwaterloo.ca/~twdedwar/cnip/cniphome.html.

Brahney, J., Bos, D. G., Pellatt, M. G., Edwards, T. W. D., and Routledge, R., 2006. The influence of nitrogen limitation on ^{15}N and carbon : nitrogen ratios in sediments from

sockeye salmon nursery lakes in British Columbia, Canada. Limnology and Oceanography 51: 2333-2340.

Brock, B. E., Wolfe, B. B., Edwards, T. W. D., 2007. Characterizing the hydrology of shallow floodplain lakes in the Slave River Delta, NWT, using water isotope tracers. Arctic, Antarctic and Alpine Research 39: 388-401.

Christopherson, R. W., and Byrne, M-L., 2006. Geosystems: An Introduction to Physical Geography. Pearson Education Canada, Inc., Toronto, Ontario, pp 706.

Coplen, T. B. 1996. New guidelines for reporting stable hydrogen, carbon and oxygen isotope-ratio data. Geochimica et Cosmochimica Acta 60: 3359-3360.

Craig, H., 1961. Isotopic variations in meteoric waters. Science 133: 1702-1703.

Craig, H., and Gordon, L. I., 1965. Deuterium and oxygen 18 variations in the ocean and marine atmosphere. In: Tongiorgi, E., (eds.), Stable Isotopes in Oceanographic Studies and Paleotemperatures. Pisa, Italy, Laboratorio di Geologia Nucleare, 9-130.

Day, J. H., 1972. Soils of the Slave River Lowland in the Northwest Territories. Research Branch, Canada Department of Agriculture, Ottawa, 60+map pp.

Dean, W. E., Jr., 1974. Determination of carbonate and organic matter in calcareous sediments and sedimentary rocks by loss on ignition: Comparison with other methods. Journal of Sedimentary Petrology 44: 242-248.

De Niro, M. J., and Epstein, S., 1981. Isotopic composition of cellulose from aquatic organisms. Geochimica et Cosmochimica Acta 45: 1885-1894.

Edwards, T. W. D., Aravena, R. O., Fritz, P., and Morgan, A. V., 1985. Interpreting paleoclimate from ^{18}O and ^{2}H in plant cellulose: comparison with evidence from fossil insects and relict permafrost in southwestern Ontario. Canadian Journal of Earth Sciences; 1720-1726.

Edwards. T. W. D., and McAndrews, J. H., 1989. Paleohydrology of a Canadian Shield lake inferred from ^{18}O in sediment cellulose. Canadian Journal of Earth Sciences; 1850-1859.

Edwards, T. W. D., 1993. Interpreting past climate from stable isotopes in continental organic matter. In: Swart, P. K., Lohmann, K. C., McKenzie, J., and Savin, S. Climate Change in Continental Isotopic Records. Geophysical Monograph 78, American Geophysical Union, Washington, pp 333-341.

Edwards, T. W. D., Wolfe, B. B., Gibson, J. J., and Hammarlund, D., 2004. Use of water isotope tracers in high-latitude hydrology and paleohydrology. In: Pienitz, R., Douglas, M. S. V., and Smol, J. P. (Eds). Long-term Environmental Change in Arctic and Antarctic Lakes. Kluwer Academic Publishers, Dordrecht, The Netherlands, Springer, pp 187-207.

English, M. C., 1984. Implications of Upstream Impoundment on the Natural Ecology and the Environment of the Slave River Delta, NWT. Northern Ecology and Resource Management. University of Alberta Press, pp 311-338.

English, M. C., Stone, M. A., Hill, B., Wolfe, P. M., and Ormson, R., 1996. Assessment of impacts on the Slave River Delta of Peace River impoundment at Hudson Hope. Northern River Basins Study. Edmonton, Alberta. NO. 74.

English, M. C., Hill, B., Stone, M. A., and Ormson, R., 1997. Geomorphological and botanical change on the outer Slave River Delta, NWT, before and after impoundment of the Peace River. Hydrological Processes 11: 1707-1724.

Environment Canada, 2004. Canadian Climate Normals 1971-2000. Accessed 4 March, 2005. http://www.climate.weatheroffice.ec.gc.ca

Flett, R., 2003. Understanding the 210-Pb Method. Flett Research Ltd. Manitoba, Canada. http://www.flettresearch.ca (accessed December, 2006).

Foster, I., Mighall, T., Proffitt, H., Walling, D. and Owens, P., 2006. Postdepositional ^{137}Cs mobility in the sediments of three shallow coastal lagoons, southwest England. Journal of Paleolimnology 35: 881-895.

Gardner, J. T., English, M. C., and Prowse, T., 2006. Wind-forced seiche events on Great Slave Lake: Hydrologic implications for the Slave River Delta, NWT, Canada. Hydrological Processes, 20: 4051-4072.

Gat, J. R., 1981. Lakes in Stable Isotope Hydrology: Deuterium and Oxygen-18 in the Water Cycle, Gat, J. R., Gonfiantini, R., (eds.), pp 203-221, IAEA Technical Report 210, International Atomic Energy Agency, Vienna.

Gibson, J. J., and Edwards, T. W. D., 2002. Regional water balance trends and evaporation-transpiration partitioning from a stable isotope survey of lakes in northern Canada. Global Biogeochemical Cycles 16: 10.1029/2001GB001839.

Glew, J. R., 1988. A portable extruding device for close internal sectioning of unconsolidated core samples. Journal of Paleolimnology 1: 235-239.

Gonfiantini, R., 1986. Environmental isotopes in lake studies. In Fritz, P., and Fontes, J. C., (eds.) Handbook of Environmental Isotope Geochemistry, vol 2. New York, Elsevier, 113-168.

Green, J. W., 1963. Wood cellulose. In: Whistler, R. L., (ed.) Methods in Carbohydrate Chemistry. Academic Press, New York 3: 9-20.

Hall, R. I., Wolfe, B. B., and Edwards, T. W. D., 2004. A Multi-Century Flood, Climatic and Ecological History of the Peace-Athabasca Delta, Northern Alberta, Canada. Final report published by B. C. Hydro.

Hecky, R. E., Campbell, P., and Hendzel, L. L., 1993. The stoichiometry of carbon, nitrogen, and phosphorus in particulate matter of lakes and oceans. Limnology and Oceanography 38: 709-724. In: Brahney, J., Bos, D. G., Pellatt, M. G., Edwards, T. W. D., and Routledge, R., 2006. The influence of nitrogen limitation on ^{15}N and carbon : nitrogen ratios in sediments from sockeye salmon nursery lakes in British Columbia, Canada. Limnology and Oceanography 51: 2333-2340.

Heiri, O., Lotter, A. F., and Lemcke, G., 2001. Loss on ignition as a method for estimating organic and carbonate content in sediments: reproducibility and comparability. Journal of Paleolimnology 25: 101-110.

Holmes, C., Marot, M., Willard, D., Weimer, L., and Brewster-Wingard, L., 2002. Methods to establish the timing of ecological changes in South Florida - good, better, best. USGS, SOFIA Project. http://sofia.er.usgs.gov/projects/sed_geochron/sedgeoab2.html (accessed on May 10, 2006).

Horita, J., and Wesolowski, D., 1994. Liquid-vapour fractionation of oxygen and hydrogen isotopes of water from the freezing to the critical temperature. Geochimica et Cosmochimica Acta 58: 3425-3497.

Jarvis, S., Brock, B. E., St. Amour, N., Hall, R. I., and Wolfe, B. B., 2006. Chronological Techniques in Paleolimnology: ^{210}Pb Measurement and Data Modelling. Technical Procedure.

Jermyn, C., 2004. Paleohydrological reconstruction of a closed basin lake in the Slave Delta, using stable isotope methods. Unpublished Undergraduate Honours Thesis, University of Waterloo, Department of Earth Sciences.

Krisnaswami, S., Lal, D., Martin, J. M., and Meybeck, M., 1971. Geochronology of Lake Sediments. Earth and Planetary Science Letters 11: 407-414

Liu, K., 2004. A paleolimnological assessment of past changes in hydrological and ecological conditions at pond SD2 in the Slave River Delta, N.W.T. Unpublished Undergraduate Honours Thesis, University of Waterloo, Department of Biology.

Longmore, M. E., 1982. The cesium dating technique and associated applications in Australia. In: Ambrose, W., and Duerden, P., (eds). Archaeometry: An Australian Perspective. ANU Press, Canberra, pp 310-321.

Mann, M. E., Raymond, B. S., and Hughes, M. K., 1999. Northern hemisphere temperatures during the past millennium: inferences, uncertainties, and limitations. Geophysical Research Letters 26: 759-762.

Meyers, P. A., and Teranes, J. L., 2001. Sediment Organic Matter. In: Last, W. M., and Smol, J. P., (eds.). Tracking Environmental Change Using Lake Sediments: Physical and Geochemical Methods, vol. 2. Kluwer Academic Publishers, Dordrect, The Netherlands, pp 239-269.

Milburn, D., MacDonald, D. D., Prowse, T. D., and Culp, J. M., 1999. Ecosystem maintenance indicators for the Slave River Delta, N. W. T., Canada. In: Pykh, Y. A., Hyatt, D. E., and Lenz, R. J. M., (eds.). Environmental Indices Systems Analysis Approach. EOLSS Publishers Co LTD, Oxford, UK, pp 329-348.

Natural Resources Canada, 2003. Discover Canada Through National Maps and Facts; Facts About Canada; Rivers. http://atlas.gc.ca/site/english/learningresources/facts/macriver.jpg/image_view (accessed January 5, 2004).

Pietroniro, A., Prowse, T., Peters, D. L., 1999. Hydrologic assessment of an inland freshwater delta using multi-temporal satellite remote sensing. Hydrological Processes 13: 2483-2498.

Prowse, T. D., and Beltaos, S., 2002. Climatic control of river-ice hydrology: a review. Hydrological Processes 16: 805-822.

Prowse, T. D., Conly, F. M., Church, M., and English, M. C., 2002. A review of hydroecological results of the Northern River Basins Study, Canada, Part 1. Peace and Slave Rivers. River and Research Applications 18: 429-446.

Prowse, T. D., Peters, D., Beltaos, S., Pietroniro, A., Romolo, L., Toyra, J., and Leconte, R. 2002. Restoring ice-jam floodwater to a drying delta ecosystem. Water International 27: 58-69.

Smol, J. P., 2002. Key Issues in Environmental Change: Pollution of Lakes and Rivers, A Paleoenvironmental Perspective. Oxford University Press Inc, New York, pp 228.

Sokal, M. A., 2007. Assessment of hydroecological changes at the Slave River Delta, NWT, using diatoms in seasonal, inter-annual and paleolimnological experiments. Unpublished PhD Thesis, Department of Biology, University of Waterloo.

Sternberg, L., DeNiro, M. J., and Keeley, J. E., 1984. Hydrogen, oxygen, and carbon isotope ratios of cellulose from submerged aquatic crassulacean acid metabolism and non-crassulacean acid metabolism plants. Plant Physiology 76: 68-70.

Timoney, K., 2002. A dying delta? A case study of a wetland paradigm. Wetlands 22: 282-300.

Tyson, R. V., 1995. Sedimentary Organic Matter. Chapman and Hall. London, pp. 615.

Water Survey of Canada, 2006. National Water Quantity Survey Program. Environment Canada.

Wesche, S., 2007. Adapting to change in Canada's North: voices from Fort Resolution, NWT. Meridian, Canadian Polar Commission. Spring/Summer issue, pp. 19-24.

Wolfe, B. B., Edwards, T. W. D., Elgood, R. J., and Beuning, K. R. M., 2001. Carbon and oxygen isotope analysis of lake sediment cellulose: methods and applications. In: Last, W. M., and Smol, J. P., (eds.). Tracking Environmental Change Using Lake Sediments: Physical and Geochemical Methods, vol. 2. Kluwer Academic Publishers, Dordrecht, Netherlands, pp 373-400.

Wolfe, B. B., Karst-Riddoch, T. L., Vardy, S. R., Falcone, M. D., Hall, R. I., and Edwards, T. W. D., 2005. Impacts of climate and river flooding on the hydro-ecology of a floodplain basin, Peace-Athabasca Delta, Canada since A.D. 1700. Quaternary Research 64: 147-162.

Wolfe, B.B., Hall, R.I., Last, W.M., Edwards, T.W.D., English, M.C., Karst-Riddoch, T.L., Paterson, A., and Palmini, R., 2006. Reconstruction of multi-century flood histories from oxbow lake sediments, Peace-Athabasca Delta, Canada. Hydrological Processes 20: 4131-4153.

Wolfe, B. B., Falcone, M. D., Clogg-Wright, K. P., Mongeon, C. L., Yi Y, Brock, B. E., St. Amour, N. A., Mark, W. A., and Edwards, T. W. D., 2007a. Progress in isotope paleohydrology using lake sediment cellulose. Journal of Paleolomnology 37: 221-231.

Wolfe, B. B., Armitage, D., Wesche S., Brock, B. E., Sokal, M. A., Clogg-Wright, K. P., Mongeon, C. L., Adam, M. E., Hall, R. I., and Edwards, T. W. D., 2007b. From Isotopes to TK interviews: towards interdisciplinary research in Fort Resolution and the Slave River Delta, Northwest Territories. Arctic 60: 75-87.

Appendix A

Water $\delta^{18}O$ and $\delta^{2}H$ Results for SD2, SD28, SD20 and the Slave River (SR3) (2003 - 2005)

	SD2		SD28		SD20		SR3	
Date	$\delta^{18}O$	$\delta^{2}H$	$\delta^{18}O$	$\delta^{2}H$	$\delta^{18}O$	$\delta^{2}H$	$\delta^{18}O$	$\delta^{2}H$
5/23/2003	-19.2	-155	-17.0	-141	-13.7	-127	-19.0	-151
6/10/2003	-17.8	-148	-16.6	-140				
6/13/2003							-18.4	-147
6/23/2003	-16.9	-144	-15.4	-134	-12.8	-122	-18.3	-147
7/6/2003	-16.0	-140	-14.7	-132				
7/9/2003							-18.5	-147
7/25/2003	-14.8	-134	-14.6	-130	-11.7	-118	-17.9	-145
8/2/2003	-14.3	-129	-14.6	-128				
8/4/2003							-17.6	-143
8/15/2003	-13.8	-127	-14.1	-128	-10.9	-114	-17.3	-141
9/4/2003	-16.3	-136	-15.1	-131			-16.8	-139
10/14/2003	-16.5	-133	-14.2	-128			-17.0	-140
5/31/2004	-16.2	-139	-16.5	-142	-12.7	-123	-17.7	-144
7/20/2004	-14.8	-126	-14.7	-134	-11.2	-118		
7/21/2004							-18.1	-146
8/18/2004	-10.9	-117						
8/19/2004			-13.7	-128			-17.5	-143
9/20/2004	-11.5	-120	-14.6	-132	-10.8	-115	-18.1	-145
5/17/2005	-19.0	-152	-18.5	-152	-12.6	-122	-18.6	-148
7/22/2005	-14.3	-132	-15.5	-134	-10.4	-115	-18.1	-144
9/22/2005	-13.6	-126	-14.8	-131	-10.5	-115	-16.8	-138

Appendix B

SD20 KB-1, SD2 KB-5 and SD28 KB-5 Sediment Core Chronologies

SD20 KB-1 Sediment Core Chronology

SD20 KB1, Slave River Delta, NWT

Dating File - using sifted Pb-210

Core Information:

	Calendar	Numeric	Decimal
Coring Date:	25-Sep-02	37524	2002.00

LOI:

DSPEC Data:

BACKGROUND Pb-210 =	1.259
Minimum positive background value =	0.101

Depth Interval (cm)		mid-depth	Section thicknes	Dry density, ρ (g/cm3)	Dry mass (g/cm2)	Cumulative dry mass	SIFTED Pb-210 (dpm/g)	Bi-214 (dpm/g)	Cs-137 (dpm/g)	Interpolated Pb-210 (dpm/g)	Interpolated Bi-214 (dpm/g)
0.0	0.5	0.25	0.5	0.0841	0.0421	0.0421	19.506	0.719	2.338	19.506	0.719
0.5	1.0	0.75	0.5	0.1025	0.0513	0.0933	15.986	1.193	1.991	15.986	1.193
1.0	1.5	1.25	0.5	0.0921	0.0461	0.1394	12.451	1.318	3.177	12.451	1.318
1.5	2.0	1.75	0.5	0.1178	0.0589	0.1983	12.320	0.794	1.693	12.320	0.794
2.0	2.5	2.25	0.5	0.1082	0.0541	0.2524	11.175	2.110	3.376	11.175	2.110
2.5	3.0	2.75	0.5	0.0943	0.0471	0.2995		1.148	2.855	10.464	1.148
3.0	3.5	3.25	0.5	0.1192	0.0596	0.3591	9.754	0.101	3.519	9.754	0.101
3.5	4.0	3.75	0.5	0.1291	0.0645	0.4237	11.505	0.340	3.836	11.505	0.340
4.0	4.5	4.25	0.5	0.1340	0.0670	0.4907	8.405	2.741	5.001	8.405	2.741
4.5	5.0	4.75	0.5	0.1677	0.0839	0.5745	6.908	2.151	3.924	6.908	2.151
5.0	5.5	5.25	0.5	0.1658	0.0829	0.6574	7.628	1.419	4.133	7.628	1.419
5.5	6.0	5.75	0.5	0.1550	0.0775	0.7349	7.927	1.060	3.918	7.927	1.060
6.0	6.5	6.25	0.5	0.1773	0.0886	0.8236				6.886	1.334
6.5	7.0	6.75	0.5	0.2298	0.1149	0.9385	5.845	1.608	1.915	5.845	1.608
7.0	7.5	7.25	0.5	0.1784	0.0892	1.0277				7.148	1.295
7.5	8.0	7.75	0.5	0.1861	0.0931	1.1207	8.451	0.981	2.627	8.451	0.981
8.0	8.5	8.25	0.5	0.2767	0.1383	1.2591				6.345	1.094
8.5	9.0	8.75	0.5	0.2688	0.1344	1.3935	4.240	1.206	1.139	4.240	1.206
9.0	9.5	9.25	0.5	0.2629	0.1315	1.5249				4.094	1.288
9.5	10.0	9.75	0.5	0.2580	0.1290	1.6539				3.948	1.370
10.0	10.5	10.25	0.5	0.3600	0.1800	1.8339				3.802	1.452
10.5	11.0	10.75	0.5	0.2944	0.1472	1.9811	3.656	1.535	0.909	3.656	1.535
11.0	11.5	11.25	0.5	0.3399	0.1699	2.1511				3.604	1.595
11.5	12.0	11.75	0.5	0.3031	0.1515	2.3026	3.552	1.654	0.545	3.552	1.654
12.0	12.5	12.25	0.5	0.3518	0.1759	2.4785				3.413	1.652
12.5	13.0	12.75	0.5	0.3902	0.1951	2.6736				3.275	1.649
13.0	13.5	13.25	0.5	0.3709	0.1854	2.8590				3.136	1.647
13.5	14.0	13.75	0.5	0.5079	0.2540	3.1130				2.998	1.644
14.0	14.5	14.25	0.5	0.4553	0.2276	3.3407				2.859	1.642
14.5	15.0	14.75	0.5	0.4414	0.2207	3.5613				2.721	1.639
15.0	15.5	15.25	0.5	0.4678	0.2339	3.7952				2.582	1.637
15.5	16.0	15.75	0.5	0.4512	0.2256	4.0209				2.444	1.634
16.0	16.5	16.25	0.5	0.6071	0.3036	4.3244				2.305	1.632
16.5	17.0	16.75	0.5	0.5883	0.2942	4.6186	2.167	1.629	-0.037	2.167	1.629
17.0	17.5	17.25	0.5	0.6522	0.3261	4.9447				1.914	1.677
17.5	18.0	17.75	0.5	0.5039	0.2520	5.1966	1.661	1.725	0.262	1.661	1.725
18.0	18.5	18.25	0.5	0.6060	0.3030	5.4997				1.661	1.725
18.5	19.0	18.75	0.5	0.4945	0.2473	5.7469				1.661	1.725
19.0	20.0	19.50	1.0	0.3489	0.3489	6.0958				1.661	1.725
20.0	20.5	20.25	0.5	0.6068	0.3034	6.3992				1.661	1.725
20.5	21.0	20.75	0.5	0.5024	0.2512	6.6504				1.661	1.725
21.0	21.5	21.25	0.5	0.5230	0.2615	6.9119				1.661	1.725
21.5	22.0	21.75	0.5	0.6655	0.3328	7.2447				1.661	1.725
22.0	22.5	22.25	0.5	0.6829	0.3414	7.5861				1.661	1.725
22.5	23.0	22.75	0.5	0.4391	0.2196	7.8057				1.661	1.725
23	23.5	23.25	0.5	0.6936	0.3468	8.1525				1.661	1.725
23.5	24.0	23.75	0.5	0.7684	0.3842	8.5367				1.661	1.725
24	24.5	24.25	0.5	0.6392	0.3196	8.8563				1.661	1.725
24.5	25.0	24.75	0.5	0.7107	0.3553	9.2116				1.661	1.725
25	25.5	25.25	0.5	0.7221	0.3611	9.5727				1.661	1.725
25.5	26.0	25.75	0.5	0.6067	0.3034	9.8761				1.661	1.725
26	26.5	26.25	0.5	0.7706	0.3853	10.2614				1.661	1.725
26.5	27.0	26.75	0.5	0.5794	0.2897	10.5511				1.661	1.725
27.0	27.5	27.25	0.5	0.8139	0.4069	10.9580				1.661	1.725

SD20 KB-1 Sediment Core Chronology

Unsupported Pb-210 (CRS Model):

Unsupported Pb-210 Measured - background (dpm/g)	Unsupported Pb-210 per interval (dpm/cm2)	Unsupported Pb-210 cumulative mass (dpm/cm2)	$t = \frac{1}{\lambda}\ln\left(\frac{A(0)}{A}\right)$ CRS Date (Year AD)
18.247	0.77	16.37	2002.0
14.727	0.75	15.60	2000.5
11.192	0.52	14.85	1998.9
11.061	0.65	14.33	1997.7
9.916	0.54	13.68	1996.2
9.205	0.43	13.14	1995.0
8.495	0.51	12.71	1993.9
10.245	0.66	12.20	1992.6
7.146	0.48	11.54	1990.8
5.649	0.47	11.06	1989.4
6.369	0.53	10.59	1988.0
6.667	0.52	10.06	1986.4
5.627	0.50	9.55	1984.7
4.586	0.53	9.05	1983.0
5.889	0.53	8.52	1981.0
7.192	0.67	7.99	1979.0
5.086	0.70	7.33	1976.2
2.981	0.40	6.62	1972.9
2.835	0.37	6.22	1970.9
2.689	0.35	5.85	1968.9
2.543	0.46	5.50	1967.0
2.397	0.35	5.04	1964.2
2.345	0.40	4.69	1961.9
2.293	0.35	4.29	1959.0
2.154	0.38	3.95	1956.3
2.016	0.39	3.57	1953.1
1.877	0.35	3.17	1949.3
1.739	0.44	2.82	1945.6
1.600	0.36	2.38	1940.1
1.462	0.32	2.02	1934.8
1.323	0.31	1.70	1929.2
1.184	0.27	1.39	1922.7
1.046	0.32	1.12	1915.9
0.907	0.27	0.80	1905.2
0.654	0.21	0.54	1892.2
0.401	0.10	0.32	1875.8
0.401	0.12	0.22	1863.7
0.401	0.10	0.10	1838.0
0.401			
0.401			
0.401			
0.401			
0.401			
0.401			
0.401			
0.401			
0.401			
0.401			
0.401			
0.401			
0.401			
0.401			
0.401			
0.401			
0.401			

Sedimentation Rate:

Sed Rate. (dry mass sedimentation) (g/cm2 yr)	Sed Rate 0.305 (cm/yr)
0.028	0.332
0.033	0.322
0.041	0.449
0.040	0.343
0.043	0.397
0.044	0.472
0.047	0.391
0.037	0.287
0.050	0.375
0.061	0.364
0.052	0.312
0.047	0.303
0.053	0.298
0.061	0.267
0.045	0.253
0.035	0.186
0.045	0.162
0.069	0.257
0.068	0.260
0.068	0.263
0.067	0.187
0.066	0.223
0.062	0.183
0.058	0.192
0.057	0.162
0.055	0.141
0.053	0.142
0.051	0.100
0.046	0.102
0.043	0.097
0.040	0.085
0.036	0.081
0.033	0.055
0.028	0.047
0.025	0.039
0.025	0.050
0.017	0.028
0.008	0.016
0.000	0.000
0.000	0.000
0.000	0.000
0.000	0.000
0.000	0.000
0.000	0.000
0.000	0.000
0.000	0.000
0.000	0.000
0.000	0.000
0.000	0.000
0.000	0.000
0.000	0.000
0.000	0.000
0.000	0.000
0.000	0.000
0.000	0.000

Extrapolating Entire Profile:

Bottom Sed Rate 0.060 (g/cm2 yr)	(sed rate method) CRS Dates + Extrapolated (year AD)	Mid-depth (cm)
	2002.0	0.25
	2000.5	0.75
	1998.9	1.25
	1997.7	1.75
	1996.2	2.25
	1995.0	2.75
	1993.9	3.25
	1992.6	3.75
	1990.8	4.25
	1989.4	4.75
	1988.0	5.25
	1986.4	5.75
	1984.7	6.25
	1983.0	6.75
	1981.0	7.25
	1979.0	7.75
	1976.2	8.25
	1972.9	8.75
	1970.9	9.25
	1968.9	9.75
	1967.0	10.25
	1964.2	10.75
	1961.9	11.25
	1959.0	11.75
	1956.3	12.25
	1953.1	12.75
	1949.3	13.25
	1945.6	13.75
	1940.1	14.25
	1934.8	14.75
	1929.2	15.25
	1922.7	15.75
	1915.9	16.25
	1905.2	16.75
	1892.2	17.25
	1875.8	17.75
	1863.7	18.25
	1859.6	18.75
	1853.8	19.50
	1848.8	20.25
	1844.6	20.75
	1840.3	21.25
	1834.8	21.75
	1829.1	22.25
	1825.5	22.75
	1819.7	23.25
	1813.4	23.75
	1808.1	24.25
	1802.2	24.75
	1796.2	25.25
	1791.1	25.75
	1784.7	26.25
	1779.9	26.75
	1773.2	27.25

SD2 KB-5 Sediment Core Chronology

SD2 KB5, Slave River Delta, NWT

Dating File - using sifted Pb-210

Core Information:

	Calendar	Numeric	Decimal
Coring Date:	25-Jul-04	38193	2004.00

LOI:

DSPEC Data:

BACKGROUND (Bi-214 avg) =	1.578
Minimum (Bi-214) background value =	1.164

Depth Interval (cm)		mid-depth	Section thickness	Dry density, ρ (g/cm3)	Dry mass (g/cm2)	Cumulative dry mass	SIFTED Pb-210 (dpm/g)	Bi-214 (dpm/g)	Cs-137 (dpm/g)	Interpolated Pb-210 (dpm/g)	Interpolated Bi-214 (dpm/g)
0.0	0.5	0.25	0.5	0.3174	0.1587	0.1587	2.435	1.348	0.187	2.435	1.348
0.5	1.0	0.75	0.5	0.2984	0.1492	0.3079	4.175	1.414	0.040	4.175	1.414
1.0	1.5	1.25	0.5	0.4303	0.2151	0.5231		1.720	0.018	4.135	1.720
1.5	2.0	1.75	0.5	0.6271	0.3136	0.8366				4.095	1.683
2.0	2.5	2.25	0.5	0.7958	0.3979	1.2346		1.647	0.078	4.055	1.647
2.5	3.0	2.75	0.5	1.0839	0.5420	1.7765				4.015	1.676
3.0	3.5	3.25	0.5	1.0358	0.5179	2.2944		1.706	0.029	3.974	1.706
3.5	4.0	3.75	0.5	1.1548	0.5774	2.8718				3.934	1.734
4.0	4.5	4.25	0.5	1.3283	0.6642	3.5360				3.894	1.761
4.5	5.0	4.75	0.5	1.1395	0.5698	4.1057				3.854	1.789
5.0	5.5	5.25	0.5	1.2696	0.6348	4.7405				3.814	1.816
5.5	6.0	5.75	0.5	1.2701	0.6351	5.3756				3.773	1.844
6.0	6.5	6.25	0.5	1.0676	0.5338	5.9094		1.871	0.019	3.733	1.871
6.5	7.0	6.75	0.5	0.9407	0.4703	6.3797				3.693	1.867
7.0	7.5	7.25	0.5	1.0536	0.5268	6.9065				3.653	1.864
7.5	8.0	7.75	0.5	1.1485	0.5743	7.4807				3.612	1.860
8.0	8.5	8.25	0.5	1.0102	0.5051	7.9858				3.572	1.856
8.5	9.0	8.75	0.5	1.0642	0.5321	8.5179	3.532	1.852	0.103	3.532	1.852
9.0	9.5	9.25	0.5	1.3029	0.6514	9.1694				3.293	1.800
9.5	10.0	9.75	0.5	1.3690	0.6845	9.8539				3.054	1.748
10.0	10.5	10.25	0.5	1.0193	0.5097	10.3635				2.814	1.695
10.5	11.0	10.75	0.5	0.9841	0.4920	10.8556	2.575	1.643	0.182	2.575	1.643
11.0	11.5	11.25	0.5	0.9745	0.4873	11.3428				2.518	1.771
11.5	12.0	11.75	0.5	0.9723	0.4861	11.8290	2.462	1.899	0.085	2.462	1.899
12.0	12.5	12.25	0.5	1.2436	0.6218	12.4508				2.582	1.793
12.5	13.0	12.75	0.5	1.0125	0.5062	12.9570				2.702	1.686
13.0	13.5	13.25	0.5	1.0477	0.5239	13.4809				2.823	1.580
13.5	14.0	13.75	0.5	1.0701	0.5350	14.0159	2.943	1.473	0.106	2.943	1.473
14.0	14.5	14.25	0.5	1.0325	0.5162	14.5321				2.857	1.596
14.5	15.0	14.75	0.5	1.4859	0.7429	15.2751				2.771	1.719
15.0	15.5	15.25	0.5	1.3771	0.6886	15.9636				2.685	1.841
15.5	16.0	15.75	0.5	1.4147	0.7073	16.6710		1.964	0.108	2.599	1.964
16.0	16.5	16.25	0.5	1.3427	0.6714	17.3423				2.513	1.749
16.5	17.0	16.75	0.5	1.4221	0.7110	18.0534	2.427	1.533	0.139	2.427	1.533
17.0	17.5	17.25	0.5	1.3272	0.6636	18.7169				2.683	1.769
17.5	18.0	17.75	0.5	1.4816	0.7408	19.4578	2.938	2.006	0.215	2.938	2.006
18.0	18.5	18.25	0.5	1.4549	0.7274	20.1852	2.645	1.779	0.291	2.645	1.779
18.5	19.0	18.75	0.5	1.5354	0.7677	20.9529	2.300	1.367	0.318	2.300	1.367
19.0	19.5	19.25	0.5	1.6166	0.8083	21.7612	1.974	1.339	0.224	1.974	1.339
19.5	20.0	19.75	0.5	1.9148	0.9574	22.7187	2.717	1.617	0.158	2.717	1.617
20.0	20.5	20.25	0.5	1.3994	0.6997	23.4183	2.227	1.519	0.268	2.227	1.519
20.5	21.0	20.75	0.5	1.5646	0.7823	24.2006	1.716	1.342	0.143	1.716	1.342
21.0	21.5	21.25	0.5	1.5704	0.7852	24.9859				1.947	1.365
21.5	22.0	21.75	0.5	1.4259	0.7129	25.6988				2.178	1.388
22.0	22.5	22.25	0.5	1.5442	0.7721	26.4709	2.409	1.412	0.225	2.409	1.412
22.5	23.0	22.75	0.5	1.4179	0.7090	27.1799				2.285	1.613
23.0	23.5	23.25	0.5	1.4012	0.7006	27.8805	2.162	1.814	0.389	2.162	1.814
23.5	24.0	23.75	0.5	1.4808	0.7404	28.6209	1.919	1.398	0.783	1.919	1.398
24.0	24.5	24.25	0.5	1.9033	0.9516	29.5725	2.505	1.405	0.479	2.505	1.405
24.5	25.0	24.75	0.5	0.7677	0.3839	29.9564				2.253	1.551
25.0	25.5	25.25	0.5	1.2501	0.6251	30.5815	2.001	1.696	1.240	2.001	1.696
25.5	26.0	25.75	0.5	1.5667	0.7834	31.3648				1.994	1.602

SD2 KB-5 Sediment Core Chronology

26.0	26.5	26.25	0.5	1.7998	0.8999	32.2647	1.987	1.508	0.194	1.987	1.508
26.5	27.0	26.75	0.5	1.2554	0.6277	32.8924	2.545	1.385	0.703	2.545	1.385
27.0	27.5	27.25	0.5	0.9414	0.4707	33.3631				2.559	1.476
27.5	28.0	27.75	0.5	1.1903	0.5952	33.9583	2.572	1.568	0.832	2.572	1.568
28.0	28.5	28.25	0.5	1.2504	0.6252	34.5835				2.208	1.524
28.5	29.0	28.75	0.5	1.1110	0.5555	35.1390	1.843	1.479	0.527	1.843	1.479
29.0	29.5	29.25	0.5	1.1433	0.5717	35.7106	2.797	1.323	0.288	2.797	1.323
29.5	30.0	29.75	0.5	0.9869	0.4934	36.2041				2.468	1.439
30.0	30.5	30.25	0.5	1.1889	0.5945	36.7985	2.138	1.554	0.172	2.138	1.554
30.5	31.0	30.75	0.5	1.2058	0.6029	37.4014	1.970	1.391	0.046	1.970	1.391
31.0	31.5	31.25	0.5	1.3265	0.6633	38.0647				2.212	1.410
31.5	32.0	31.75	0.5	1.2165	0.6082	38.6729				2.453	1.430
32.0	32.5	32.25	0.5	1.2499	0.6249	39.2978	2.695	1.449	0.053	2.695	1.449
32.5	33.0	32.75	0.5	1.5077	0.7538	40.0517				2.324	1.307
33.0	33.5	33.25	0.5	1.4154	0.7077	40.7594	1.953	1.164	0.005	1.953	1.164
33.5	34.0	33.75	0.5	1.1962	0.5981	41.3575				1.945	1.257
34.0	34.5	34.25	0.5	1.4237	0.7119	42.0693				1.937	1.350
34.5	35.0	34.75	0.5	1.5765	0.7882	42.8576				1.929	1.443
35.0	35.5	35.25	0.5	1.2180	0.6090	43.4666	1.921	1.536	0.002	1.921	1.536
35.5	36.0	35.75	0.5	1.5419	0.7710	44.2375				1.842	1.558
36.0	36.5	36.25	0.5	1.5277	0.7639	45.0014				1.763	1.581
36.5	37.0	36.75	0.5	1.5485	0.7742	45.7756	1.684	1.604	0.022	1.684	1.604
37.0	37.5	37.25	0.5	1.4030	0.7015	46.4771				1.841	1.595
37.5	38.0	37.75	0.5	1.6671	0.8336	47.3107	1.997	1.586	0.042	1.997	1.586
38.0	38.5	38.25	0.5	1.4346	0.7173	48.0280				1.936	1.556
38.5	39.0	38.75	0.5	1.4594	0.7297	48.7577	1.875	1.526	-0.071	1.875	1.526
39.0	39.5	39.25	0.5	1.5379	0.7690	49.5267				1.968	1.483
39.5	40.0	39.75	0.5	1.6000	0.8000	50.3267				2.062	1.439
40.0	40.5	40.25	0.5	1.5863	0.7931	51.1198				2.155	1.396
40.5	41.0	40.75	0.5	1.7121	0.8560	51.9758				2.248	1.352
41.0	41.5	41.25	0.5	1.7365	0.8682	52.8441				2.342	1.308
41.5	42.0	41.75	0.5	1.3809	0.6904	53.5345	2.435	1.265	0.116	2.435	1.265
42.0	42.5	42.25	0.5	1.3821	0.6911	54.2255				2.687	1.412
42.5	43.0	42.75	0.5	0.8617	0.4308	54.6564	2.939	1.559	-0.011	2.939	1.559
43.0	43.5	43.25	0.5	1.0860	0.5430	55.1994				2.571	1.587
43.5	44.0	43.75	0.5	1.1499	0.5749	55.7743				2.203	1.614
44.0	44.5	44.25	0.5	1.4304	0.7152	56.4895	1.836	1.642	-0.077	1.836	1.642
44.5	45.0	44.75	0.5	1.8379	0.9190	57.4085				2.050	1.859
45.0	45.5	45.25	0.5	1.3220	0.6610	58.0694	2.265	2.076	-0.073	2.265	2.076
45.5	46.0	45.75	0.5	1.5784	0.7892	58.8586				2.359	1.849
46.0	46.5	46.25	0.5	1.2008	0.6004	59.4591	2.453	1.623	-0.094	2.453	1.623
46.5	47.5	47.00	1.0	1.0042	1.0042	60.4632				2.617	1.652
47.5	48.0	47.75	0.5	1.3900	0.6950	61.1582				2.781	1.682
48.0	48.5	48.25	0.5	0.9864	0.4932	61.6514	2.945	1.712	-0.037	2.945	1.712
48.5	49.0	48.75	0.5	1.3943	0.6972	62.3486	2.827	1.717	0.055	2.827	1.717

SD2 KB-5 Sediment Core Chronology

Unsupported Pb-210 (CRS Model):

Cesium-137 Peak:

Cs-137 depth	Cs-137 (Year AD)	Cs-137 ± error
25.25	1963	1 cm

Sedimentation Rate:

Sed Rate. (dry mass sedimentation) (g/cm2 yr)	Sed Rate 0.653 (cm/yr)
1.944	6.124
0.640	2.145
0.645	1.500
0.649	1.035
0.649	0.816
0.648	0.597
0.641	0.619
0.636	0.551
0.629	0.473
0.619	0.543
0.612	0.482
0.603	0.475
0.594	0.556
0.588	0.625
0.585	0.555
0.580	0.505
0.573	0.567
0.569	0.534
0.629	0.483
0.708	0.517
0.819	0.804
0.996	1.012
1.040	1.067
1.090	1.121
0.946	0.761
0.828	0.817
0.733	0.700
0.654	0.611
0.680	0.659
0.712	0.479
0.742	0.539
0.781	0.552
0.829	0.618
0.890	0.626
0.667	0.503
0.525	0.355
0.640	0.440
0.913	0.594
1.618	1.001
0.554	0.289
0.921	0.658
4.221	2.698

Final Chronology:

137Cs Model *constant sed rate=* 0.616 cm/yr Year
2004.0
2003.2
2002.4
2001.6
2000.8
1999.9
1999.1
1998.3
1997.5
1996.7
1995.9
1995.1
1994.3
1993.4
1992.6
1991.8
1991.0
1990.2
1989.4
1988.6
1987.8
1987.0
1986.1
1985.3
1984.5
1983.7
1982.9
1982.1
1981.3
1980.5
1979.6
1978.8
1978.0
1977.2
1976.4
1975.6
1974.8
1974.0
1973.1
1972.3
1971.5
1970.7

Unsupported Pb-210 Measured - background (dpm/g)	Unsupported Pb-210 per interval (dpm/cm2)	Unsupported Pb-210 cumulative mass (dpm/cm2)	$t = \frac{1}{\lambda}\ln\left(\frac{A(0)}{A}\right)$ CRS Date (Year AD)
0.857	0.14	53.52	2004.00
2.597	0.39	53.38	2003.92
2.557	0.55	52.99	2003.68
2.517	0.79	52.44	2003.35
2.477	0.99	51.65	2002.86
2.437	1.32	50.67	2002.24
2.396	1.24	49.35	2001.40
2.356	1.36	48.11	2000.58
2.316	1.54	46.75	1999.66
2.276	1.30	45.21	1998.58
2.236	1.42	43.91	1997.65
2.195	1.39	42.49	1996.59
2.155	1.15	41.10	1995.52
2.115	0.99	39.95	1994.61
2.075	1.09	38.95	1993.80
2.034	1.17	37.86	1992.89
1.994	1.01	36.69	1991.88
1.954	1.04	35.69	1990.99
1.715	1.12	34.65	1990.04
1.476	1.01	33.53	1988.98
1.236	0.63	32.52	1988.00
0.997	0.49	31.89	1987.37
0.940	0.46	31.40	1986.88
0.884	0.43	30.94	1986.40
1.004	0.62	30.51	1985.95
1.125	0.57	29.89	1985.29
1.245	0.65	29.32	1984.67
1.365	0.73	28.66	1983.95
1.279	0.66	27.93	1983.12
1.193	0.89	27.27	1982.35
1.107	0.76	26.39	1981.29
1.021	0.72	25.62	1980.35
0.935	0.63	24.90	1979.43
0.849	0.60	24.27	1978.61
1.105	0.73	23.67	1977.80
1.360	1.01	22.94	1976.79
1.067	0.78	21.93	1975.35
0.722	0.55	21.15	1974.19
0.396	0.32	20.60	1973.34
1.139	1.09	20.28	1972.84
0.649	0.45	19.19	1971.06
0.138	0.11	18.73	1970.29

SD2 KB-5 Sediment Core Chronology

0.369	0.29	18.63	1970.11
0.600	0.43	18.34	1969.60
0.831	0.64	17.91	1968.85
0.707	0.50	17.27	1967.67
0.584	0.41	16.77	1966.73
0.341	0.25	16.36	1965.93
0.927	0.88	16.10	1965.44
0.675	0.26	15.22	1963.63
0.423	0.26	14.96	1963.08
0.416	0.33	14.70	1962.50
0.409	0.37	14.37	1961.78
0.967	0.61	14.01	1960.95
0.981	0.46	13.40	1959.53
0.994	0.59	12.94	1958.40
0.630	0.39	12.35	1956.90
0.265	0.15	11.95	1955.86
1.219	0.70	11.80	1955.46
0.890	0.44	11.11	1953.50
0.560	0.33	10.67	1952.21
0.392	0.24	10.34	1951.19
0.634	0.42	10.10	1950.45
0.875	0.53	9.68	1949.08
1.117	0.70	9.15	1947.27
0.746	0.56	8.45	1944.72
0.375	0.27	7.89	1942.50
0.367	0.22	7.62	1941.40
0.359	0.26	7.40	1940.46
0.351	0.28	7.14	1939.34
0.343	0.21	6.87	1938.07
0.264	0.20	6.66	1937.08
0.185	0.14	6.46	1936.08
0.106	0.08	6.31	1935.37
0.263	0.18	6.23	
0.419	0.35	6.05	
0.358	0.26	5.70	
0.297	0.22	5.44	
0.390	0.30	5.23	
0.484	0.39	4.93	
0.577	0.46	4.54	
0.670	0.57	4.08	
0.764	0.66	3.51	
0.857	0.59	2.84	
1.109	0.77	2.25	
1.361	0.59	1.49	
0.993	0.54	0.90	
0.626	0.36	0.36	
0.258			
0.472			
0.687			
0.781			
0.875			
1.039			
1.203			
1.367			
1.249			

1.572	1.001
0.952	0.668
0.671	0.435
0.760	0.536
0.894	0.638
1.495	1.010
0.541	0.284
0.702	0.915
1.102	0.881
1.101	0.703
1.095	0.608
0.451	0.359
0.425	0.452
0.405	0.340
0.611	0.488
1.403	1.263
0.302	0.264
0.389	0.394
0.593	0.499
0.822	0.681
0.496	0.374
0.344	0.283
0.255	0.204
0.352	0.234
0.654	0.462
0.646	0.540
0.642	0.451
0.634	0.402
0.624	0.512
0.786	0.510
1.086	0.711
1.849	1.194
0.739	0.527
0.450	0.270
0.496	0.346
0.571	0.391
0.417	0.271
0.317	0.198
0.245	0.154
0.190	0.111
0.143	0.082
0.103	0.075
0.063	0.046
0.034	0.039
0.028	0.026
0.018	0.016

1969.9
1969.1
1968.3
1967.5
1966.7
1965.8
1965.0
1964.2
1963.4
1962.6
1961.8
1961.0
1960.2
1959.3
1958.5
1957.7
1956.9
1956.1
1955.3
1954.5
1953.7
1952.9
1952.0
1951.2
1950.4
1949.6
1948.8
1948.0
1947.2
1946.4
1945.5
1944.7
1943.9
1943.1
1942.3
1941.5
1940.7
1939.9
1939.0
1938.2
1937.4
1936.6
1935.8
1935.0
1934.2
1933.4
1932.6
1931.7
1930.9
1930.1
1929.3
1928.1
1926.9
1926.1
1925.2

SD28 KB-5 Sediment Core Chronology

SD28 KB5, Slave River Delta, NWT

Dating File - using sifted Pb-210

Core Information:

	Calendar	Numeric	Decimal
Coring Date:	25-Sep-02	**37524**	2002.00

LOI:

DSPEC Data:

BACKGROUND Pb-210 =	**1.607**
Minimum positive background value =	**0.956**

Depth Interval (cm)		mid-depth	Section thickness	Dry density, ρ (g/cm3)	Dry mass (g/cm2)	Cumulative dry mass (g/cm2)	SIFTED Pb-210 (dpm/g)	Bi-214 (dpm/g)	Cs-137 (dpm/g)	Interpolated Pb-210 (dpm/g)	Interpolated Bi-214 (dpm/g)
0.0	0.5	0.25	0.5	0.1996	0.0998	0.0998	3.771	1.884	0.122	3.771	1.884
0.5	1.0	0.75	0.5	0.3881	0.1941	0.2939	4.370	0.956	-0.046	4.370	0.956
1.0	1.5	1.25	0.5	0.1996	0.0998	0.3936	3.753	2.208	0.017	3.753	2.208
1.5	2.0	1.75	0.5	0.4003	0.2002	0.5938				3.338	2.197
2.0	2.5	2.25	0.5	0.5684	0.2842	0.8780				2.923	2.186
2.5	3.0	2.75	0.5	0.7041	0.3521	1.2301		2.175	0.120	2.508	2.175
3.0	3.5	3.25	0.5	1.0361	0.5181	1.7481	2.092	1.255	0.021	2.092	1.255
3.5	4.0	3.75	0.5	0.9333	0.4666	2.2148				2.774	1.312
4.0	4.5	4.25	0.5	0.8171	0.4085	2.6233				3.456	1.370
4.5	5.0	4.75	0.5	0.8332	0.4166	3.0399	4.137	1.427	0.141	4.137	1.427
5.0	5.5	5.25	0.5	0.7353	0.3676	3.4075	3.152	1.668	-0.030	3.152	1.668
5.5	6.0	5.75	0.5	0.7004	0.3502	3.7577		1.852	0.220	3.004	1.852
6.0	6.5	6.25	0.5	0.8092	0.4046	4.1624				2.857	1.579
6.5	7.0	6.75	0.5	1.0359	0.5179	4.6803		1.306	0.285	2.709	1.306
7.0	7.5	7.25	0.5	0.9404	0.4702	5.1505		1.684	0.214	2.562	1.684
7.5	8.0	7.75	0.5	0.9838	0.4919	5.6424				2.415	1.603
8.0	8.5	8.25	0.5	0.8509	0.4254	6.0678				2.267	1.522
8.5	9.0	8.75	0.5	0.9020	0.4510	6.5188	2.120	1.442	0.232	2.120	1.442
9.0	9.5	9.25	0.5	1.2829	0.6414	7.1603				2.185	1.505
9.5	10.0	9.75	0.5	1.1132	0.5566	7.7169				2.251	1.568
10.0	10.5	10.25	0.5	0.9716	0.4858	8.2027				2.316	1.631
10.5	11.0	10.75	0.5	0.9304	0.4652	8.6679				2.382	1.694
11.0	11.5	11.25	0.5	0.8469	0.4235	9.0913				2.447	1.757
11.5	12.0	11.75	0.5	0.7748	0.3874	9.4787	2.513	1.820	0.164	2.513	1.820
12.0	12.5	12.25	0.5	0.9545	0.4773	9.9560				2.280	1.743
12.5	13.0	12.75	0.5	1.1361	0.5681	10.5240	2.047	1.666	0.152	2.047	1.666
13.0	13.5	13.25	0.5	0.7570	0.3785	10.9025				2.286	1.682
13.5	14.0	13.75	0.5	0.9966	0.4983	11.4008				2.525	1.698
14.0	14.5	14.25	0.5	1.0101	0.5050	11.9058				2.765	1.715
14.5	15.0	14.75	0.5	1.0834	0.5417	12.4475		1.731	0.336	3.004	1.731
15.0	15.5	15.25	0.5	0.9169	0.4584	12.9060		1.427	0.312	3.243	1.427
15.5	16.0	15.75	0.5	0.9140	0.4570	13.3630				3.482	1.586
16.0	16.5	16.25	0.5	1.0400	0.5200	13.8830	3.721	1.744	0.498	3.721	1.744
16.5	17.0	16.75	0.5	0.9985	0.4992	14.3822				3.636	1.708
17.0	17.5	17.25	0.5	2.0073	1.0037	15.3859				3.552	1.671
18.0	18.5	18.25	0.5	1.1299	0.5649	15.9508		1.635	0.310	3.467	1.635
18.5	19.0	18.75	0.5	1.0322	0.5161	16.4669		1.590	0.407	3.382	1.590
19.0	19.5	19.25	0.5	1.0517	0.5259	16.9928		1.515	0.465	3.298	1.515
19.5	20.0	19.75	0.5	1.0472	0.5236	17.5164				3.213	1.670
20.0	20.5	20.25	0.5	1.1171	0.5585	18.0749				3.129	1.826
20.5	21.0	20.75	0.5	0.7970	0.3985	18.4734		1.982	0.253	3.044	1.982
21.0	21.5	21.25	0.5	1.2601	0.6300	19.1035				2.959	1.638
21.5	22.0	21.75	0.5	0.9190	0.4595	19.5629	2.875	1.294	0.355	2.875	1.294
22.0	22.5	22.25	0.5	1.1871	0.5935	20.1565		1.667	0.336	2.750	1.667

SD28 KB-5 Sediment Core Chronology

22.5	23.0	22.75	0.5	1.0866	0.5433	20.6998				2.625	1.637
23.0	23.5	23.25	0.5	0.8817	0.4409	21.1407				2.500	1.606
23.5	24.0	23.75	0.5	0.8976	0.4488	21.5895	2.375	1.576	0.293	2.375	1.576
24.0	24.5	24.25	0.5	0.9472	0.4736	22.0630				2.318	1.456
24.5	25.0	24.75	0.5	0.7056	0.3528	22.4158	2.261	1.336	0.209	2.261	1.336
25.0	25.5	25.25	0.5	1.0154	0.5077	22.9235				2.246	1.438
25.5	26.0	25.75	0.5	0.9107	0.4554	23.3789				2.231	1.540
26.0	26.5	26.25	0.5	0.8834	0.4417	23.8206				2.217	1.642
26.5	27.0	26.75	0.5	0.8794	0.4397	24.2603		1.744	0.125	2.202	1.744
27.0	27.5	27.25	0.5	0.9614	0.4807	24.7410				2.187	1.528
27.5	28.0	27.75	0.5	1.0168	0.5084	25.2494	2.172	1.312	0.162	2.172	1.312
28.0	28.5	28.25	0.5	0.9320	0.4660	25.7153				2.009	1.590
28.5	29.0	28.75	0.5	0.8257	0.4128	26.1282		1.868	0.369	1.845	1.868
29.0	29.5	29.25	0.5	1.0670	0.5335	26.6617	1.682	1.434	0.350	1.682	1.434
29.5	30.0	29.75	0.5	1.2051	0.6026	27.2642				1.618	1.632
30.0	30.5	30.25	0.5	1.1496	0.5748	27.8390		1.830	0.368	1.554	1.830
30.5	31.0	30.75	0.5	0.9816	0.4908	28.3298				1.491	1.837
31.0	31.5	31.25	0.5	1.1635	0.5817	28.9116		1.844	0.462	1.427	1.844
31.5	32.0	31.75	0.5	1.1200	0.5600	29.4716	1.363	1.484	0.524	1.363	1.484
32.0	32.5	32.25	0.5	0.8328	0.4164	29.8880		1.081	0.402	1.363	1.081
32.5	33.0	32.75	0.5	1.2070	0.6035	30.4915				1.363	1.081

SD28 KB-5 Sediment Core Chronology

Unsupported Pb-210 (CRS Model):

Sedimentation Rate:

Unsupported **Pb-210** Measured - background (dpm/g)	Unsupported **Pb-210** per interval (dpm/cm2)	Unsupported **Pb-210** cumulative mass (dpm/cm2)	$t = \frac{1}{\lambda}\ln\left(\frac{A(0)}{A}\right)$ CRS Date (Year AD)	Sed Rate. (dry mass sedimentation) (g/cm2 yr)	Sed Rate 0.620 (cm/yr)	Bottom Sed Rate 0.231 (g/cm2 yr)	(sed rate method) CRS Dates + Extrapolated (year AD)
2.164	0.22	31.92	2002.0	0.459	2.301		2002.0
2.763	0.54	31.71	2001.8	0.357	0.921		2001.8
2.146	0.21	31.17	2001.2	0.452	2.267		2001.2
1.731	0.35	30.96	2001.0	0.557	1.391		2001.0
1.315	0.37	30.61	2000.7	0.725	1.275		2000.7
0.900	0.32	30.24	2000.3	1.046	1.485		2000.3
0.485	0.25	29.92	1999.9	1.921	1.854		1999.9
1.167	0.54	29.67	1999.6	0.792	0.848		1999.6
1.848	0.76	29.12	1999.1	0.491	0.601		1999.1
2.530	1.05	28.37	1998.2	0.349	0.419		1998.2
1.544	0.57	27.31	1997.0	0.551	0.749		1997.0
1.397	0.49	26.75	1996.3	0.596	0.851		1996.3
1.249	0.51	26.26	1995.7	0.654	0.809		1995.7
1.102	0.57	25.75	1995.1	0.728	0.702		1995.1
0.955	0.45	25.18	1994.4	0.821	0.874		1994.4
0.807	0.40	24.73	1993.8	0.954	0.970		1993.8
0.660	0.28	24.34	1993.3	1.149	1.350		1993.3
0.512	0.23	24.05	1992.9	1.462	1.621		1992.9
0.578	0.37	23.82	1992.6	1.284	1.001		1992.6
0.643	0.36	23.45	1992.1	1.135	1.020		1992.1
0.709	0.34	23.10	1991.6	1.015	1.044		1991.6
0.774	0.36	22.75	1991.1	0.915	0.983		1991.1
0.840	0.36	22.39	1990.6	0.830	0.980		1990.6
0.905	0.35	22.03	1990.1	0.758	0.978		1990.1
0.673	0.32	21.68	1989.6	1.004	1.052		1989.6
0.440	0.25	21.36	1989.1	1.513	1.331		1989.1
0.679	0.26	21.11	1988.7	0.968	1.279		1988.7
0.918	0.46	20.86	1988.3	0.707	0.710		1988.3
1.157	0.58	20.40	1987.6	0.549	0.543		1987.6
1.396	0.76	19.81	1986.7	0.442	0.408		1986.7
1.635	0.75	19.06	1985.4	0.363	0.396		1985.4
1.874	0.86	18.31	1984.1	0.304	0.333		1984.1
2.114	1.10	17.45	1982.6	0.257	0.247		1982.6
2.029	1.01	16.35	1980.5	0.251	0.251		1980.5
1.944	1.95	15.34	1978.5	0.246	0.122		1978.5
1.860	1.05	13.39	1974.1	0.224	0.198		1974.1
1.775	0.92	12.34	1971.5	0.216	0.210		1971.5
1.690	0.89	11.42	1969.0	0.210	0.200		1969.0
1.606	0.84	10.53	1966.4	0.204	0.195		1966.4
1.521	0.85	9.69	1963.7	0.198	0.178		1963.7
1.437	0.57	8.84	1960.8	0.192	0.240		1960.8
1.352	0.85	8.27	1958.6	0.190	0.151		1958.6
1.267	0.58	7.42	1955.1	0.182	0.198		1955.1
1.142	0.68	6.84	1952.5	0.186	0.157		1952.5

SD28 KB-5 Sediment Core Chronology

1.018	0.55	6.16	1949.2	0.188	0.173		1949.2
0.893	0.39	5.60	1946.1	0.196	0.222		1946.1
0.768	0.34	5.21	1943.8	0.211	0.235		1943.8
0.711	0.34	4.87	1941.6	0.213	0.225		1941.6
0.653	0.23	4.53	1939.3	0.216	0.306		1939.3
0.639	0.32	4.30	1937.6	0.210	0.206		1937.6
0.624	0.28	3.98	1935.1	0.198	0.218		1935.1
0.609	0.27	3.69	1932.7	0.189	0.214		1932.7
0.594	0.26	3.42	1930.3	0.179	0.204		1930.3
0.580	0.28	3.16	1927.7	0.170	0.177		1927.7
0.565	0.29	2.88	1924.8	0.159	0.156		1924.8
0.401	0.19	2.59	1921.4	0.201	0.216		1921.4
0.238	0.10	2.41	1919.0	0.315	0.381		1919.0
0.726	0.39	2.31	1917.7	0.099	0.093		1917.7
0.662	0.40	1.92	1911.8	0.090	0.075		1915.1
0.598	0.34	1.52	1904.3	0.079	0.069		1912.6
0.535	0.26	1.18	1896.1	0.069	0.070		1910.4
0.471	0.27	0.92	1888.0	0.061	0.052		1907.9
0.407	0.23	0.64	1876.6	0.049	0.044		1905.5
0.407	0.17	0.42	1862.5	0.032	0.038		1903.7
0.407	0.25	0.25	1845.7	0.019	0.016		1901.1

Appendix C

SD20 KB-1, SD2 KB-5 and SD28 KB-5 LOI Data

SD20 KB-1 LOI Data

LOSS-ON-IGNITION DATA SHEET

Date: 16-May-03
Technician Courtney
Lake name SD 20
Core #: Kb-1

	90°C	550°C	1000°C
Time In	**May 16, 1:00pm**	**May 20, 10:00am**	**May 22, 10:15am**
Time Out	**May 20, 9:30am**	**May 21, 1:00pm**	**May 23, 9:30am**

Sediment Depth (cm)			Crucible #	Crucible	Cruc. + Wet	Cruc. + Dry Sed.	Cruc. + Burnt sed.	Cruc. + Ashed sed.
(Top)	(Bottom)	center		Weight (g)	Sediment (g)	after 90°C (g)	after 550°C (g)	after 1000°C (g)
0.0	0.5	0.25	137	9.1268	9.6496	9.1363	9.1303	9.1301
0.5	1.0	0.75	61	8.5873	9.1152	8.6144	8.5983	8.5977
1.0	1.5	1.25	60	8.5646	9.0571	8.5892	8.5748	8.5739
1.5	2.0	1.75	157	8.3686	8.9025	8.4032	8.3828	8.3813
2.0	2.5	2.25	58	8.2118	8.715	8.2409	8.2237	8.2231
2.5	3.0	2.75	110	8.4789	8.984	8.5159	8.4946	8.4935
3.0	3.5	3.25	156	8.315	8.8138	8.3578	8.3347	8.3335
3.5	4.0	3.75	73	8.5722	9.0564	8.6148	8.593	8.5918
4.0	4.5	4.25	24	8.3947	8.909	8.4489	8.4212	8.4197
4.5	5.0	4.75	70	8.0684	8.5925	8.1225	8.0942	8.0925
5.0	5.5	5.25	95	7.7832	8.2393	7.8393	7.8123	7.8104
5.5	6.0	5.75	120	7.7772	8.2863	7.8506	7.8191	7.8169
6.0	6.5	6.25	133	8.1186	8.6186	8.1868	8.1562	8.1549
6.5	7.0	6.75	2	8.9759	8.4919	9.0374	9.0101	9.0085
7.0	7.5	7.25	37	8.7276	8.2002	8.7843	8.759	8.7579
7.5	8.0	7.75	102	9.436	9.9505	9.5071	9.4775	9.4763
8.0	8.5	8.25	108	8.4962	8.9989	8.5843	8.5524	8.5503
8.5	9.0	8.75	19	8.6462	9.1285	8.7602	8.7255	8.7209
9.0	9.5	9.25	81	8.8546	9.3549	8.9755	8.9385	8.9345
9.5	10.0	9.75	100	8.744	9.1998	8.8457	8.8139	8.8101
10.0	10.5	10.25	101	8.2711	8.819	8.3865	8.3545	8.3483
10.5	11.0	10.75	106	7.7334	8.2361	7.8445	7.8095	7.806
11.0	11.5	11.25	154	8.1355	8.5949	8.2372	8.2089	8.2039
11.5	12.0	11.75	56	8.5044	9.0488	8.6346	8.6009	8.5935
12.0	12.5	12.25	59	8.3685	8.8454	8.5045	8.4712	8.4639
12.5	13.0	12.75	54	9.3584	9.8656	9.4977	9.4632	9.4558
13.0	13.5	13.25	15	8.0487	8.5191	8.191	8.1562	8.149
13.5	14.0	13.75	148	8.4285	8.9528	8.5791	8.5373	8.5315
14.0	14.5	14.25	134	7.9738	8.4425	8.1197	8.0827	8.0774
14.5	15.0	14.75	5	7.7643	8.2403	7.9143	7.8751	7.8689
15.0	15.5	15.25	142	7.8088	8.2627	7.9713	7.9346	7.9272
15.5	16.0	15.75	138	8.2432	8.6944	8.388	*crucible broke lost sediments*	
16.0	16.5	16.25	90	7.2296	7.6847	7.3847	7.3465	7.3393
16.5	17.0	16.75	31	8.4446	8.9758	8.6393	8.592	8.5869
17.0	17.5	17.25	99	8.3864	8.8956	8.5835	8.5412	8.5322
17.5	18.0	17.75	167	8.909	9.4364	9.1147	9.0741	9.0656
18.0	18.5	18.25	77	8.396	8.8874	8.574	8.5341	8.5259
18.5	19.0	18.75	65	8.3105	8.8469	8.497	8.4539	8.4441
19.0	19.5	19.25	*this section was not found. Only 19.0-20.0 was found in the bag					
19	20.0	19.75	34	8.868	9.3445	9.0435	9.002	8.9955
20.0	20.5	20.25	17	8.2422	8.749	8.4282	8.3897	8.3808
20.5	21.0	20.75	11	8.6049	9.1446	8.7937	8.7503	8.7418
21.0	21.5	21.25	38	8.6608	9.1889	8.8557	8.8125	8.8034
21.5	22.0	21.75	98	8.7447	9.2147	8.9327	8.8958	8.8868
22.0	22.5	22.25	12	8.4794	8.9901	8.6671	8.6243	8.6141
22.5	23.0	22.75	92	8.4535	8.9475	8.6515	8.6131	8.6034
23	23.5	23.25	162	8.3347	8.8387	8.5693	8.5301	8.5226
23.5	24.0	23.75	55	8.6693	9.1789	8.888	8.8474	8.8375
24	24.5	24.25	9	8.6353	9.131	8.865	8.8262	8.816
24.5	25.0	24.75	147	7.5016	7.8905	7.7433	7.7075	7.6988
25	25.5	25.25	123	8.3335	8.8583	8.5993	8.5616	8.5529
25.5	26.0	25.75	18	8.2956	8.7699	8.5231	8.4893	8.4801
26	26.5	26.25	25	8.6454	9.1306	8.8974	8.8627	8.8533
26.5	27.0	26.75	29	8.3144	8.8436	8.5629	8.5233	8.513
27.0	27.5	27.25	127	8.6912	9.2045	8.9238	8.8839	8.8758

SD20 KB-1 LOI Data

SD20 KB-		LOI			= LOI
Mid	%H2	%O	%M	LOI	%CaCO
Depth	(g/g wet	(% dry	(%dry	(% dry	(% dry
0.25	98.1	63.1	34.7	2.11	4.78
0.75	94.8	59.4	38.3	2.21	5.03
1.25	95.0	58.5	37.8	3.66	8.31
1.75	93.5	58.9	36.7	4.34	9.85
2.25	94.2	59.1	38.8	2.06	4.69
2.75	92.6	57.5	39.4	2.97	6.76
3.25	91.4	53.9	43.2	2.80	6.37
3.75	91.2	51.1	46.0	2.82	6.40
4.25	89.4	51.1	46.1	2.77	6.29
4.75	89.6	52.3	44.5	3.14	7.14
5.25	87.7	48.1	48.4	3.39	7.70
5.75	85.5	42.9	54.0	3.00	6.81
6.25	86.3	44.8	53.2	1.91	4.33
6.75	112.7	44.3	53.0	2.60	5.91
7.25	110.7	44.6	53.4	1.94	4.41
7.75	86.1	41.6	56.6	1.69	3.84
8.25	82.4	36.2	61.4	2.38	5.42
8.75	76.3	30.4	65.5	4.04	9.17
9.25	75.8	30.6	66.0	3.31	7.52
9.75	77.6	31.2	65.0	3.74	8.49
10.2	78.9	27.7	66.9	5.37	12.2
10.7	77.9	31.5	65.3	3.15	7.16
11.2	77.8	27.8	67.2	4.92	11.1
11.7	76.0	25.8	68.4	5.68	12.9
12.2	71.4	24.4	70.1	5.37	12.2
12.7	72.5	24.7	69.9	5.31	12.0
13.2	69.7	24.4	70.4	5.06	11.5
13.7	71.2	27.7	68.3	3.85	8.75
14.2	68.8	25.3	71.0	3.63	8.26
14.7	68.4	26.1	69.7	4.13	9.39
15.2	64.2	22.5	72.8	4.55	10.3
15.7	67.9				0.00
16.2	65.9	24.6	70.7	4.64	10.5
16.7	63.3	24.2	73.0	2.62	5.95
17.2	61.2	21.4	73.9	4.57	10.3
17.7	61.0	19.7	76.1	4.13	9.39
18.2	63.7	22.4	72.9	4.61	10.4
18.7	65.2	23.1	71.6	5.25	11.9
19.2					0.00
19.7	63.1	23.6	72.6	3.70	8.42
20.2	63.3	20.7	74.5	4.78	10.8
20.7	65.0	22.9	72.5	4.50	10.2
21.2	63.0	22.1	73.1	4.67	10.6
21.7	60.0	19.6	75.5	4.79	10.8
22.2	63.2	22.8	71.7	5.43	12.3
22.7	59.9	19.3	75.7	4.90	11.1
23.2	53.4	16.7	80.0	3.20	7.27
23.7	57.0	18.5	76.9	4.53	10.2
24.2	53.6	16.8	78.6	4.44	10.0
24.7	37.8	14.8	81.5	3.60	8.18
25.2	49.3	14.1	82.5	3.27	7.44
25.7	52.0	14.8	81.1	4.04	9.19
26.2	48.0	13.7	82.5	3.73	8.48
26.7	53.0	15.9	79.9	4.14	9.42
27.2	54.6	17.1	79.3	3.48	7.91

SD2 KB-5 LOI Data

LOSS-ON-IGNITION DATA SHEET

Date: September 23, 2004 **90°C** **550°C** **1000°C**

Technician: Cherie **Time In: 3 pm**

Lake name: SD2 KB-5 (July 2004) **Time Out: 3 pm (Next day)**

Sediment Depth (cm)		Crucible #	Crucible	Cruc. + Wet	Cruc. + Dry Sed.	Cruc. + Burnt sed.	Cruc. + Ashed sed.
(Top)	(Bottom)		Weight (g)	Sediment (g)	after 90°C (g)	after 550°C (g)	after 1000°C (g)
0.0	0.5	72	8.7127	9.0143	8.7808	8.7727	8.7699
0.5	1.0	137	9.1271	9.4317	9.1941	9.1865	9.1835
1.0	1.5	156	8.3148	8.6095	8.4094	8.3986	8.3937
1.5	2.0	128	8.7767	9.0909	8.9159	8.9038	8.8982
2.0	2.5	94	8.3525	8.6697	8.5056	8.4915	8.4857
2.5	3.0	Z7	8.6664	8.8785	8.8014	8.7938	8.7885
3.0	3.5	56	8.4704	8.7583	8.6366		
3.5	4.0	J	7.5171	7.7625	7.6691	7.6631	7.6580
4.0	4.5	115	7.1346	7.3459	7.2761	7.2690	7.2653
4.5	5.0	149	8.4929	8.7735	8.6805	8.6697	8.6646
5.0	5.5	29	8.2968	8.5762	8.4752	8.4641	8.4589
5.5	6.0	132	8.5679	8.8051	8.7346	8.7277	8.7218
6.0	6.5	144	9.3570	9.5102	9.4557	9.4499	9.4465
6.5	7.0	141	8.2326	8.3825	8.3154	8.3071	8.3040
7.0	7.5	62	8.3181	8.5129	8.4334	8.4268	8.4226
7.5	8.0	165	8.5465	8.7629	8.6844	8.6769	8.6723
8.0	8.5	27	9.7106	9.9195	9.8325	9.8235	9.8183
8.5	9.0	42	8.0819	8.2383	8.1782	8.1721	8.1679
9.0	9.5	104	8.0867	8.2832	8.2088	8.2001	8.1949
9.5	10.0	18	8.2943	8.4563	8.4003	8.3908	8.3889
10.0	10.5	Z6	8.1590	8.3566	8.2851	8.2752	8.2721
10.5	11.0	126	8.1105	8.2255	8.1770	8.1707	8.1687
11.0	11.5	152	7.9526	8.0643	8.0136	8.0075	8.0052
11.5	12.0	4	8.0073	8.1245	8.0746	8.0682	8.0658
12.0	12.5	31	8.4427	8.5414	8.5028	8.4978	8.4957
12.5	13.0	Z5	7.4698	7.5958	7.5504	7.5447	7.5418
13.0	13.5	Z9	7.5960	7.6726	7.6436	7.6392	7.6377
13.5	14.0	123	8.3322	8.4296	8.3908	8.3856	8.3832
14.0	14.5	164	8.1059	8.1974	8.1552	8.1498	8.1481
14.5	15.0	64	8.7880	8.9046	8.8706	8.8648	8.8630
15.0	15.5	Z26	7.8682	7.9921	7.9555	7.9501	7.9481
15.5	16.0	83	8.8409	8.9473	8.9187	8.9129	8.9115
16.0	16.5	77	8.3973	8.4989	8.4701	8.4653	8.4628
16.5	17.0	71	8.4105	8.5129	8.4831	8.4774	8.4755
17.0	17.5	39	8.7895	8.9267	8.8812	8.8749	8.8711
17.5	18.0	51	8.6046	8.7007	8.6728	8.6678	8.6651
18.0	18.5	14	8.4439	8.5923	8.5424	8.5351	8.5313
18.5	19.0	47	9.0502	9.1660	9.1322	9.1267	9.1232
19	19.5	88	8.1677	8.3045	8.2694	8.2624	8.2597
19.5	20.0	Z28	8.0675	8.2098	8.1755	8.1681	8.1651
20.0	20.5	114	7.5775	7.6693	7.6446	7.6410	7.6390
20.5	21.0	107	7.8249	7.9694	7.9361	7.9291	7.9267
21.0	21.5	92	8.4495	8.6072	8.5622	8.5566	8.5530
21.5	22.0	13	8.5161	8.7493	8.6844	8.6757	8.6702
22.0	22.5	12	8.4770	8.5980	8.5698	8.5647	8.5618
22.5	23.0	Z1	8.2366	8.3938	8.3486	8.3408	8.3374
23	23.5	Z14	8.2088	8.2968	8.2723	8.2661	8.2647

SD2 KB-5 LOI Data

23.5	24.0	17	8.2433	8.3601	8.3274	8.3218	8.3179
24	24.5	147	7.4954	7.6099	7.5793	7.5737	7.5714
24.5	25.0	Z20	8.7342	8.8397	8.7856	8.7815	8.7799
25	25.5	L	7.3272	7.4022	7.3776	7.3738	7.3716
25.5	26.0	26	8.1199	8.2365	8.2040	8.2001	8.1968
26	26.5	59	8.3682	8.5054	8.4716	8.4678	8.4640
26.5	27.0	127	8.6899	8.7952	8.7633	8.7566	8.7553
27.0	27.5	122	8.0967	8.1791	8.1423	8.1350	8.1341
27.5	28.0	111	8.1742	8.2881	8.2476	8.2396	8.2376
28.0	28.5	19	8.6452	8.7593	8.7198	8.7135	8.7109
28.5	29.0	Z23	8.3970	8.5194	8.4733	8.4656	8.4631
29.0	29.5	Z4	7.7112	7.7859	7.7561	7.7519	7.7497
29.5	30.0	H	9.1921	9.2689	9.2413	9.2368	9.2350
30.0	30.5	Z15	9.3026	9.3933	9.3626	9.3578	9.3563
30.5	31.0	6	8.4478	8.5163	8.4919	8.4890	8.4867
31.0	31.5	Z19	8.5652	8.6391	8.6176	8.6143	8.6132
31.5	32.0	Z3	8.8924	9.0004	8.9677	8.9626	8.9610
32.0	32.5	Z16	7.4780	7.5887	7.5530	7.5482	7.5465
32.5	33.0	Z30	9.0484	9.1841	9.1417	9.1371	9.1343
33.00	33.50	Z13	8.5744	8.6420	8.6204	8.6178	8.6168
33.50	34.00	Z27	8.8078	8.8843	8.8639		
34.00	34.50	Z11	8.4488	8.5258	8.5043	8.5026	8.5007
34.50	35.00	I	8.5924	8.6749	8.6540	8.6522	8.6501
35.00	35.50	30	8.7030	8.8881	8.8401	8.8345	8.8301
35.50	36.00	B	8.3936	8.6176	8.5543	8.5475	8.5419
36.00	36.50	D	7.6428	7.7630	7.7317	7.7268	7.7251
36.50	37.00	67	7.8136	7.9266	7.8961	7.8927	7.8898
37.00	37.50	Z18	8.3124	8.4426	8.4071	8.4028	8.3995
37.50	38.00	Z22	8.3234	8.4233	8.3996	8.3958	8.3939
38.00	38.50	151	8.4734	8.6157	8.5752	8.5706	8.5673
38.50	39.00	112	8.1760	8.2422	8.2253	8.2232	8.2218
39.00	39.50	118	8.4632	8.5774	8.5472	8.5443	8.5416
39.50	40.00	110	8.4779	8.5720	8.5502	8.5477	8.5448
40.00	40.50	102	9.4317	9.5213	9.4981	9.4953	9.4935
40.50	41.00	Z12	8.6791	8.7765	8.7498	8.7456	8.7436
41.00	41.50	Z24	7.4850	7.5646	7.5434	7.5404	7.5385
41.50	42.00	Z17	7.6871	7.7562	7.7358	7.7317	7.7304
42.00	42.50	F	8.5176	8.6029	8.5729	8.5676	8.5648
42.50	43.00	A	7.7546	7.8187	7.7953	7.7913	7.7904
43.00	43.50	Z2	7.8837	7.9539	7.9277	7.9234	7.9218
43.50	44.00	Z21	8.1213	8.1631	8.1467	8.1434	8.1430
44.00	44.50	34	8.8656	8.9447	8.9233	8.9196	8.9173
44.50	45.00	63	8.2803	8.3572	8.3389	8.3354	8.3336
45.00	45.50	46	8.6974	8.7708	8.7525	8.7490	8.7474
45.50	46.00	169	8.4615	8.5634	8.5343	8.5296	8.5266
46.00	46.50	97	8.3110	8.4293	8.3968	8.3915	8.3891
46.50	47.50	3	8.6486	8.7415	8.7035	8.6972	8.6950
47.50	48.00	68	8.1719	8.2659	8.2360	8.2303	8.2276
48.00	48.50	160	8.2127	8.3103	8.2731	8.2668	8.2653
48.50	49.00	70	8.0629	8.1571	8.1268	8.1217	8.1188

SD2 KB-5 LOI Data

SD2 KB-		LOI			= LOI
Mid	%H2	%O	%M	LOI	%CaCO
Depth	(g/g wet	(% dry	(%dry	(% dry	(% dry
0.25	77.4	11.8	83.9	4.11	9.34
0.75	78.0	11.3	84.1	4.48	10.1
1.25	67.9	11.4	83.4	5.18	11.7
1.75	55.7	8.69	87.2	4.02	9.14
2.25	51.7	9.21	87.0	3.79	8.61
2.75	36.3	5.63	90.4	3.93	8.92
3.25	42.2				
3.75	38.0	3.95	92.7	3.36	7.63
4.25	33.0	5.02	92.3	2.61	5.94
4.75	33.1	5.76	91.5	2.72	6.18
5.25	36.1	6.22	90.8	2.91	6.62
5.75	29.7	4.14	92.3	3.54	8.04
6.25	35.5	5.88	90.6	3.44	7.83
6.75	44.7	10.0	86.2	3.74	8.51
7.25	40.8	5.72	90.6	3.64	8.28
7.75	36.2	5.44	91.2	3.34	7.58
8.25	41.6	7.38	88.3	4.27	9.69
8.75	38.4	6.33	89.3	4.36	9.91
9.25	37.8	7.13	88.6	4.26	9.68
9.75	34.5	8.96	89.2	1.79	4.07
10.2	36.1	7.85	89.6	2.46	5.59
10.7	42.1	9.47	87.5	3.01	6.84
11.2	45.3	10.0	86.2	3.77	8.57
11.7	42.5	9.51	86.9	3.57	8.10
12.2	39.1	8.32	88.1	3.49	7.94
12.7	36.0	7.07	89.3	3.60	8.18
13.2	37.8	9.24	87.6	3.15	7.16
13.7	39.8	8.87	87.0	4.10	9.31
14.2	46.1	10.9	85.6	3.45	7.84
14.7	29.1	7.02	90.8	2.18	4.95
15.2	29.5	6.19	91.5	2.29	5.21
15.7	26.8	7.46	90.7	1.80	4.09
16.2	28.3	6.59	89.9	3.43	7.80
16.7	29.1	7.85	89.5	2.62	5.95
17.2	33.1	6.87	88.9	4.14	9.42
17.7	29.0	7.33	88.7	3.96	9.00
18.2	33.6	7.41	88.7	3.86	8.77
18.7	29.1	6.71	89.0	4.27	9.70
19.2	25.6	6.88	90.4	2.65	6.03
19.7	24.1	6.85	90.3	2.78	6.31
20.2	26.9	5.37	91.6	2.98	6.77
20.7	23.0	6.29	91.5	2.16	4.91
21.2	28.5	4.97	91.8	3.19	7.26
21.7	27.8	5.17	91.5	3.27	7.43
22.2	23.3	5.50	91.3	3.13	7.10
22.7	28.7	6.96	90.0	3.04	6.90
23.2	27.8	9.76	88.0	2.20	5.01
23.7	28.0	6.66	88.7	4.64	10.5
24.2	26.7	6.67	90.5	2.74	6.23
24.7	51.2	7.98	88.9	3.11	7.07
25.2	32.8	7.54	88.1	4.37	9.92
25.7	27.8	4.64	91.4	3.92	8.92
26.2	24.6	3.68	92.6	3.68	8.35
26.7	30.2	9.13	89.1	1.77	4.03

Note: Crucible broke for sample 3.25 mid-pint depth

SD28 KB-5 LOI Data

LOSS-ON-IGNITION DATA SHEET

Date: Oct. 31/02 90°C 550°C 1000°C
Technician: Time In
Lake name: SD 28 Time Out
Core #: KB-5

Sediment Depth (cm)		Crucible #	Crucible	Cruc. + Wet	Cruc. + Dry Sed.	Cruc. + Burnt sed.	Cruc. + Ashed sed.
(Top)	(Bottom)		Weight (g)	Sediment (g)	after 90°C (g)	after 550°C (g)	after 1000°C (g)
0.0	0.5		8.2669	8.7298	8.3995	8.3888	8.3818
0.5	1.0		8.4688	8.9896	8.6295	8.6168	8.6086
1.0	1.5		8.3960	8.9632	8.5535	8.5393	8.5322
1.5	2.0		7.7637	8.3224	7.9549	7.9380	7.9268
2.0	2.5		8.6682	9.1827	8.9046	8.8879	8.8771
2.5	3.0		9.2760	9.7356	9.5240	9.5093	9.4983
3.0	3.5		8.3967	8.8838	8.7039	8.6883	8.6768
3.5	4.0		9.3688	9.8638	9.6660	9.6532	9.6410
4.0	4.5		8.1357	8.6429	8.4343	8.4175	8.4064
4.5	5.0		8.4448	8.9769	8.7751	8.7591	8.7471
5.0	5.5		9.1238	9.6984	9.4369	9.4201	9.4087
5.5	6.0		8.6929	9.0845	8.8773	8.8591	8.8488
6.0	6.5		8.3929	8.9531	8.7236	8.7047	8.6924
6.5	7.0		8.0493	8.5131	8.3460	8.3280	8.3187
7.0	7.5		8.4769	8.9830	8.7857	8.7682	8.7581
7.5	8.0		8.4283	8.8697	8.7041	8.6871	8.6771
8.0	8.5		8.4755	8.9671	8.7699	8.7518	8.7418
8.5	9.0		8.2946	8.7838	8.6029	8.5853	8.5751
9.0	9.5		8.2117	8.6393	8.5017	8.4871	8.4759
9.5	10.0		8.6692	9.1923	9.0068	8.9913	8.9785
10.0	10.5		8.7894	9.2094	9.0552	9.0443	9.0333
10.5	11.0		8.0632	8.5457	8.3444	8.3279	8.3174
11.0	11.5		9.7094	10.1997	9.9893	9.9725	9.9591
11.5	12.0		8.1185	8.7106	8.4695	8.4508	8.4349
12.0	12.5		9.1262	9.6180	9.4165	9.3988	9.3857
12.5	13.0		8.1717	8.6883	8.4829	8.4650	8.4528
13.0	13.5		8.2434	8.7333	8.5289	8.5135	8.5017
13.5	14.0		8.2318	8.7507	8.5588	8.5409	8.5275
14.0	14.5		7.9734	8.4958	8.3006	8.2860	8.2737
14.5	15.0		8.5902	9.0154	8.8770	8.8640	8.8527
15.0	15.5		8.5041	8.9685	8.7990	8.7844	8.7736
15.5	16.0		8.5675	9.1163	8.9013	8.8835	8.8713
16.0	16.5		9.3581	9.8254	9.6608	9.6464	9.6355
16.5	17.0		7.7264	8.2967	8.0860	8.0668	8.0536
17.0	17.5		8.4472	8.9767	8.7911	8.7745	8.7618
17.5	18.0						
18.0	18.5		8.4096	8.8794	8.7196	8.7027	8.6918
18.5	19.0		7.3918	7.8924	7.7024	7.6848	7.6726
19.0	19.5		9.4302	10.0187	9.8285	9.8117	9.7974
19.5	20.0		8.3554	8.8355	8.6625	8.6464	8.6345
20.0	20.5		7.7824	8.3410	8.1225	8.1023	8.0881
20.5	21.0		7.4959	7.9515	7.7897	7.7738	7.7621
21.0	21.5		8.6898	9.1039	8.9540	8.9388	8.9294
21.5	22.0		8.1951	8.6937	8.5133	8.4988	8.4870
22.0	22.5		8.7259	9.2783	9.0874	9.0692	9.0562
22.5	23.0		7.6197	8.0820	7.9289	7.9122	7.9009
23	23.5		7.7770	8.2022	8.0132	7.9985	7.9893

23.5	24.0		8.6423	9.1351	8.9289	8.9120	8.8990
24	24.5		8.1101	8.6569	8.4488	8.4305	8.4176
24.5	25.0		8.3861	8.8462	8.6199	8.6047	8.5940
25	25.5		8.2965	8.7541	8.5813	8.5665	8.5552
25.5	26.0		8.8513	9.3769	9.1467	9.1272	9.1159
26	26.5		7.1333	7.5808	7.3963	7.3824	7.3720
26.5	27.0		8.6476	9.1751	8.9572	8.9403	8.9284
27.0	27.5		8.0842	8.6356	8.4206	8.4022	8.3889
27.5	28.0		8.7429	9.2953	9.0768	9.0570	9.0428
28.0	28.5		8.3331	8.7423	8.5644	8.5500	8.5383
28.5	29.0		8.2973	8.7993	8.5627	8.5457	8.5358
29.0	29.5		8.2116	8.7943	8.5966	8.5764	8.5625
29.5	30.0		8.7021	9.2227	9.0286	9.0114	8.9992
30.0	30.5		8.6449	9.1898	8.9919	8.9730	8.9608
30.5	31.0		8.3146	8.8445	8.6341	8.6177	8.6065
31.0	31.5		8.2340	8.7343	8.5718	8.5551	8.5421
31.5	32.0		8.7431	9.3279	9.1157	9.0969	9.0836
32.0	32.5		8.9058	9.4218	9.2619	9.2453	9.2329
32.5	33.0		7.8089	8.3853	8.1818	8.1620	8.1486

SD28 KB-5 LOI Data

SD28 KB-5		LOI 550			= LOI 1000/0.44
Mid Point	%H2O	%OM	%MM	LOI 1000	%CaCO3
Depth (cm)	(g/g wet wt.)	(% dry wt)	(%dry wt)	(% dry wt)	(% dry wt)
0.25	71.35	8.07	86.65	5.28	12.00
0.75	69.14	7.90	86.99	5.10	11.60
1.25	72.23	9.02	86.48	4.51	10.25
1.75	65.78	8.84	85.30	5.86	13.31
2.25	54.05	7.06	88.37	4.57	10.38
2.75	46.04	5.93	89.64	4.44	10.08
3.25	36.93	5.08	91.18	3.74	8.51
3.75	39.96	4.31	91.59	4.10	9.33
4.25	41.13	5.63	90.66	3.72	8.45
4.75	37.93	4.84	91.52	3.63	8.26
5.25	45.51	5.37	90.99	3.64	8.28
5.75	52.91	9.87	84.54	5.59	12.69
6.25	40.97	5.72	90.57	3.72	8.45
6.75	36.03	6.07	90.80	3.13	7.12
7.25	38.98	5.67	91.06	3.27	7.43
7.75	37.52	6.16	90.21	3.63	8.24
8.25	40.11	6.15	90.46	3.40	7.72
8.75	36.98	5.71	90.98	3.31	7.52
9.25	32.18	5.03	91.10	3.86	8.78
9.75	35.46	4.59	91.62	3.79	8.62
10.25	36.71	4.10	91.76	4.14	9.41
10.75	41.72	5.87	90.40	3.73	8.49
11.25	42.91	6.00	89.21	4.79	10.88
11.75	40.72	5.33	90.14	4.53	10.30
12.25	40.97	6.10	89.39	4.51	10.26
12.75	39.76	5.75	90.33	3.92	8.91
13.25	41.72	5.39	90.47	4.13	9.39
13.75	36.98	5.47	90.43	4.10	9.31
14.25	37.37	4.46	91.78	3.76	8.54
14.75	32.55	4.53	91.53	3.94	8.95
15.25	36.50	4.95	91.39	3.66	8.32
15.75	39.18	5.33	91.01	3.65	8.31
16.25	35.22	4.76	91.64	3.60	8.18
16.75	36.95	5.34	90.99	3.67	8.34
17.25	35.05	4.83	91.48	3.69	8.39
18.25					-
18.75	34.01	5.45	91.03	3.52	7.99
19.25	37.95	5.67	90.41	3.93	8.93
19.75	32.32	4.22	92.19	3.59	8.16
20.25	36.03	5.24	90.88	3.87	8.81
20.75	39.12	5.94	89.89	4.18	9.49
21.25	35.51	5.41	90.61	3.98	9.05
21.75	36.20	5.75	90.69	3.56	8.09
22.25	36.18	4.56	91.73	3.71	8.43
22.75	34.56	5.03	91.37	3.60	8.17
23.25	33.12	5.40	90.94	3.65	8.31
23.75	44.45	6.22	89.88	3.90	8.85
24.25	41.84	5.90	89.57	4.54	10.31
24.75	38.06	5.40	90.79	3.81	8.66
25.25	49.18	6.50	88.92	4.58	10.40
25.75	37.76	5.20	90.84	3.97	9.02
26.25	43.80	6.60	89.57	3.83	8.69
26.75	41.23	5.29	90.76	3.95	8.99
27.25	41.31	5.46	90.70	3.84	8.74
27.75	38.99	5.47	90.58	3.95	8.99
28.25	39.55	5.93	89.82	4.25	9.67
28.75	43.48	6.23	88.72	5.06	11.50
29.25	47.13	6.41	89.86	3.73	8.48
29.75	33.93	5.25	91.14	3.61	8.21
30.25	37.28	5.27	91.00	3.74	8.49
30.75	36.32	5.45	91.04	3.52	7.99
31.25	39.71	5.13	91.36	3.51	7.97
31.75	32.48	4.94	91.21	3.85	8.75
32.25	36.29	5.05	91.38	3.57	8.11
32.75	30.99	4.66	91.86	3.48	7.91
	35.31	5.31	91.10	3.59	8.17

Appendix D

SD20 KB-1, SD2 KB-5 and SD28 KB-5
Carbon and Nitrogen Elemental and Stable Isotope Results

SD20 KB-1 Carbon and Nitrogen Elemental and Stable Isotope Results

				Carbon Range is 3e-8 to 20e-8				
SD20 KB-1				Nitrogen range is 4.5e-8 to 22e-8				
		Major Peak	Major Peak	Elemental		Reported		
Mid Point	Weight	Area (E-8)	Area (E-8)	% Comp		Delta		
Depth (cm)	(mg)	(C)	(N)	(C)	(N)	(C13)	(N15)	C/N
0.25	4.061	22.96	16.11	36.08	3.39	-26.77	0.55	10.6519
0.75	3.998	21.94	15.27	35.03	3.26	-27.03	0.39	10.74716
1.25	3.973	22.17	15.38	35.61	3.31	-27.17	0.45	10.76572
1.75	4.008	21.98	14.96	35.00	3.19	-27.23	0.43	10.97022
2.25	4.037	21.83	14.85	34.51	3.14	-27.26	0.46	10.97964
2.75	4.054	21.11	14.20	33.23	2.99	-27.47	0.54	11.12115
2.75	4.014	21.02	14.14	33.42	3.01	-27.44	0.62	11.11743
3.25	3.992	19.81	13.29	31.66	2.83	-27.22	0.53	11.1988
3.75	4.069	19.78	13.21	31.02	2.77	-27.23	0.72	11.20889
4.25	4.134	18.92	12.59	29.21	2.60	-27.11	0.65	11.25549
4.75	4.101	18.53	12.30	28.83	2.54	-26.98	0.63	11.33779
5.25	4.622	19.32	12.83	26.68	2.35	-26.89	0.67	11.33702
5.75	4.533	18.24	12.11	25.68	2.26	-26.52	0.69	11.34099
5.75	4.439	16.75	11.22	24.07	2.13	-26.33	0.66	11.28458
6.25	4.482	17.56	11.67	25.00	2.21	-26.26	0.65	11.32623
6.75	4.586	15.02	9.93	20.88	1.83	-25.11	0.35	11.41553
7.25	4.675	17.70	11.58	24.15	2.10	-25.85	0.64	11.51287
7.75	4.788	16.27	10.84	21.65	1.91	-25.41	0.57	11.31087
8.25	4.487	13.60	9.15	19.30	1.71	-24.56	-0.17	11.30639
8.75	4.659	12.26	8.20	16.73	1.47	-23.50	0.47	11.37254
8.75	4.502	11.63	7.83	16.43	1.45	-23.65	0.41	11.29849
9.25	4.752	12.72	8.48	17.03	1.50	-23.53	0.40	11.37809
9.75	4.564	10.99	7.38	15.29	1.35	-23.09	0.17	11.30917
10.25	8.37	20.10	13.12	15.31	1.33	-22.71	0.42	11.48687
10.75	8.126	20.78	13.36	16.32	1.40	-22.82	0.63	11.62179
11.25	8.235	19.31	12.78	14.95	1.32	-22.72	0.58	11.32424
11.75	7.904	18.14	11.95	14.63	1.28	-22.71	0.48	11.39408
11.75	8.061	18.84	12.39	14.91	1.31	-22.68	0.39	11.41424
12.25	7.953	17.47	11.60	14.01	1.24	-22.56	0.55	11.31502
12.75	7.938	16.60	11.00	13.32	1.18	-22.48	0.40	11.33787
13.25	8.294	18.11	11.89	13.92	1.22	-22.43	0.37	11.44408
13.75	8.185	17.10	11.30	13.31	1.17	-22.38	0.29	11.3655
14.25	8.166	16.77	11.11	13.07	1.15	-22.15	0.26	11.32842
14.75	8.051	17.22	11.45	13.60	1.21	-22.47	0.34	11.26761
14.75	7.986	17.26	11.44	13.75	1.21	-22.45	0.33	11.32619

SD20 KB-1 Carbon and Nitrogen Elemental and Stable Isotope Results

			Carbon Range is 3e-8 to 20e-8				
SD20 KB-1			Nitrogen range is 4.5e-8 to 22e-8				
	Major Peak	Major Peak	Elemental		Reported		
Midpoint	Area (E-8)	Area (E-8)	% Comp		Delta		
Depth (cm)	(C)	(N)	(C)	(N)	(C13)	(N15)	C/N
15.25	18.8962	12.6606	11.97	1.072	-22.3405	0.342127	11.16604
15.75	18.2706	12.3391	11.708	1.058	-22.4301	0.203502	11.06616
16.25	17.1959	11.7305	10.542	0.958	-22.269	0.325818	11.00418
16.75	13.8448	9.72341	8.724	0.81	-22.252	0.019009	10.77037
17.25	15.8897	10.9475	9.798	0.898	-22.2156	0.042453	10.91091
17.75	17.165	11.578	10.858	0.977	-22.0743	0.259564	11.11361
17.75	17.5884	11.9188	10.896	0.986	-22.0494	0.291162	11.05071
18.25	17.5032	11.9345	10.855	0.985	-22.091	0.320722	11.0203
18.75	18.2279	12.4178	11.267	1.021	-22.0311	0.199425	11.03526
19.5	17.2536	11.7823	11.023	1.005	-22.0459	0.156615	10.96816
19.5	17.4572	11.9942	11.161	1.023	-21.9533	0.092399	10.91007
20.25	17.9841	12.3544	10.493	0.961	-21.9372	0.202483	10.91883
20.75	16.5746	11.4091	10.304	0.945	-22.1448	0.158653	10.9037
20.75	16.469	11.3173	10.379	0.951	-22.1174	0.138267	10.91377
21.25	17.1198	11.7424	10.694	0.979	-21.8763	0.200444	10.92339
21.75	14.7465	10.2505	9.485	0.876	-21.9533	0.073032	10.82763
22.25	27.9566	19.0951	8.884	0.814	-21.9418	0.374745	10.914
22.75	28.5718	19.4131	8.977	0.82	-22.0316	0.239178	10.94756
23.25	25.5744	17.6564	8.086	0.748	-22.1232	0.113804	10.81016
23.75	22.4138	15.4991	7.152	0.662	-22.2881	0.051627	10.80363
23.75	22.3796	15.5313	7.101	0.66	-22.2203	0.079148	10.75909
24.25	24.7598	16.9999	7.867	0.726	-22.2472	0.432845	10.83609
24.75	23.7204	16.5526	7.458	0.699	-22.2172	0.026144	10.66953
25.25	24.9945	17.2954	7.794	0.724	-22.1816	-0.16141	10.76519
25.75	24.9722	17.3684	7.856	0.729	-22.1432	-0.13083	10.77641
26.25	26.391	18.2882	8.388	0.778	-21.972	-0.087	10.78149
26.75	25.2225	17.5919	8.05	0.753	-22.2254	-0.0238	10.69057
26.75	25.2552	17.5592	7.879	0.736	-22.2066	-0.11248	10.70516
27.25	22.6121	15.8492	7.187	0.676	-22.2934	-0.32959	10.63166

SD2 KB-5 Carbon and Nitrogen Elemental and Stable Isotope Results

SD2 KB-5	Carbon and Nitrogen Results						
Midpoint Depth (cm)	Major Peak Area (E-8) (C)	Major Peak Area (E-8) (N)	Elemental % Comp (C)	Elemental % Comp (N)	Reported Delta (C13)	Reported Delta (N15)	C/N
0.25	22.872	13.508	5.647	0.614	-24.617	-0.158	9.197
0.75	13.458	8.248	3.301	0.371	-26.173	-0.221	8.898
1.25	12.598	7.220	3.109	0.326	-25.413	-0.572	9.537
1.75	18.638	9.986	2.285	0.224	-25.452	-0.318	10.201
2.25	18.572	8.968	2.266	0.200	-25.089	-0.017	11.330
2.25	13.535	6.232	1.651	0.138	-25.180	0.062	11.964
2.75	13.318	6.073	1.616	0.133	-25.320	0.392	12.150
3.25	14.729	6.551	1.799	0.144	-24.897	0.171	12.493
3.75	22.100	8.969	2.728	0.201	-23.847	0.005	13.572
4.25	16.597	6.875	2.009	0.151	-24.848	0.181	13.305
4.75	9.750	3.896	1.184	0.083	-24.877	0.195	14.265
5.25	10.927	4.251	1.324	0.091	-25.398	0.351	14.549
5.75	10.041	3.950	1.190	0.084	-25.722	0.146	14.167
5.75	10.330	4.149	1.237	0.088	-25.503	0.084	14.057
6.25	9.419	3.719	1.146	0.081	-26.005	-0.016	14.148
6.75	5.377	2.552	1.303	0.106	-25.304	0.144	12.292
7.25	12.892	5.567	1.589	0.125	-25.398	0.282	12.712
7.75	18.990	9.335	1.883	0.170	-25.044	0.020	11.076
8.25	15.828	8.046	1.938	0.180	-24.979	-0.435	10.767
8.75	15.558	7.693	1.869	0.168	-24.921	-0.264	11.125
8.75	16.170	8.019	1.961	0.178	-24.804	-0.240	11.017
9.25	16.660	7.922	2.043	0.176	-24.959	0.001	11.608
9.75	20.311	9.405	2.485	0.210	-24.975	0.579	11.833
10.25	15.807	7.236	1.921	0.160	-24.937	-0.381	12.006
10.75	25.415	13.579	3.122	0.306	-23.702	-0.363	10.203
11.25	17.388	8.994	2.835	0.268	-24.322	-0.450	10.578
11.75	19.858	10.323	2.463	0.234	-24.667	0.070	10.526
11.75	19.517	10.167	2.395	0.228	-24.735	-0.190	10.504
12.25	18.604	9.107	2.272	0.203	-24.983	0.099	11.192
12.75	17.575	8.755	2.143	0.194	-25.162	-0.099	11.046
13.25	20.010	10.205	2.421	0.225	-24.884	-0.074	10.760
13.75	24.381	12.311	2.982	0.275	-24.299	-0.195	10.844
14.25	8.457	3.707	1.991	0.155	-23.767	0.717	12.845
14.75	14.736	5.434	1.794	0.119	-24.605	1.402	15.076
14.75	12.135	4.660	1.474	0.101	-24.906	1.243	14.594
15.25	16.663	5.610	2.022	0.123	-24.974	0.858	16.439
15.75	14.134	4.892	1.727	0.107	-25.997	0.462	16.140
16.25	16.408	6.648	1.995	0.146	-25.385	0.518	13.664
16.75	17.366	6.358	2.148	0.142	-25.173	1.091	15.127
17.25	16.340	6.269	1.961	0.136	-25.154	0.526	14.419
17.75	16.782	6.981	2.063	0.156	-25.245	0.299	13.224
17.75	15.527	6.470	1.876	0.141	-25.327	0.463	13.305
18.25	17.491	7.431	2.157	0.166	-24.594	0.297	12.994
18.75	19.238	7.802	2.342	0.173	-23.849	0.271	13.538
19.25	12.862	4.806	1.568	0.105	-25.709	0.482	14.933
19.75	13.553	4.562	1.631	0.098	-24.632	1.108	16.643
20.25	10.466	3.539	1.273	0.076	-26.441	0.760	16.750
20.75	10.135	3.311	1.207	0.069	-26.254	0.333	17.493
20.75	9.995	3.181	1.207	0.067	-26.235	0.788	18.015
21.25	10.818	3.543	1.313	0.076	-26.174	1.663	17.276
21.75	13.167	4.425	1.268	0.076	-26.071	1.449	16.684
22.25	12.836	4.602	1.244	0.080	-25.893	0.991	15.550
22.75	14.157	5.127	1.716	0.111	-25.394	0.616	15.459
23.25	13.877	5.232	1.653	0.112	-25.767	2.187	14.759
23.75	14.495	5.783	1.742	0.125	-25.638	1.556	13.936
23.75	14.407	5.936	1.709	0.126	-25.605	1.508	13.563

SD2 KB-5 Carbon and Nitrogen Elemental and Stable Isotope Results

SD2 KB-5 Carbon and Nitrogen Results							
Midpoint Depth (cm	Major Pea Area (E-8) (C)	Major Pea Area (E-8) (N)	Elemental % Comp (C)	Elemental % Comp (N)	Reported Delta (C13)	Reported Delta (N15)	C/N
24.25	14.99	5.73963	1.773	0.121	-24.95591	1.291985	14.65289
24.75	10.2883	4.80538	2.485	0.205	-24.05345	0.218597	12.12195
25.25	17.3311	7.64933	2.101	0.167	-24.59384	0.806841	12.58084
25.75	15.0302	5.85014	1.428	0.099	-25.6617	1.312605	14.42424
26.25	14.2436	4.84403	1.369	0.082	-24.14221	1.314595	16.69512
26.75	12.2639	5.39469	1.443	0.113	-24.77943	0.669872	12.76991
26.75	11.9795	5.24112	1.418	0.11	-24.82586	0.507574	12.89091
27.25	9.9023	5.73098	4.539	0.469	-23.43999	-0.907991	9.678038
27.75	11.7818	6.21041	2.859	0.269	-24.61895	-0.350148	10.62825
28.25	27.4103	14.2333	3.304	0.312	-24.76726	-0.147269	10.58974
28.75	20.8502	10.975	3.292	0.314	-24.91304	-0.669591	10.48408
29.25	23.2482	11.9871	3.75	0.351	-24.53905	-0.14488	10.68376
29.75	25.6797	12.9714	3.045	0.281	-24.74498	-0.175033	10.8363
29.75	25.0908	12.7501	2.973	0.275	-24.69251	-0.381941	10.81091
30.25	24.5662	11.8517	2.963	0.259	-24.50501	-0.163582	11.44015
30.75	20.6199	9.372	2.458	0.202	-24.57595	-0.059454	12.16832
31.25	14.149	6.42127	1.675	0.136	-25.13848	0.441646	12.31618
31.75	14.1338	6.22691	1.703	0.134	-24.96189	0.525639	12.70896
32.25	14.2944	6.40654	1.693	0.135	-24.93891	0.598981	12.54074
32.75	15.1666	6.72735	1.429	0.113	-24.98257	0.728766	12.64602
32.75	15.6555	6.79251	1.49	0.116	-25.01406	0.482891	12.84483
33.25	10.529	4.62336	1.247	0.096	-25.09246	0.736447	12.98958
33.75	9.10594	3.75208	1.063	0.077	-25.11155	0.793958	13.80519
34.25	15.2701	5.94531	1.461	0.1	-25.12515	1.269729	14.61
34.75	10.3299	4.127	0.974	0.068	-25.67864	1.215184	14.32353
35.25	11.56	4.44891	1.098	0.074	-25.69298	1.294002	14.83784
35.75	15.2583	5.61015	1.469	0.095	-25.0584	1.258931	15.46316
35.75	14.302	5.04712	1.353	0.084	-24.8777	1.009899	16.10714
36.25	12.9398	4.3628	1.232	0.073	-23.91205	1.37639	16.87671
36.75	15.2341	5.17768	1.457	0.087	-24.3198	1.310809	16.74713
37.25	10.5077	3.84045	0.998	0.063	-26.03018	1.205186	15.84127
37.75	10.2008	3.93453	0.976	0.065	-26.07958	1.088668	15.01538
38.25	9.55614	3.55738	0.898	0.058	-25.90639	1.43079	15.48276
38.75	9.69289	3.46714	0.924	0.057	-26.01922	1.146476	16.21053
38.75	10.1565	3.66374	0.956	0.06	-26.04001	1.071167	15.93333
39.25	11.5008	3.99744	0.911	0.055	-25.8695	1.247787	16.56364
39.75	11.664	4.44251	0.933	0.062	-25.96776	1.535991	15.04839
40.25	9.81041	3.54033	0.929	0.058	-24.15309	1.065548	16.01724
40.75	13.7885	5.84093	1.299	0.099	-25.18231	1.440783	13.12121
41.25	15.954	7.05156	1.545	0.122	-25.16145	0.771366	12.66393
41.75	16.2889	7.92366	1.925	0.168	-24.6039	0.265159	11.45833
41.75	16.0235	7.70203	1.945	0.167	-24.55205	0.24155	11.64671
42.25	10.4939	5.73193	2.55	0.246	-24.17525	-0.010738	10.36585
42.75	13.3465	7.16267	3.105	0.298	-24.23819	0.029374	10.41946
43.25	12.8798	7.15059	3.133	0.311	-24.11983	0.113697	10.07395
43.75	12.4373	6.56652	3.001	0.282	-24.33722	0.174297	10.64184
44.25	19.2686	8.88136	2.34	0.194	-24.71081	0.748123	12.06186
44.75	16.9967	7.04861	2.052	0.152	-25.54836	1.095202	13.5
44.75	17.6237	7.28032	2.107	0.156	-25.53103	1.207615	13.50641
45.25	13.3762	5.70456	1.598	0.12	-25.15518	0.838412	13.31667
45.75	17.4777	8.44366	2.062	0.179	-25.04332	0.47842	11.51955
46.25	15.7429	7.52226	1.916	0.164	-25.13102	0.233486	11.68293
47	13.9464	7.59713	3.336	0.325	-24.08405	-0.220614	10.26462
47.75	21.9154	11.0766	2.638	0.242	-24.38314	0.824376	10.90083
47.75	21.6049	10.8563	2.633	0.24	-24.35875	0.011329	10.97083
48.25	11.2874	5.69071	2.68	0.24	-24.81333	-0.131392	11.16667
48.75	23.7608	11.6343	2.823	0.25	-24.70273	0.580252	11.292

SD28 KB-5 Carbon and Nitrogen Elemental and Stable Isotope Results

			Carbon Range is 2.5e-8 to 20e-8				
SD28 KB-5			Nitrogen range is 4.5e-8 to 20e-8				
	Major Peak	Major Peak	Elemental		Reported		
Mid Point	Area (E-8)	Area (E-8)	% Comp		Delta		
Depth (cm)	(C)	(N)	(C)	(N)	(C13)	(N15)	C/N
0.25	12.2763	10.6349	3.2880	0.3210	-25.7214	1.2037	10.2430
0.75	12.1907	10.4005	3.2950	0.3180	-25.8122	1.2617	10.3616
1.25	12.5913	10.9342	3.3520	0.3280	-25.4955	1.0626	10.2195
1.75	11.3152	9.7001	3.0640	0.2960	-25.9281	1.1381	10.3514
2.25	9.2705	7.5039	2.5230	0.2260	-26.2482	1.2170	11.1637
2.75	8.1502	6.3699	2.1990	0.1910	-26.4020	1.3876	11.5131
2.75	8.9919	6.6480	2.3150	0.1970	-26.3785	1.2093	11.7513
3.25	7.3612	5.4528	1.9770	0.1610	-26.3869	1.4796	12.2795
3.75	6.8266	4.9302	1.8250	0.1440	-26.2959	1.8082	12.6736
4.25	6.6808	5.1221	1.8140	0.1500	-26.3827	1.9677	12.0933
4.75	7.0758	5.5291	1.9010	0.1620	-26.3644	1.7824	11.7346
5.25	15.2563	11.3357	2.0670	0.1750	-26.2219	1.5683	11.8114
5.75	14.5905	11.0704	1.9780	0.1690	-26.2423	1.1769	11.7041
5.75	7.5473	5.7441	1.9310	0.1680	-25.9754	1.2324	11.4940
6.25	15.0665	11.3561	2.0490	0.1750	-26.1172	1.1802	11.7086
6.75	14.9416	11.3267	2.0110	0.1730	-26.1693	1.3135	11.6243
7.25	14.4859	10.8775	1.9750	0.1670	-26.2059	1.3630	11.8263
7.75	14.7289	10.8673	1.9970	0.1660	-26.1688	1.2432	12.0301
8.25	14.9997	11.2048	2.0440	0.1730	-26.1601	1.0371	11.8150
8.75	15.2194	11.1167	2.0580	0.1690	-26.0142	1.0794	12.1775
8.75	7.7439	5.8091	1.9860	0.1700	-25.8899	1.0996	11.6824
9.25	13.9672	9.8243	1.8940	0.1500	-26.1615	1.0844	12.6267
9.75	13.8118	9.7112	1.8800	0.1490	-26.1354	1.1449	12.6174
10.25	14.4488	10.2299	1.9600	0.1570	-25.9509	1.3088	12.4841
10.75	14.6291	10.5709	1.9730	0.1610	-26.0353	1.1614	12.2547
11.25	15.7611	11.7767	2.1380	0.1820	-26.1840	0.9675	11.7473
11.75	16.8050	12.6692	2.2870	0.1950	-26.2869	0.8405	11.7282
11.75	17.1380	12.5733	2.2560	0.1940	-26.5961	1.2098	11.6289
12.25	16.2520	12.0964	2.2010	0.1840	-26.2121	0.9953	11.9620
12.75	16.2760	11.9369	2.2230	0.1860	-26.3067	1.5687	11.9516
13.25	17.0091	12.8696	2.3020	0.1980	-26.3825	1.0901	11.6263
13.75	16.4819	12.2875	2.2440	0.1890	-26.2098	0.8633	11.8730
14.25	15.7715	11.6929	2.1390	0.1800	-26.3351	0.7510	11.8833
14.75	15.2733	11.4347	2.0850	0.1750	-26.2951	0.8937	11.9143
14.75	16.4094	11.8096	2.1480	0.1810	-26.4988	0.9612	11.8674
15.25	15.0280	11.1225	2.0520	0.1700	-26.3634	1.1783	12.0706
15.75	14.5876	10.7168	1.9890	0.1650	-26.3406	1.2120	12.0545

SD28 KB-5 Carbon and Nitrogen Elemental and Stable Isotope Results

			Carbon Range is 2.5e-8 to 20e-8				
SD28 KB-5			Nitrogen range is 4.5e-8 to 20e-8				
	Major Peak	Major Peak	Elemental		Reported		
Mid Point	Area (E-8)	Area (E-8)	% Comp		Delta		
Depth (cm)	(C)	(N)	(C)	(N)	(C13)	(N15)	C/N
16.25	14.1758	10.4117	1.9150	0.1580	-26.2254	1.2200	12.1203
16.75	14.4345	10.7099	1.9590	0.1630	-26.1692	1.3881	12.0184
17.25	14.7685	10.7458	2.0070	0.1660	-26.2160	1.3014	12.0904
17.75	14.0298	10.1838	1.9020	0.1550	-26.2059	1.0085	12.2710
17.75	15.6022	11.1282	2.0420	0.1690	-26.4862	0.9815	12.0828
18.25	14.1053	10.2160	1.9020	0.1540	-26.1806	0.8276	12.3506
18.75	13.6977	9.6698	1.8680	0.1470	-26.1386	0.7715	12.7075
19.25	13.2002	9.3517	1.7960	0.1430	-26.0282	1.1782	12.5594
19.75	13.7836	10.0200	1.8580	0.1510	-26.0918	0.9542	12.3046
20.25	13.3469	9.5546	1.8060	0.1440	-26.0229	0.8214	12.5417
20.75	13.9120	9.9473	1.8950	0.1530	-26.1285	1.7439	12.3856
20.75	15.4673	11.0980	2.0280	0.1700	-26.4237	1.0697	11.9294
21.25	14.0463	10.1435	1.9020	0.1540	-26.1485	1.0645	12.3506
21.75	13.8859	9.8991	1.8870	0.1500	-26.0910	0.7961	12.5800
22.25	13.9060	9.7908	1.8870	0.1490	-26.1232	1.0202	12.6644
22.75	13.9333	10.0028	1.8890	0.1520	-26.2331	1.1325	12.4276
23.25	14.6410	10.4719	1.9870	0.1590	-26.3041	1.1277	12.4969
23.75	14.7673	10.6181	2.0000	0.1610	-26.3304	1.0472	12.4224
23.75	15.7777	11.4300	2.0740	0.1750	-26.6312	1.0896	11.8514
24.25	16.0358	11.6636	2.1830	0.1790	-26.3798	0.8922	12.1955
24.75	16.1353	11.7363	2.1910	0.1800	-26.4447	0.8236	12.1722
25.25	16.0776	11.7052	2.1840	0.1790	-26.5676	0.9153	12.2011
25.75	16.4975	12.0932	2.2370	0.1850	-26.5490	0.8668	12.0919
26.25	16.4369	11.9724	2.2300	0.1830	-26.4528	0.8431	12.1858
26.75	16.3905	11.8690	2.2250	0.1810	-26.4597	0.8245	12.2928
26.75	17.5080	12.9635	2.3000	0.1990	-26.8077	0.8994	11.5578
27.25	16.6882	12.3485	2.2620	0.1880	-26.6190	0.8145	12.0319
27.75	15.6364	11.1303	2.1220	0.1690	-26.3347	0.9484	12.5562
28.25	14.8869	10.4264	2.0220	0.1580	-26.1405	1.0147	12.7975
28.75	14.5912	10.0071	1.9810	0.1530	-26.1941	1.5275	12.9477
29.25	14.7903	10.1557	2.0140	0.1550	-26.2342	1.3137	12.9935
29.75	14.7603	10.1463	2.0120	0.1540	-26.0820	1.2254	13.0649
29.75	15.4990	11.1471	2.0330	0.1700	-26.2935	0.9487	11.9588
30.25	14.7240	10.0420	2.0070	0.1530	-26.0400	1.2681	13.1176
30.75	13.9479	9.4787	1.8940	0.1430	-26.1354	1.2745	13.2448
31.25	14.1546	9.6561	1.9190	0.1460	-26.0817	1.2577	13.1438
31.75	13.4421	9.0060	1.8290	0.1360	-26.1062	1.2689	13.4485
32.25	12.8969	8.6933	1.7490	0.1310	-26.0292	1.2934	13.3511
32.75	6.3485	4.7862	0.8510	0.0690	-26.0433	1.1022	12.3333
32.75	14.0272	10.0316	1.8380	0.1520	-26.3065	0.8223	12.0921

Appendix E

SD20 KB-1 and SD28 KB-5 Cellulose-inferred $\delta^{18}O_{LW}$ Results and E/I Values

SD20 KB-1 Cellulose-inferred $\delta^{18}O_{LW}$ Results and E/I Values

SD20 Sample ID	Mid Point Core Depth	SED CRS Dates	Cell 18O	Repeats	Three Point Mean	Cell-Infrrd 18O lw	Calculated E/I
SD20 0-0.5 cm	0.25	2002.00	18.6		-10.8	-9.1	3.98
SD20 0.5-1cm	0.75	2000.17	15.2		-11.5	-12.4	0.68
SD20 1-1.5cm	1.25	1998.24	14.6		-12.5	-13.1	0.54
SD20 1.5-2cm	1.75	1996.82	15.7		-12.7	-12.0	0.80
SD20 2-2.5cm	2.25	1994.93	14.5	14.2, 14.8	-12.7	-13.1	0.52
SD20 2.5-3cm	2.75	1993.26	14.7		-13.5	-13.0	0.56
SD20 3-3.5cm	3.25	1989.37	13.2		-13.5	-14.4	0.33
SD20 3.5-4cm	3.75	1987.46	14.5		-14.0	-13.1	0.52
SD20 4-4.5cm	4.25	1984.84	13.0		-14.6	-14.6	0.31
SD20 4.5-5cm	4.75	1982.71	11.6	11.0, 12.1	-15.4	-16.0	0.18
SD20 5-5.5cm	5.25	1980.36	11.8		-16.0	-15.7	0.19
SD20 5.5-6cm	5.75	1977.59	11.1		-16.6	-16.4	0.14
SD20 6-6.5cm	6.25	1974.63	10.0		-16.5	-17.5	0.07
SD20 6.5-7cm	6.75	1971.41	12.0		-15.6	-15.6	0.21
SD20 7-7.5cm	7.25	1967.45	14.1	14.6, 13.7	-14.7	-13.5	0.45
SD20 7.5-8cm	7.75	1963.17	12.6		-14.4	-15.0	0.26
SD20 8-8.5cm	8.25	1956.95	12.9		-14.3	-14.7	0.29
SD20 8.5-9cm	8.75	1948.22	14.5		-13.4	-13.2	0.52
SD20 9-9.5cm	9.25	1941.01	15.4		-13.3	-12.2	0.74
SD20 9.5-10cm	9.75	1938.47	13.1	13.7, 12.6	-13.9	-14.5	0.32
SD20 10-10.5cm	10.25	1934.93	12.7		-14.5	-14.9	0.27
SD20 10.5-11cm	10.75	1932.03	13.4		-14.0	-14.2	0.35
SD20 11-11.5cm	11.25	1928.68	14.7		-14.3	-12.9	0.57
SD20 11.5-12cm	11.75	1925.70	11.9		-13.5	-15.7	0.20
SD20 12-12.5cm	12.25	1922.24	15.9	16.3, 15.4	-14.1	-11.8	0.88
SD20 12.5-13cm	12.75	1918.39	12.8		-12.3	-14.8	0.28
SD20 13-13.5cm	13.25	1914.74	17.4		-13.2	-10.3	1.75
SD20 13.5-14cm	13.75	1909.74	13.2		-13.6	-14.4	0.33
SD20 14-14.5cm	14.25	1905.26	11.5		-14.5	-16.1	0.17
SD20 14.5-15cm	14.75	1900.91	14.5	16.0, 12.9	-14.4	-13.1	0.52
SD20 15-15.5cm	15.25	1896.31	13.6		-13.8	-14.0	0.38
SD20 15.5-16cm	15.75	1891.87	13.4		-13.6	-14.2	0.35
SD20 16-16.5cm	16.25	1885.89	15.1		-13.5	-12.5	0.65
SD20 16.5-17cm	16.75	1880.10	13.8		-13.0	-13.8	0.41
SD20 17-17.5cm	17.25	1873.68	14.9	14.2, 15.7	-13.5	-12.7	0.60
SD20 17.5-18cm	17.75	1868.71	13.5		-12.9	-14.1	0.37
SD20 18-18.5cm	18.25	1862.75	15.7		-12.5	-12.0	0.81
SD20 18.5-19cm	18.75	1857.88	16.3		-12.0	-11.4	1.01
SD20 19-20cm	19.5	1851.01	14.9		-12.4	-12.7	0.60
SD20 20-20.5cm	20.25	1845.03	14.7		-12.6	-13.0	0.56
SD20 20.5-21cm	20.75	1840.09	15.7		-11.4	-12.0	0.81
SD20 21-21.5cm	21.25	1834.94	18.6		-11.0	-9.2	3.70
SD20 21.5-22cm	21.75	1828.39	15.7		-11.2	-11.9	0.82
SD20 22-22.5cm	22.25	1821.66	15.1	14.7, 15.4	-12.0	-12.5	0.65
SD20 22.5-23cm	22.75	1817.34	16.1		-12.0	-11.6	0.95
SD20 23-23.5cm	23.25	1810.51	15.7		-12.0	-12.0	0.81
SD20 23.5-24cm	23.75	1802.95	15.1		-12.1	-12.5	0.65
SD20 24-24.5cm	24.25	1796.65	15.9	16.1, 15.8	-12.4	-11.8	0.88
SD20 24.5-25cm	24.75	1789.66	14.8		-12.4	-12.9	0.57
SD20 25-25.5cm	25.25	1782.55	15.2		-12.6	-12.5	0.67
SD20 25.5-26cm	25.75	1776.57	15.1		-11.7	-12.5	0.66
SD20 26-26.5cm	26.25	1768.99	17.5		-11.3	-10.2	1.83
SD20 26.5-27cm	26.75	1763.28	16.5		-10.6	-11.2	1.12
SD20 27-27.5cm	27.25	1755.27	17.4	18.1, 16.6	-10.7	-10.3	1.71

SD28 KB-5 Cellulose-inferred $\delta^{18}O_{LW}$ Results and E/I Values

SD28 Sample ID	Mid Point Core Depth	SED CRS Dates	Cell 18O	Repeats	Three Point Mean	Cell-Infrrd 18O lw	Calculated E/I
0-0.5	0.25	2002.00	9.3		-19.4	-18.2	0.04
0.5-1	0.75	2001.78	6.8	6.3, 7.3	-20.1	-20.6	-0.06
1-1.5	1.25	2001.23	6.0		-21.0	-21.4	-0.08
1.5-2	1.75	2001.01	6.6		-21.3	-20.8	-0.06
2-2.5	2.25	2000.65	5.8		-21.1	-21.6	-0.09
2.5-3	2.75	2000.26	6.4	6.5, 6.3	-21.7	-21.0	-0.07
3-3.5	3.25	1999.92	4.9	4.2, 5.6	-19.6	-22.5	-0.11
3.5-4	3.75	1999.65	12.4		-19.3	-15.2	0.24
4-4.5	4.25	1999.05	7.3		-18.2	-20.1	-0.04
4.5-5	4.75	1998.21	8.1		-19.8	-19.4	-0.02
5-5.5	5.25	1996.99	7.7		-19.5	-19.8	-0.03
5.5-6	5.75	1996.32	8.2		-19.3	-19.3	-0.01
6-6.5	6.25	1995.73	8.6		-19.2	-18.9	0.01
6.5-7	6.75	1995.10	8.0		-18.7	-19.4	-0.02
7-7.5	7.25	1994.38	9.7	9.4, 10.0	-18.4	-17.8	0.06
7.5-8	7.75	1993.80	9.6		-18.1	-17.9	0.05
8-8.5	8.25	1993.28	9.0		-18.2	-18.5	0.02
8.5-9	8.75	1992.91	9.3		-18.1	-18.2	0.03
9-9.5	9.25	1992.60	9.9		-18.0	-17.6	0.07
9.5-10	9.75	1992.10	9.3	8.7, 10.0	-17.9	-18.1	0.04
10-10.5	10.25	1991.60	9.7	9.5, 9.8	-17.7	-17.8	0.05
10.5-11	10.75	1991.12	10.5		-17.5	-17.1	0.10
11-11.5	11.25	1990.61	9.9		-17.2	-17.6	0.07
11.5-12	11.75	1990.10	10.5		-17.5	-17.0	0.10
12-12.5	12.25	1989.58	9.6	9.4, 9.8	-16.6	-17.9	0.05
12.5-13	12.75	1989.10	12.8		-16.3	-14.8	0.28
13-13.5	13.25	1988.72	11.3		-15.7	-16.2	0.15
13.5-14	13.75	1988.33	11.6		-16.2	-16.0	0.18
14-14.5	14.25	1987.62	11.2		-16.5	-16.4	0.15
14.5-15	14.75	1986.68	10.5	10.5, 10.4	-16.6	-17.0	0.10
15-15.5	15.25	1985.43	11.0		-17.0	-16.5	0.14
15.5-16	15.75	1984.15	10.1		-16.8	-17.4	0.08
16-16.5	16.25	1982.61	11.0		-17.1	-16.6	0.13
16.5-17	16.75	1980.52	10.1		-17.0	-17.4	0.08
17-17.5	17.25	1978.46	10.5	9.8, 11.3	-16.8	-17.0	0.10
17.5-18			11.7		-16.4	-15.9	0.18
18-18.5	18.25	1974.10	11.1		-15.7	-16.4	0.14
18.5-19	18.75	1971.47	12.8		-15.6	-14.8	0.29
19-19.5	19.25	1968.99	11.9		-15.3	-15.7	0.20
19.5-20	19.75	1966.39	12.1	12.3, 11.9	-15.7	-15.5	0.21
20-20.5	20.25	1963.72	11.6		-15.6	-15.9	0.18
20.5-21	20.75	1960.77	12.2		-15.5	-15.4	0.23
21-21.5	21.25	1958.62	12.3		-15.3	-15.2	0.24
21.5-22	21.75	1955.13	12.3		-15.1	-15.2	0.24
22-22.5	22.25	1952.51	12.8	13.3, 12.4	-14.7	-14.8	0.29
22.5-23	22.75	1949.15	13.6		-14.4	-14.0	0.38
23-23.5	23.25	1946.13	13.1		-14.2	-14.5	0.32
23.5-24	23.75	1943.79	13.6		-14.1	-14.0	0.38
24-24.5	24.25	1941.60	13.8	14.1, 13.4	-14.2	-13.8	0.41
24.5-25	24.75	1939.30	12.9		-14.4	-14.7	0.30
25-25.5	25.25	1937.62	12.9		-14.9	-14.7	0.29
25.5-26	25.75	1935.10	12.2		-15.0	-15.4	0.23
26-26.5	26.25	1932.72	12.7		-14.3	-14.9	0.28
26.5-27	26.75	1930.29	14.9		-13.9	-12.7	0.61
27-27.5	27.25	1927.74	13.4	14.1, 12.6	-13.8	-14.2	0.35
27.5-28	27.75	1924.77	13.3		-14.7	-14.3	0.34
28-28.5	28.25	1921.40	12.0		-14.8	-15.6	0.21
28.5-29	28.75	1919.00	13.2	12.7, 13.7	-14.5	-14.4	0.33
29-29.5	29.25	1917.66	14.1		-14.1	-13.5	0.45
29.5-30	29.75	1915.05	13.2		-13.6	-14.4	0.33
30-30.5	30.25	1912.56	14.7		-13.6	-12.9	0.57
30.5-31	30.75	1910.44	14.2		-13.5	-13.4	0.47
31-31.5	31.25	1907.92	13.3	13.5, 13.2	-13.8	-14.3	0.35
31.5-32	31.75	1905.49	13.8		-14.0	-13.8	0.41
32-32.5	32.25	1903.69	13.5		-14.0	-14.1	0.37
32.5-33	32.75	1901.07	13.5		-14.1	-14.1	0.37